DEVELOPMENT OF CI ENGINE OPERATED MICRO TRIGENERATION SYSTEM FOR POWER, HEATING AND SPACE COOLING

by

RAHUL GOYAL

(2010RME102)

Department of Mechanical Engineering

MALAVIYA NATIONAL INSTITUTE OF TECHNOLOGY, JAIPUR

INDIA

November, 2015

DEVELOPMENT OF CI ENGINE OPERATED MICRO TRIGENERATION SYSTEM FOR POWER, HEATING AND SPACE COOLING

by

RAHUL GOYAL

(2010RME102)

Department of Mechanical Engineering

Submitted in Fulfillment of the requirements for the degree of

DOCTOR OF PHILOSOPHY

to the

MALAVIYA NATIONAL INSTITUTE OF TECHNOLOGY, JAIPUR

INDIA

November, 2015

DEPARTMENT OF MECHANICAL ENGINEERING

MALAVIYA NATIONAL INSTITUTE OF TECHNOLOGY, JAIPUR

CERTIFICATE

This is to certify that the thesis entitled **"Development of CI Engine Operated Micro Trigeneration System for Power, Heating and Space Cooling"** submitted by **Mr. Rahul Goyal (2010RME102)**, to the Malaviya National Institute of Technology, Jaipur for the award for the degree of **Doctor of Philosophy** is a bonafide record of original research work carried out by him. He has worked under our guidance and supervision and has fulfilled the requirement for the submission of this thesis.

The results contained in thesis have not been submitted in part or full, to any other University or Institute for the award of any degree or diploma.

(Prof. Dilip Sharma)
Professor
Department of Mechanical Engineering
Malaviya National Institute of Technology
Jaipur

(Prof. S.L.Soni)
Professor
Department of Mechanical Engineering
Malaviya National Institute of Technology
Jaipur

Date:

ACKNOWLEDGEMENT

I wish to express my deep regards and profound sense of gratitude to my reverend and learned supervisors **Prof. Dilip Sharma** and **Prof. S. L. Soni**, Department of Mechanical Engineering, Malaviya National Institute of Technology Jaipur, who through their excellent guidance has enabled me to accomplish this work. They have been great source of inspiration to me, all through. I am very grateful to them for guiding me how to conduct research and how to clearly & effectively present the work done.

I extend my sincere thanks to my doctoral guidance committee members, **Prof. Jyotirmay Mathur, Dr. G.D. Agrawal and Dr. N. Rathogi**, for their valuable suggestions and cooperation throughout the course of study.

I also would like to thank **Mr. Pradeep Kumar Gupta,** Research Scholar for his continuous help during preparation of thesis.

I am also thankful to **Mr. Ramesh Meena,** Lab. Technician (I.C. Engine Lab), **Mr. Deepesh Sonar,** Research Scholar, Department of Mechanical Engineering, Malaviya National Institute of Technology, Jaipur for helping me in Labs and conducting the experiments.

Words will never be adequate to express the sense of reverence, veneration and gratitude to my dear parents **Mr. Madhukar Goyal** and **Mrs. Meena Goyal**, who have always wished to this to happen. I'd like to express my thanks and gratitude to my father in-laws **Dr. Laxmi Chand Agrawal** and mother in-laws **Mrs. Usha Agrawal** for their blessing and encouragement. I would also like thanks to my brothers, brothers in laws, sister in laws and their families for their support and assistance in every respect.

Things would never have been possible without my wife **Mrs. Preeti Goyal**. Her understanding, cooperation, patience and undoubted faith in my potential had motivated me to complete this research. Since inception of the work till thesis writing she has been a continuous moral support to me and had bear all responsibilities to keep myself much focused. It's incomplete without

mentioning the sweetest smiles and cheerful faces of my lovely kids **Aradhya and Pragyan**, who eased the pressure of the last crucial phase of work with their joyful company.
Last but not the least I would like to express deep sense of gratitude to all my relatives, colleagues, friends and junior fellows for their encouragement and assistance.

Place: Jaipur

Date:

Rahul Goyal

ABSTRACT

To achieve an optimal solution for the current energy crisis, the world needs to focus more on (a) renewable sources of energy or (b) look for recycling / appropriate utilization of energy being wasted. An alarming amount of heat is wasted from exhaust systems of various engines - stationary or in automobiles. Cogeneration and trigeneration have emerged as the most effective techniques for achieving the goal of efficient utilization of energy resources. Trigeneration systems use waste heat from prime movers to generate heating and cooling along with power. They are more efficient, less polluting & more economical than conventional systems.

The present study describes the performance and emission characteristics of a micro trigeneration system based on a single cylinder, 5 hp, and water cooled diesel engine. In this trigeneration system, in addition to the electricity generated from the genset, waste heat from hot exhaust gas of diesel engine was used to drive a combination of four units of Electrolux vapor absorption (VA) system for space cooling, and compact type heat exchanger was used for hot water production. The capacity and heat input of each unit of VA system was 51 liters and 95 Watts respectively. A cabin (3' X 5' X 6') made of ply wood was fabricated as a space for cooling. The performance and emission analysis for the trigeneration system was divided in various steps to suit the conditions of single generation, combined cooling and power (CCP), combined heating and power (CHP) and combined cooling, heating and power (CCHP) modes.

The test results show that a temperature drop of 6.5^0C was obtained in cabin at full engine load about 6 hours after system start up. The reduction of CO_2 emission in kg per kWh of useful energy output was 53.83% in combined heating and power (CHP), 57.46% in combined cooling, heating and power (CCHP) and 8.02% in combined cooling and power (CCP) mode compared to that of single generation (power generation only) at full load. The decrease in specific fuel consumption was 53.24%, 51.29% and 6.89% in case of CHP, CCHP and CCP mode respectively compared to that in single generation at full load. The test results also show that the useful energy output and total thermal efficiency of trigeneration system were much higher than that of single generation. From the exergetic point of view, exergy efficiency of either of the integrated systems was marginally higher compared to the traditional power generation system

(Single generation). For the optimization of trigeneration system in CCHP mode, different VA units were operated one by one to obtain the best energy output in terms of space cooling and water heating.

Hence, the results show that micro trigeneration system using single cylinder CI engine for power, heating and space cooling is very effective and that they can be projected as strategic means to achieve energy security and efficiency, with positive impact on economy, simultaneously reducing environmental threats, leading to sustainable development.

CONTENTS

LIST OF FIGURES

Appendix

LIST OF TABLES

NOMENCLATURE

BSFC	Break specific fuel consumption (kg/kWh)
BTE	Break thermal efficiency (%)
CHP	Combined heating and power
CCP	Combined cooling and power
CCHP	Combined cooling, heating and power
CO	Carbon monoxide
COP	Coefficient of performance
HC	Unburned hydrocarbons
NO_x	Oxides of nitrogen
NTU	Number of transfer units
PEM	Proton exchange membrane
SFC	Specific fuel consumption (kg/kWh)
U	overall heat transfer coefficient (kW/m^2K)
A	Area (m^2)
VAR	Vapor absorption refrigerator
Btu	British thermal unit
Mtoe	Million ton of oil equivalent

Symbols

μ	Viscosity (N-s/m)
ρ	Density (kg/m^3)
K	Thermal conductivity (W/mK)

$\dot{m}$	Mass flow rate (kg/s)
E	Energy
C_p	Specific heat (kJ/kgK)
T	Temperature (K)
H	Efficiency (%)
T_0	Ambient temperature (K)
P	pressure
Pr	Prandtl number
Re	Reynolds number
St	Stanton number
Nu	Nusselt number
bp	Break power of engine
kWh	Kilo watt hour
CV	Calorific value

Subscripts

f	Fuel
ex.	Exhaust
eng.	Engine
Cw	Cold water
H.E.	Heat exchanger
ref	Refrigeration
Cab	Cabin

T	Total
Gen	Generator
h_i	Hot fluid in
c_i	Cold fluid in
E	Exergy
eva	Evaporator
I	Inlet
O	Outlet

CHAPTER 1

INTRODUCTION

1.1 Research Background

1.1.1 World Energy Demand

World energy consumption is expected to increase from 524 quadrillion Btu in 2010 to 630 quadrillion Btu in 2020 and 820 quadrillion Btu in 2040. Hence, in the next 30 years energy consumption will increase by 56% [1]. More than 85% of the increase in global energy demand shall occur among the developing nations outside the organization for Economic Cooperation and Development (i.e. non OECD) from 2010 to 2040. World total energy consumption during 1990 to 2040 for Non OECD and OECD nations is shown in Fig 1.1.

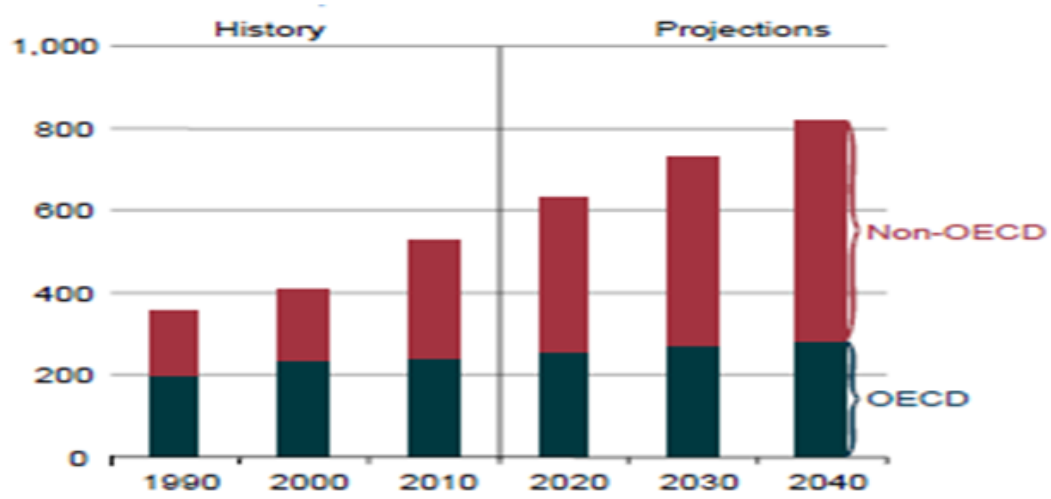

Fig.1.1 World total energy consumption in(quadrillion Btu) 1990-2040 [1]

1.1.2 Energy supply by various sources

Fossil fuels continue to satisfy most of the world's current energy demand. In 2012, liquid fuels (mainly crude), natural gas, and coal were the source for more than three-fourth of world's total energy consumption. Hence, petroleum and other liquid fuels remain to be the largest source of energy. Liquid fuels' consumption is increasing in the industrial and transportation sectors while decreasing in commercial and power sector.

According to WEO 2014, world's coal consumption rises at an average rate of 1.3% per year (increased from 640Mtoe in 1973 to 909Mtoe in 2012) [2]. Coal consumption rose mainly in industrial sector from 56.6% in 1973 to 80% in 2012 as shown in Fig. 1.2.

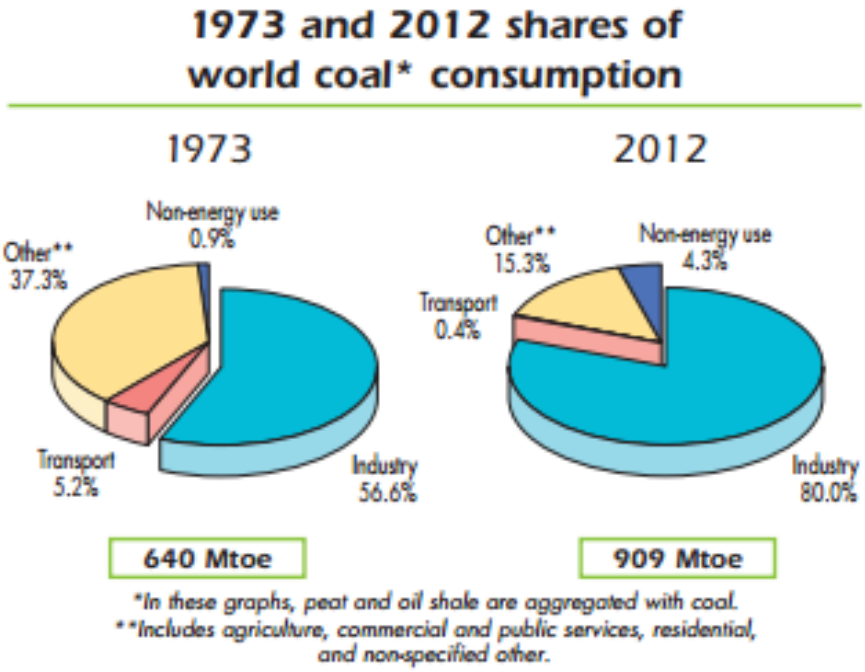

Fig.1.2 Worldwide coal consumption [2]

Figure 1.3 shows that world's oil consumption rises at an average rate of 1.1% per year (increased from 2251Mtoe in 1973 to 3652Mtoe in 2012) [2]. The report shows that the oil consumption is mainly increased in transport sector (which includes all on-road vehicles) with an increase from 45.4% of the total oil consumption in 1973 to 63.7% of the total oil consumption in 2012.

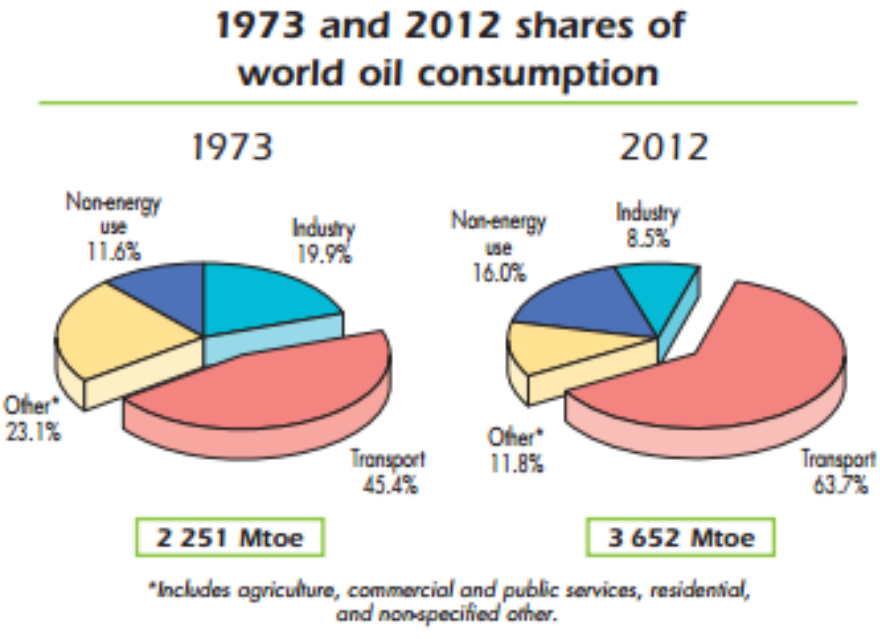

Fig.1.3 Worldwide oil consumption [2]

Figure 1.4 shows that world's total natural gas consumption increases by an average of 1.7% per year (increased from 652Mtoe in 1973 to 1366Mtoe in 2012) [2]. As in case of coal consumption, the world's natural gas consumption is mainly in the industrial sector. However, the percentage consumption of natural gas in industrial sector is reduced from 54.8% in 1973 to 36.5% in 2012. Other sectors have accounted for majority of the increased consumption.

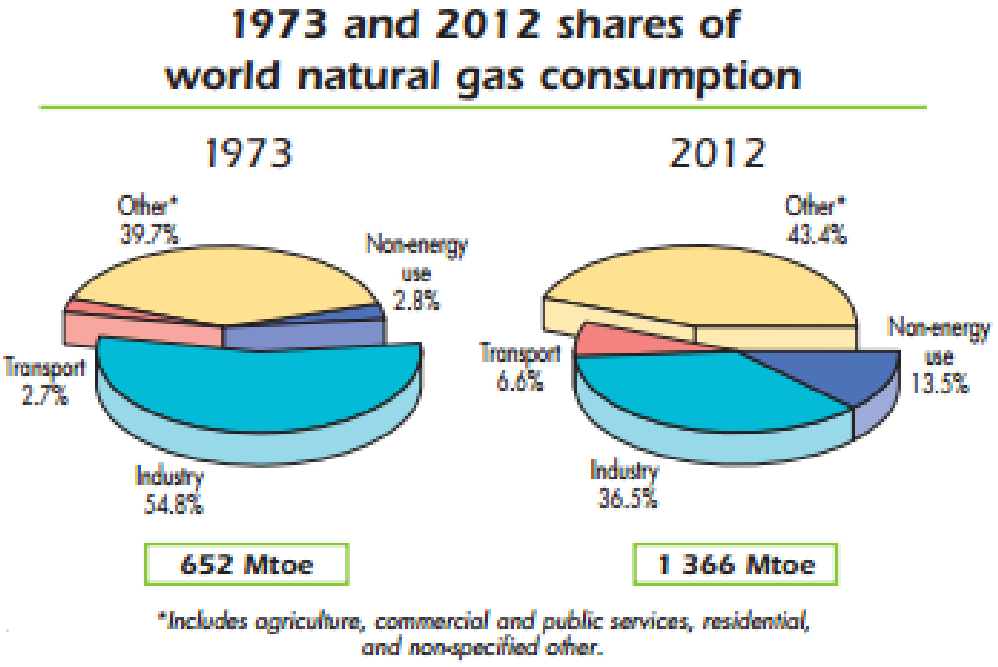

Fig.1.4 Worldwide natural gas consumption [2]

Figure 1.5 shows that world's total electricity consumption increases by an average of 1.87% per year (increased from 440Mtoe in 1973 to 1626Mtoe in 2012) [2]. World's electricity consumption is increased in 'others' sector (which includes buildings/residential) and decreased in industry and transport sector in terms of percentage of overall world's electricity consumption.

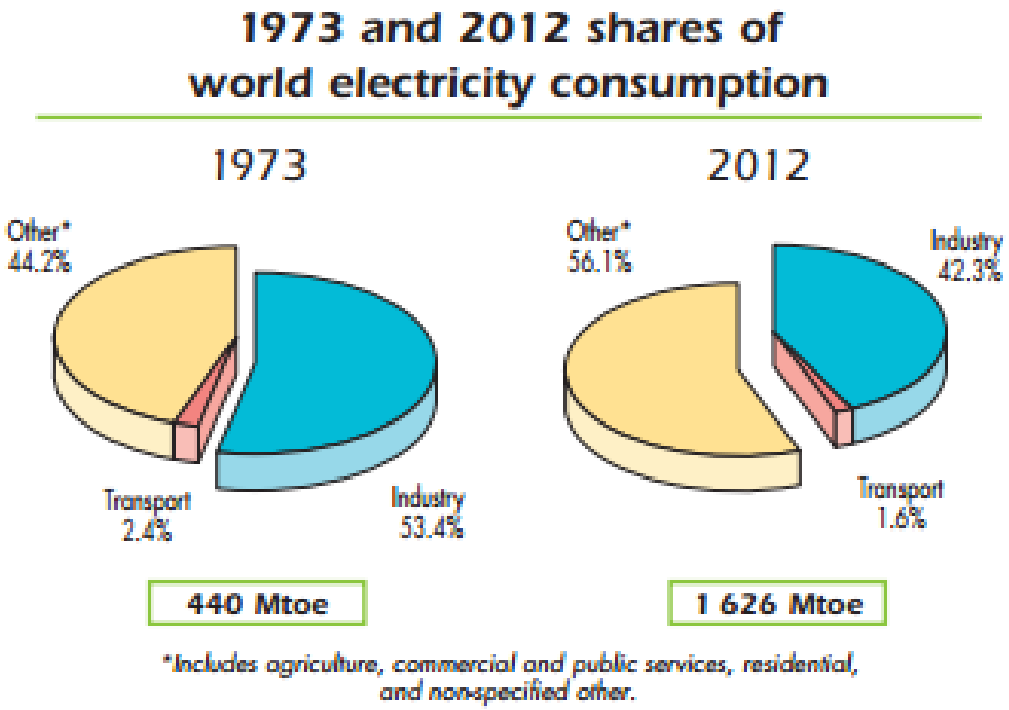

Fig.1.5 Worldwide electricity consumption [2]

1.1.3 Sector wise consumption of energy in world

Energy use in the residential sector is defined as the energy consumed by households, excluding their transportation use. As per IEO 2013, energy use by residential sector shall account for about 14% of world's total energy consumption in 2040. World's residential energy consumption is expected to increase by 57% from 2010 to 2040, mainly as a result of growing residential demand in the non OECD countries. Total non OECD residential energy consumption increases at an average annual rate of 2.5%, compared with an average of 0.4% per year in OECD countries as shown in Fig 1.6 [1].

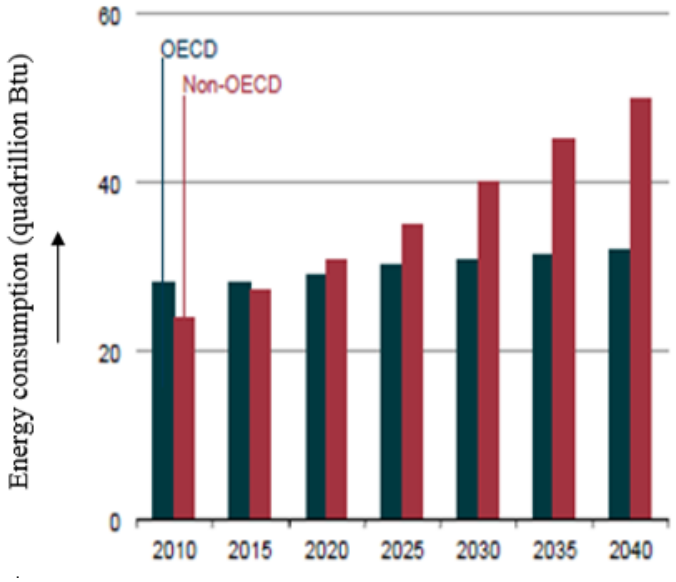

Fig.1.6 World residential sector delivered energy consumption in (quadrillion Btu) [1]

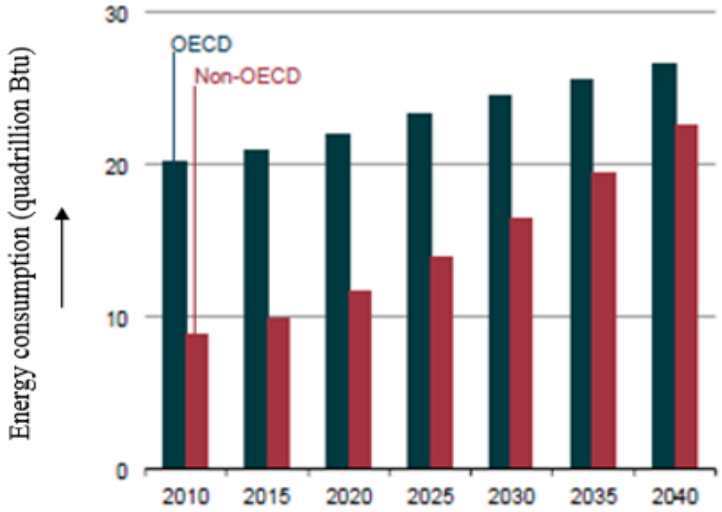

Fig.1.7 World commercial sector delivered energy consumption in (quadrillion Btu) [1]

As per IEO 2013, energy use by commercial sector accounted for nearly 8% of world's total energy consumption in 2010 [1]. World's commercial energy consumption is expected to increase by around 80% from 2010 to 2040, mainly as a result of growing commercial demand in the non OECD countries. Total non OECD commercial energy consumption increases at an average annual rate of 5.5%, compared with an average of 1.7% per year in OECD countries as shown in Fig. 1.7 [1].

Energy use in transportation sector includes energy consumed in moving people and goods by road, rail, air, water and pipeline. The transportation sector accounts for 26% of world's total energy consumption in 2010 and transportation energy use is expected to increase by 1.1% per year from 2010 to 2040 as per IEO 2013 as shown in Fig. 1.8 [1].

India's transportation energy use grows at the fastest rate in the world, averaging at 5.1% per year, compared with the world average of 1.1% per year as discussed above. Transportation energy use in India is expected to grow from 2.4 quadrillion Btu in 2010 to 10.9 quadrillion Btu in 2040, considering the increase in demand for passenger and freight transportation resulting from India's fast growing economy and increasing population. The rapid enhancement in the road infrastructure in India shall lead to the exponential expansion of transportation energy use.

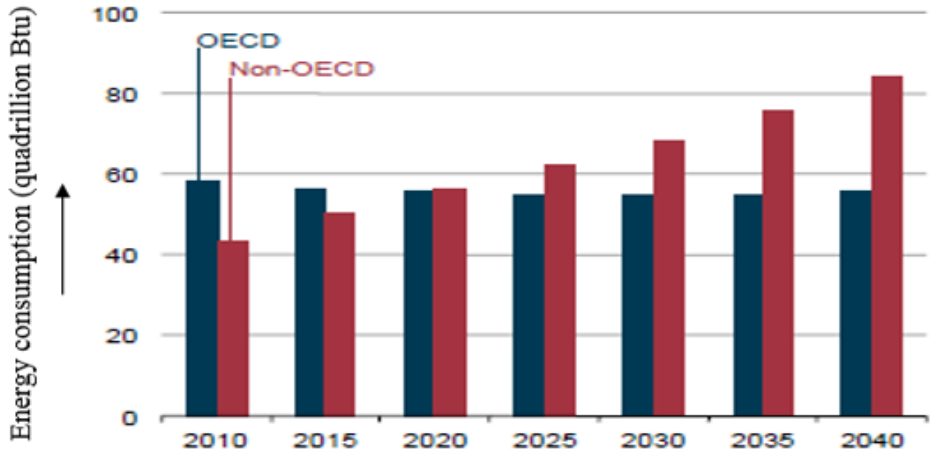

Fig.1.8 World transportation sector delivered energy consumption in (quadrillion Btu) [1]

In 2011, the global transport sector consumed about 2200 Mtoe, constituting about 25% of global energy supplies. As Fig. 1.9 shows, about 96% of the total energy consumption in transportation sector was fulfilled by oil (Gasoline, Diesel, Jet and Residual), while the rest of the energy consumed in transportation sector was obtained from natural gas, bio fuels, and electricity. More than 60% of the oil consumed globally goes to the transportation sector. As per Fig. 1.9, road transport accounts for 76% (LDV, Truck, Bus and Other) of the transportation energy consumption. The light-duty vehicles (LDVs), including light trucks, light commercial vehicles, and minibuses accounted for about 52%, while trucks, including medium and heavy-duty, accounted for 17%,full-sized buses and two-three wheelers accounted 4%&3% respectively. Air and marine each accounted for about 10% of total transport energy consumption, while the railways accounted for only 3% [3].

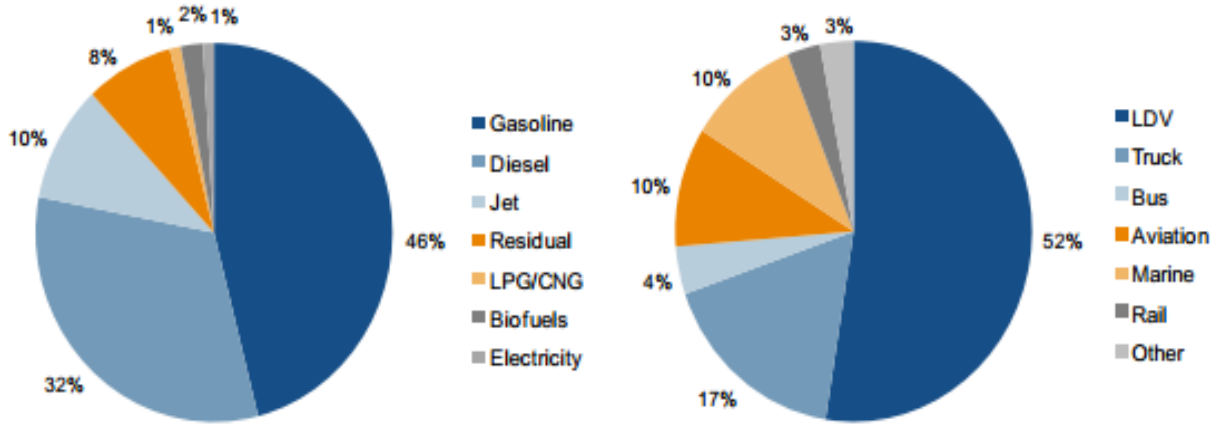

Fig.1.9 Transport energy consumption by source and by mode in 2011[3]

1.1.4 Energy demand in India

India has the third largest energy demand in the world after China and the United States and just ahead of Russia. China and India continue to lead both world economic growth and energy demand growth. According to WEO 2011, India's energy demand is more than doubled from 319 Mtoe in 1990 to 669 Mtoe in 2009. Since 1990, energy consumption in both the countries has increased significantly in terms of percentage of world's total energy use; together, they accounted for about 10% of world's total energy consumption in 1990 and nearly 24% in 2010 [4]. It is further predicted that their combined energy use will be more than doubled from 2010 to 2040. Per-capita Energy Consumption (PEC) during a year is computed as the ratio of the total energy consumption during the year to the mid-year population for that year. Energy Intensity is defined as the amount of energy consumed for generating one unit of Gross Domestic Product (at constant prices). PEC and energy intensity are the most used policy indicators, both at national and international levels. In the absence of data on consumption of non-conventional energy from various sources, particularly in rural areas in the developing countries, including India, these two indicators are generally computed on the basis of consumption of conventional energy. Per-capita Energy Consumption (PEC) increased from 1, 3694.83 Mega Joules in 2005-06 to 19522.15 Mega Joules in 2013-14 as shown in Fig.1.10. The annual decrease in PEC from 2013-14 to 2012-13 was 0.60% [4].

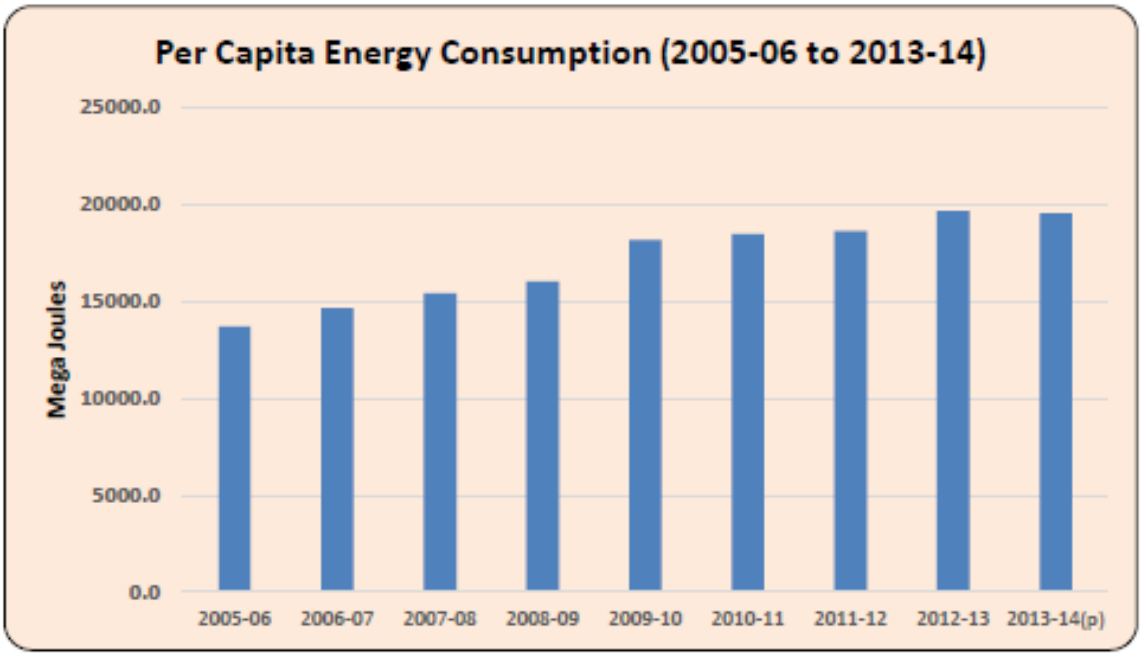

Fig.1.10 Per Capita energy consumption from 1970-71 to 2011-12 [4]

The energy intensity (amount of energy consumed for generating one unit of Gross Domestic Product at 2004-05 prices) increased from 0.4656 Mega Joules in 2005-06 to 0.4192 Mega Joules in 2013-14 as shown in Fig. 1.11 [4].

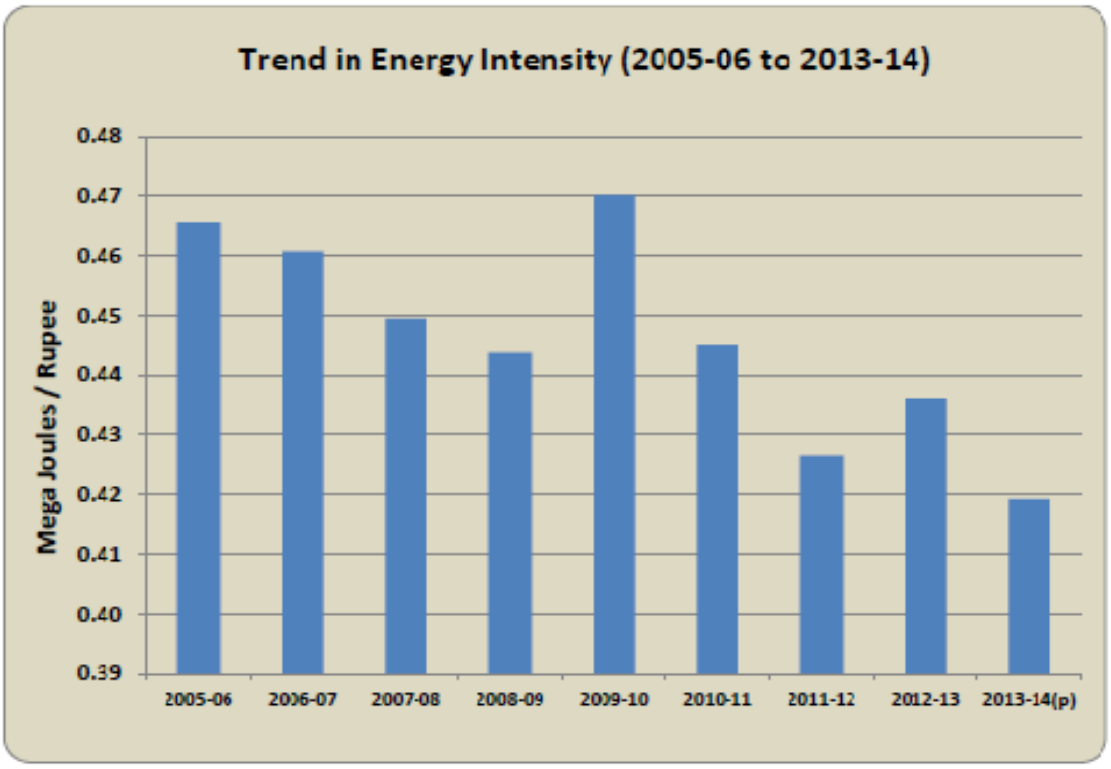

Fig. 1.11 Energy intensity from 1970- 71 to 2011- 12 [4]

1.1.5 Sector wise energy consumption in India

India's total primary energy demand is expected to grow by 2.3 times in the next two decades due to sustained economic growth in the building, transportation and industrial sectors and is expected to reach an energy consumption level of 40 EJ [5].Sector wise consumption of electricity in India during 2013-14 is shown in Fig. 1.12. The electricity consumption in India increased from 4, 11,887 GWh during 2005-06 to 8, 82,592 GWh during 2013-14, showing a cumulative annual growth rate (CAGR) of 8.84%. The increase in electricity consumption from 2012-13 (8,24,302 GWh) to 2013-14 (8,82,592 GWh) was 7.06%.The contribution of electricity in industry, domestic, agriculture and commercial sectors was 43.83, 22.46%, 18.03% and 8.72% respectively. The electricity consumption in industry sector and commercial sector has increased at a much faster rate compared to other sectors during 2005-06 to 2013-14, with CAGRs of 10.97% and 8.83% respectively [4].

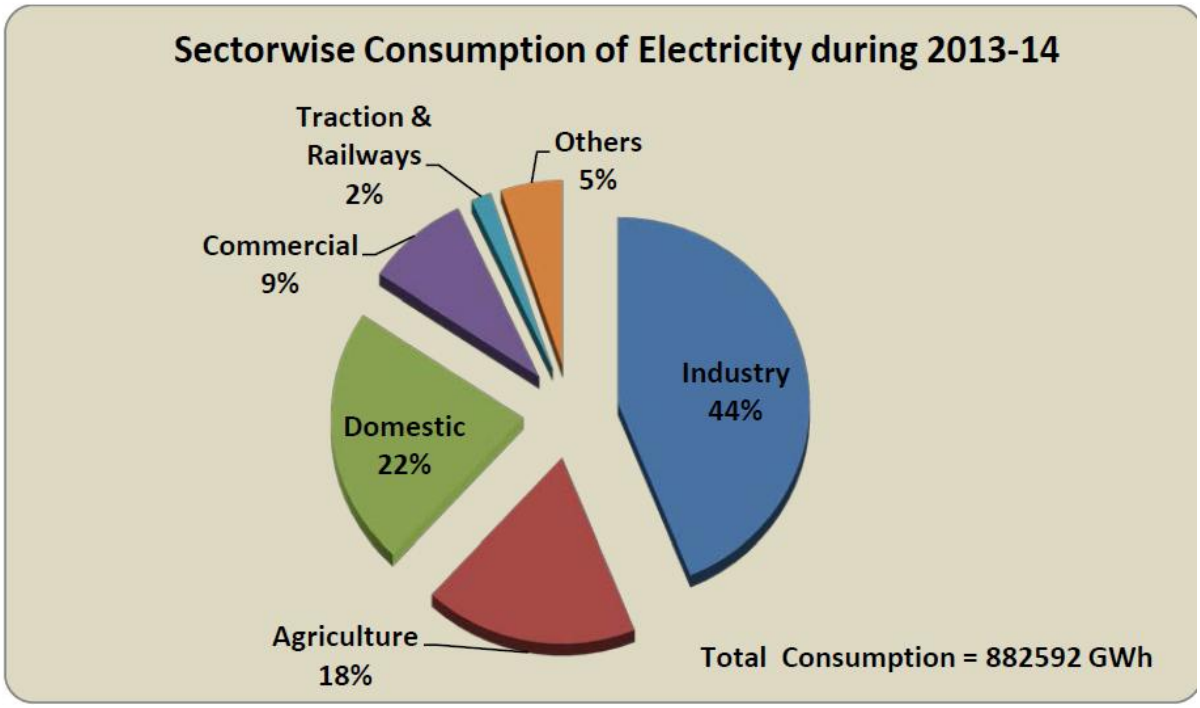

Fig.1.12 Sector wise electricity consumption in India during 2013-14 [4]

The Bureau of Energy Efficiency predicts that India's constructed floor area will increase by around five times from 2005 to 2030 [6]. This study also predicts that India's total residential floor area will be much larger than its total commercial floor area in 2030. Central European University (CEU) estimates that, by 2050, 85% of floor space will be in residential use, while

15% will be used for commercial purposes. Figure 1.13 shows the energy consumption by buildings in India in years 2005, 2030 and 2050.

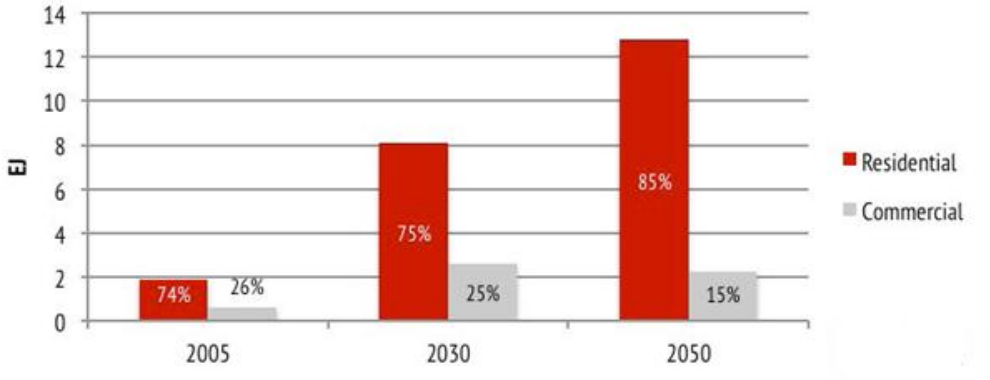

Fig.1.13 Energy consumption of India's buildings in 2005, 2030 and 2050 [6]

1.1.6 Distribution of energy use in residential sector in India

A study was conducted on rural and urban residential energy consumption in India by the Pacific Northwest National Laboratory (PNNL) and IIM Ahmadabad. The study found that, in the residential buildings, energy consumption due to space cooling and lighting accounts for one third of the total energy consumption; whereas, in commercial buildings, it accounts for nearly two-thirds. Figure1.14 shows the energy consumption by service in rural and urban area [5, 6].

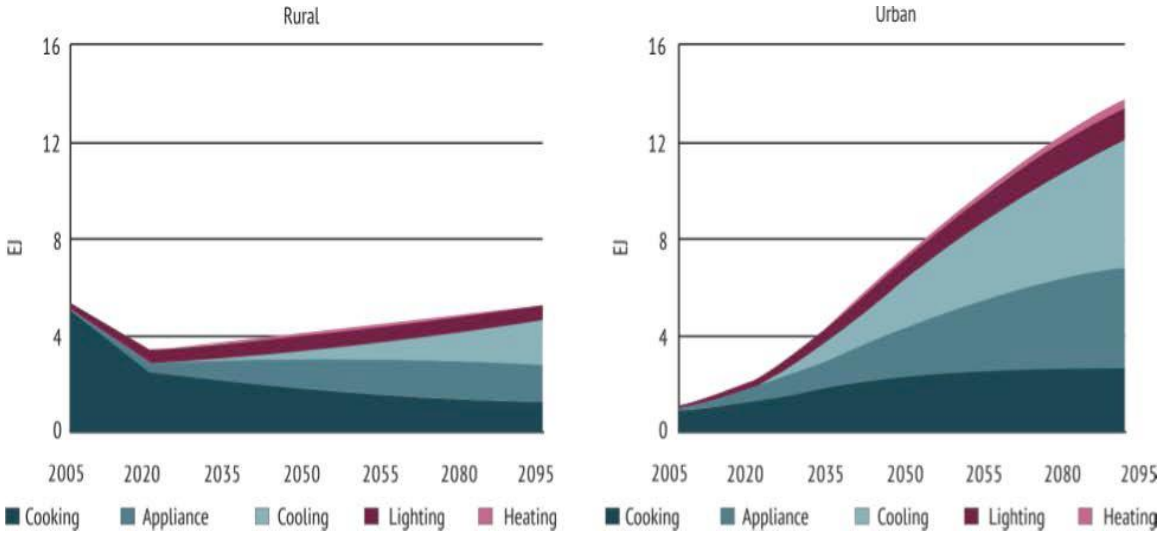

Fig.1.14 Energy consumption by service in rural and urban areas in India [5, 6]

The Climate Works Foundation study [7] indicates that the residential sector accounts for 21% of total electricity consumption. The energy consumption distribution in the residential

sector is shown in Fig. 1.15 where ceiling fans and lighting constitute the majority of energy use at 62%.

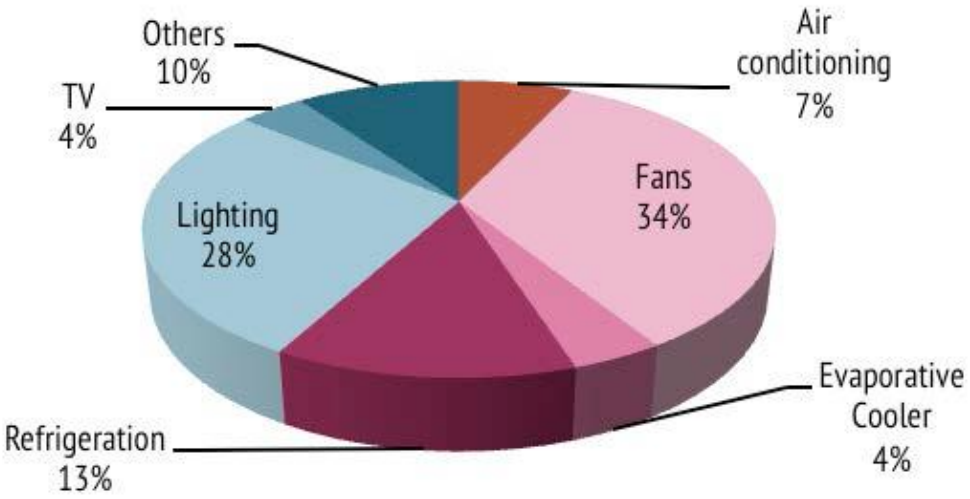

Fig.1.15 Energy consumption in residential sector in India [7]

1.2 CO_2 Emissions

Global CO_2 emission is increased due to growing fossil fuel consumption. World energy outlook (WEO 2012) states that CO_2 emission from combustion of coal was 13.1 $GtCO_2$ in 2010 and it will expected to grow to 15.3 $GtCO_2$ in 2035. Similarly, CO_2 emission from oil consumption was 10.9 $GtCO_2$ in 2010 and it is expected to grow to 12.6 $GtCO_2$ in 2035, primarily due to increased demand in transport sector. Also, CO_2emissionfrom burning of gas in 2010 was 6.2 $GtCO_2$and the same is expected to grow to 9.2 $GtCO_2$ in 2035 [8].

Figure 1.16 shows that 10 large developed / developing countries contribute two third of the total global CO_2emissions in 2013. Out of this, China and US emit 13.3 $GtCO_2$, which is about 42% of world's total CO_2 emissions in 2013. India emits more than 5% of global CO_2emissions and is showing a clear trend of rapid increase.CO_2 emissions have almost tripled between 1990 and 2013.The WEO 2012 new policies scenario projects that CO_2 emission in India is expected to increase by 3.5% per year from 2010 to 2035, at which time India would probably account for 10% of the global CO_2emissions.

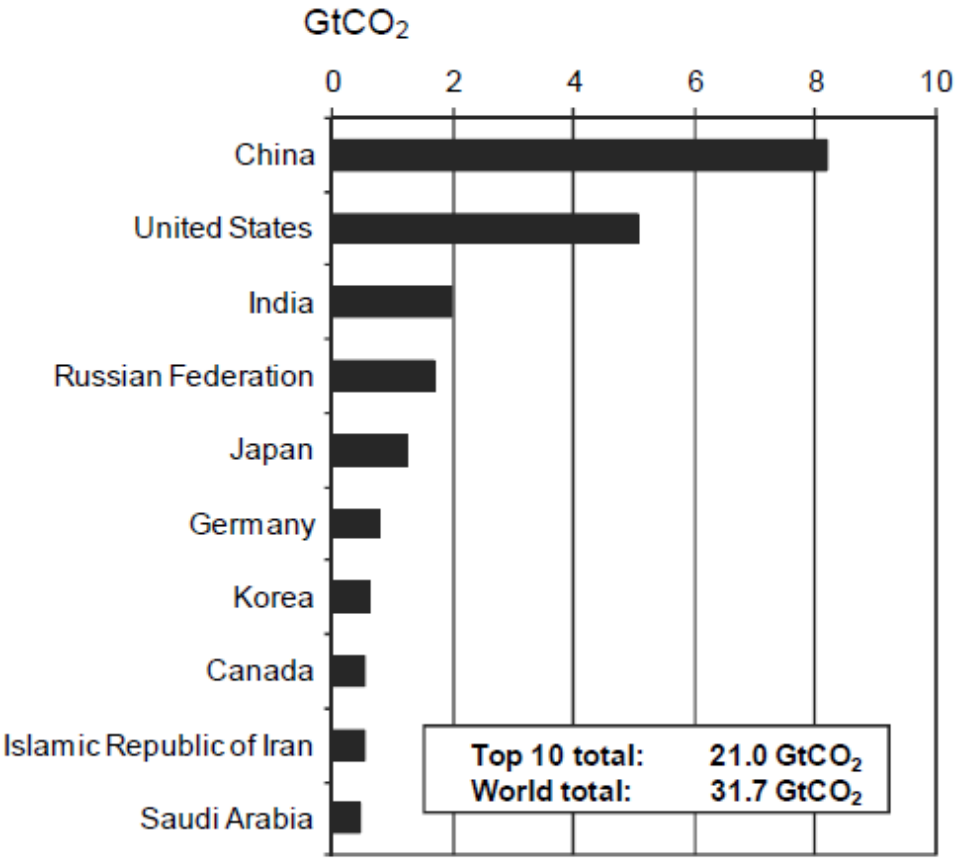

Fig.1.16 Top 10 emitting countries in 2013 [8]

In India, two sectors namely electricity & heat generation produced nearly 42% of total CO_2 emissions in India during 2013 while transport accounted for 23%, as shown in Fig. 1.17.

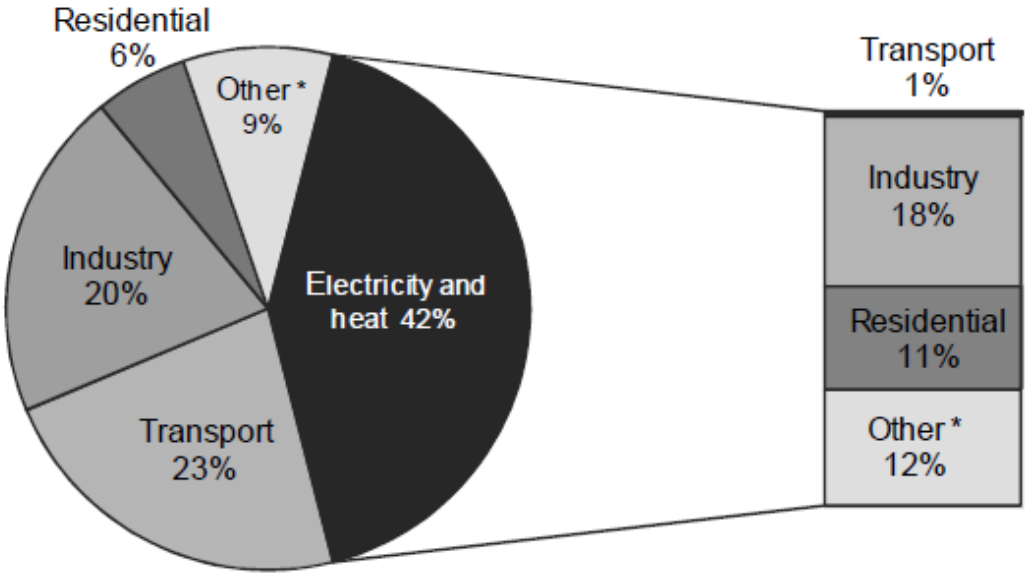

Fig.1.17 World CO_2 emissions by Sector in India (in 2013) [8]

India's emissions of 1.6 tons CO_2 per capita per year were much lower than those of other countries in 2013. The world average was 5.29 tons CO_2 per capita per year, compared to that of China at 6.1 tons CO_2 per capita per year and the United States at 16.1 tons CO_2 per capita per year [8]. According to New Policies Scenario (NPS) it is assumed that in 2035, when India is projected to be the world's most populated nation, India's carbon emissions could reach 2.34 tons CO_2 per capita, which is an increase of around 70% in 26 years from that of 2012.

Based on the current conventional prime energy consumption rate, British Petroleum predicted that major fossil sources, i.e. crude oil, natural gas and coal, would be depleted within 46, 59 and 118 years respectively [9]. Hence, considering the fast growing energy demand, limited energy resources and increasing CO_2 emissions, for a sustainable future, there is a great need to identify alternative and clean sources of energy as also energy conservation techniques to enhance the efficiency of various systems. Since a lot of work has already been done in the direction of alternative fuels like hydrogen, bio-diesel, and other additives like alcohols, the current work focused mainly on improvement in energy efficiency of the existing systems by way of minimizing energy loss. Hence, the prime focus here was on waste energy (heat) utilization techniques in heating and space cooling.

1.3 Waste Heat Recovery system

The energy available at the exit stream of prime mover goes waste if it is not utilized properly. With effective means, more than half of this waste heat could be recovered so that a considerable amount of primary fuel can be saved. It is established fact that in an internal combustion engine, a great amount (almost two-third) of energy is wasted in the form of heat carried away by exhaust gases and cooling water / air to the environment. If this waste heat is utilized for cooling and/or heating purpose, then this heat is known as recovered heat and the system which is used to recover waste heat is known as waste heat recovery system. There are various techniques which utilize the waste heat from internal combustion engines. These techniques comprise Thermoelectric generator, Simple Rankine cycle, Organic Rankine cycle, Kalina cycle, Supercritical Rankine cycle using zeotropic mixture, and others technologies like combined heating and power systems (CHP or cogeneration),combined cooling, heating and power systems (CCHP or trigeneration), six strokes internal combustion engines, etc. Detailed descriptions of all these techniques are given below:

1.3.1 Thermoelectric Generator (TEG)

TEG is one of the most important and outstanding devices. TEG is solid state device that produce electricity from heat flow across a temperature gradient. As the heat flows from hot to cold end, free charge carriers in the material are also driven to the cold end. This phenomenon was discovered by Thomas Johann Seebeck in 1821 and is called the Seebeck effect. Seebeck observed that if two dissimilar materials were joined together and the junctions were held at different temperature a potential (voltage) difference was developed. This voltage difference (dV) was proportional to the temperature difference (dT). The ratio of the voltage difference to the temperature difference is related to an intrinsic property of the material called the Seebeck coefficient [10]. The fuel efficiency of diesel engine is as low as 30% whereas around 35% of fuel energy is lost in the form of waste heat through an exhaust pipe [11].TEG can utilize this waste heat into electricity. By converting the waste heat into electricity, engine performance, reliability, efficiency, and design flexibility could be improved significantly. Free maintenance, silent operation and no moving or complex mechanical parts are the main advantages of TEG [12]. For an automobile engine, there are two main sources for capturing exhaust heat, one is radiator and another is flue gas system. An automotive waste heat energy recovery system consists of an exhaust gas system, a heat exchanger, a TEG system, a power conditioning system, and a battery pack as shown in Fig. 1.18.

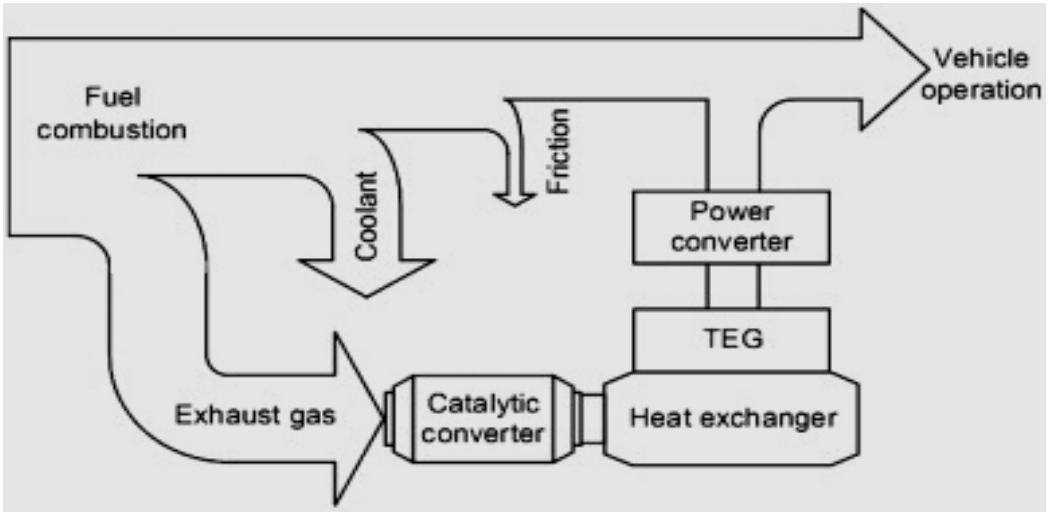

Fig.1.18 A Typical waste heat energy recovery system [13]

The major drawback of TEG is their relatively low conversion efficiency which is up to 5% only [14]. Thermoelectric material efficiency depends on the thermoelectric figure of merit,

Z. The performance of thermoelectric material can be expressed as $ZT = \alpha^2 T/kR$, where Z is the thermoelectric material figure of merit, α is the Seebeck coefficient, R is the electric resistivity, k is total thermal conductivity and T is average absolute temperature of hot and cold plates of the thermoelectric module [15]. The figure of merit is often expressed in its dimensionless form, ZT. With higher value of the thermoelectric figure of merit, higher efficiency can be obtained. The conversion efficiency as a function of operating temperature difference and for a range of value of the material's figure of merit is displayed in Fig. 1.19 [16]. Materials such as BiTe, CeFeSb, ZnBe, SiGe, SnTe and new nano crystalline thermoelectric materials are currently in development stage to improve the conversion efficiency of TEGs [17].

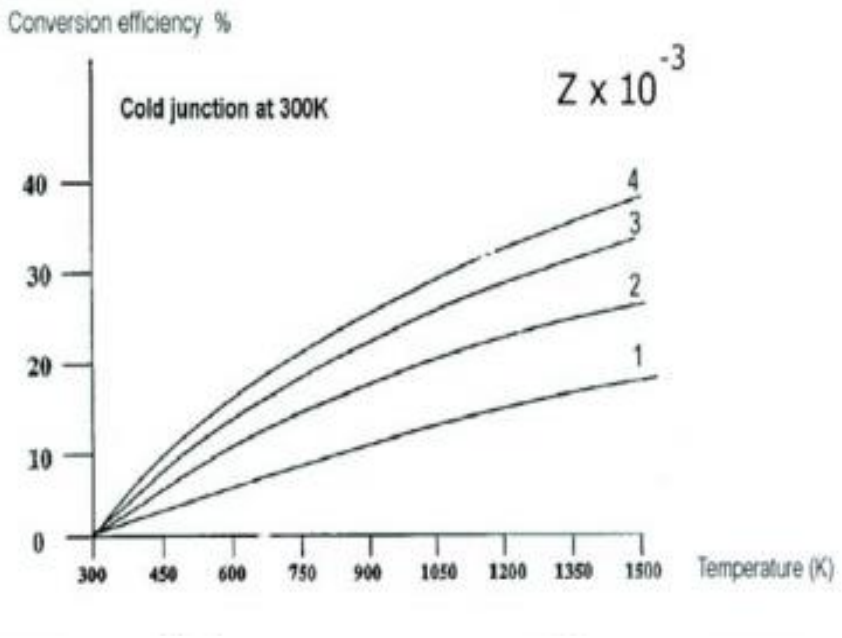

Fig.1.19: Efficiency vs. temperature for various thermoelectric figures of merit [16]

The cost of TEG consists of the device cost and running cost. The running cost is governed by the generator's conversion efficiency, while the device cost is determined by the cost of its construction to produce the desired electrical power output [18]. Since the conversion efficiency of TEG is low, therefore running cost is low as compare to device cost. So, an important objective in thermo electric power generation is to reduce the cost per watt of the device. Cost per watt can be reduced by optimizing the device geometry, improving the manufacturing quality [19].

1.3.2 Bottoming Cycle Techniques

Within waste heat recovery technology, the terms bottoming cycle and topping cycle are used. A bottoming cycle is a thermodynamic cycle which generates electricity from waste heat, while topping cycle is a thermodynamic cycle in which waste heat from electricity generation is rejected to the environment or used for heating purposes in industry. Suitable bottoming cycle for diesel and gas engines is the simple Rankine cycle, Organic Rankine cycle, Kalina cycle, and Supercritical Rankine cycle using Zeotropic mixture. The descriptions of these bottoming cycles are as follows:

1.3.2.1 Simple Steam Rankine cycle as a bottoming cycle

A waste heat recovery Rankine Bottoming cycle system consists of a pump to circulate the working fluid i.e. water/steam, an evaporator/boiler to absorb exhaust heat energy, an expander/turbine to release power by bringing the fluid to a lower pressure level, and a condenser to release the heat from the fluid. In a Rankine cycle evaporator/boiler is usually a heat exchanger that operates at a constant level of evaporating pressure. Fig. 1.20 shows configuration of a Rankine cycle system [20].

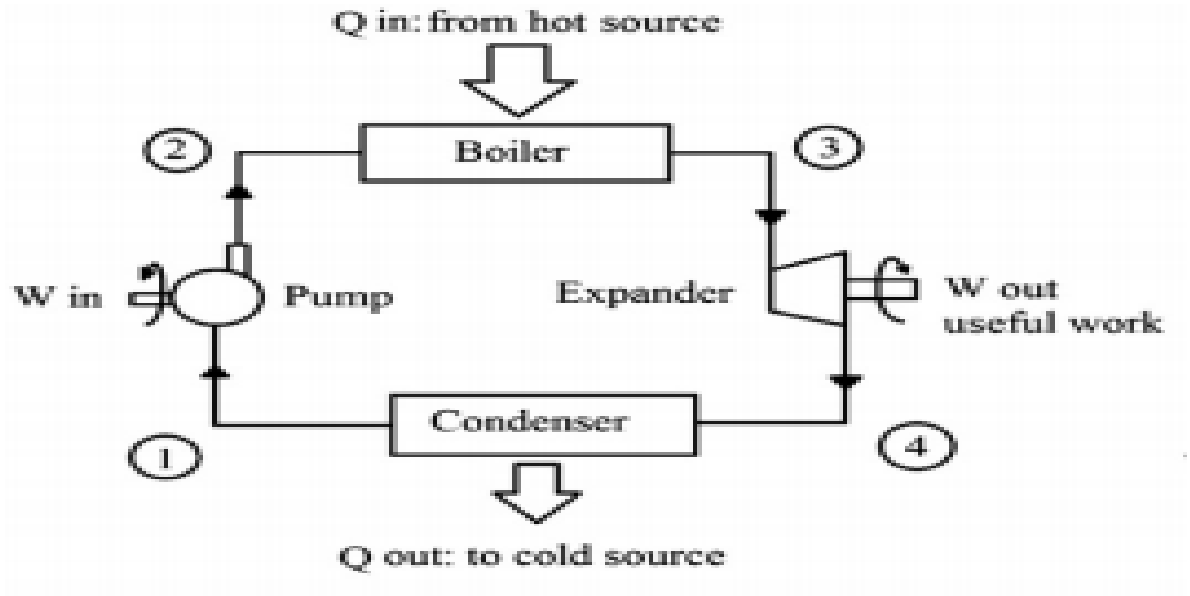

Fig. 1.20: Simple Rankine Cycle System [20]

1.3.2.2 Organic Rankine Cycle (ORC)

The organic Rankine cycle applies the principles of the steam Rankine cycle but the basic difference is the working fluid. In a simple Rankine cycle the working fluid is water/steam but ORC utilizes organic fluid such as benzene, toluene, p-xylene, R113 and R123 with low

boiling points [21]. It can be said that efficiency of cycle is greatly dependent on the selection of working fluid and operating conditions. The cycle consists of an expansion turbine, a condenser, a pump, a boiler and a super heater, if needed (as shown in Fig.1.21) [21].

However, the efficiency of ORC would vary according to different types of working fluids and heat source. It has been mentioned that for simple Rankine cycle working fluid is wet fluid i.e. liquid and for ORC working fluid is organic i.e. dry and isentropic. Thus working fluid can be classified as a dry, isentropic, or wet fluid depending on the slope of the saturation vapor curve on a T-S diagram (dT/ds), ds/dt is used to express how dry or wet a fluid is, because dT/ds leads to infinity for isentropic fluids. Since, Q = ds/dT, the type of working fluid can be classified by the value of Q i.e. Q > 0 a dry fluid, Q = 0 an isotropic fluid and Q < 0 a wet fluid. Fig 1.22 show the three types of fluids in a T-S diagram [22]. Liu et al. [23] derived an expression to determine Q, which is:

$$Q = \frac{C_p}{T_H} - \frac{\left[\left(n\frac{T_{rH}}{(1-T_{rH})}\right) + 1\right]}{T_H^2}\nabla H_H$$

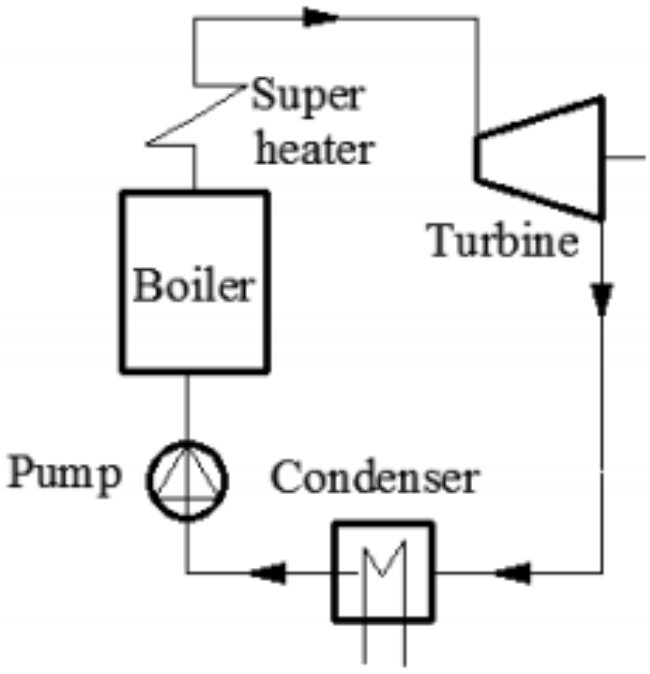

Fig.1.21: A schematic diagram of simple ORC system [21]

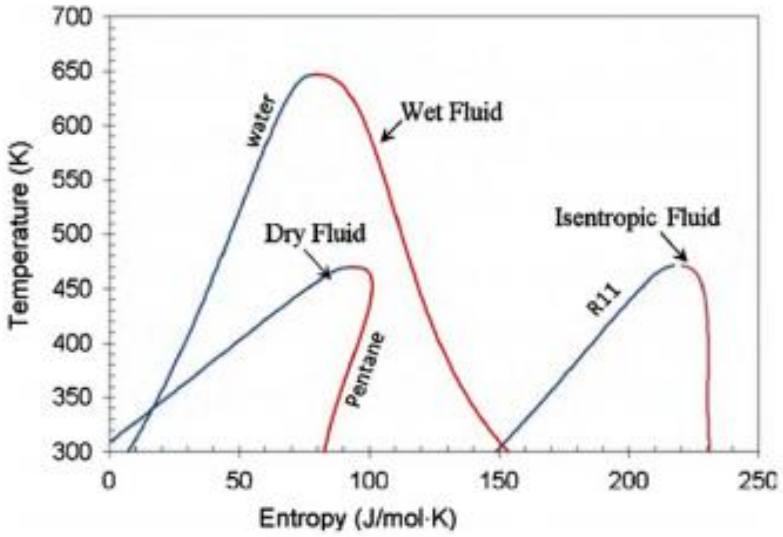

Fig.1.22: T-s diagram for 3 types of working fluids [22]

1.3.2.3 Kalina Cycle

The Kalina cycle is principally a modified Rankine cycle. The Kalina cycle uses a mixture as the working fluid, the mixture being composed of at least two different components, typically water and ammonia. The use of mixture results in a good thermal match in the waste heat boiler, but requires a recuperator after the turbine. This makes the plant more complex. Chen [22] states that Kalina cycle performs substantially better than a steam Rankine cycle. The Kalina cycle can produce 10-30 % more power than a steam Rankine cycle. Smaller size of the whole unit is another advantage of Kalina cycle. One drawback of the Kalina cycle is corrosion. Impurities such as air or carbon dioxide in liquid ammonia may cause stress corrosion cracking of mild steel. Dipippo [24] reported that there have been claims of up to 50% more power output from Kalina cycle as opposed to ORC using the same input from actual operations.

1.3.2.4 Supercritical Rankine cycle using zeotropic mixture

Unlike a conventional organic Rankine cycle, a supercritical Rankine cycle does not go through the two phase region during the heating process. By adopting the zeotropic mixture as working fluid, this cycle can improve the system efficiency. H Chen et al. [25] proposed and analyzed a supercritical Rankine cycle using zeotropic mixture working fluids for the conversion of low grade heat into power. The proposed cycle can achieve thermal efficiency of 10.8 to 13.4 % with the cycle high temperature of 393k - 473k as compare to 9.7 – 10.1 % for the ORC. Figure 1.23 shows the configuration and process of a zeotropic mixture supercritical Rankine cycle. Yamaguchi et al. [26] proposed a super critical CO_2 Rankine

cycle for solar energy production. The system utilizes evacuated solar collector to convert CO_2 into high temperature supercritical fluid, used to drive a turbine and thereby producing mechanical energy & hence electricity as shown in Fig. 1.24.

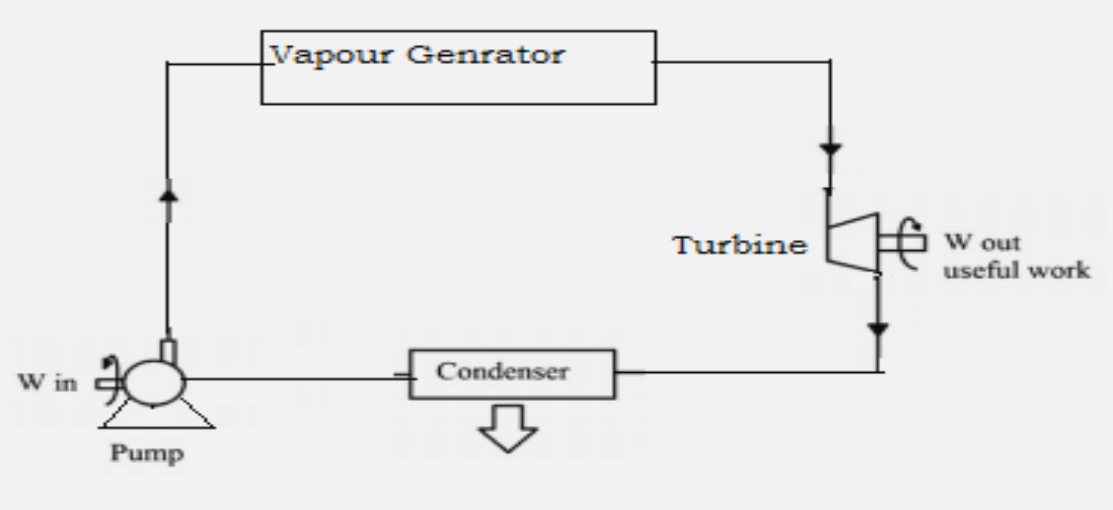

Fig.1.23: Supercritical Rankine Cycle [24]

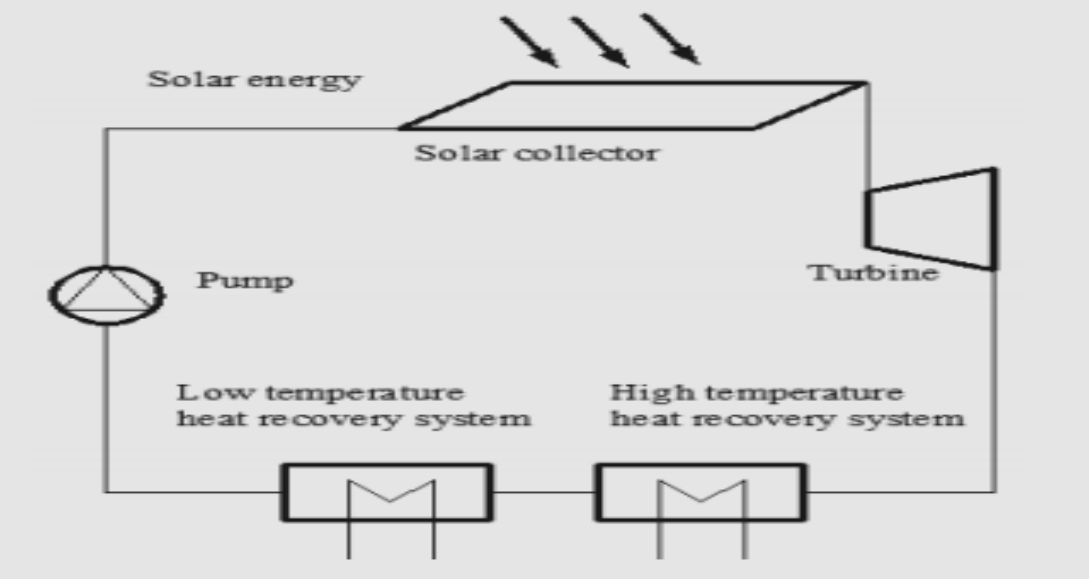

Fig.1.24: The solar operated Rankine cycle [25]

1.3.3 Six stroke internal combustion engines

A typical four stroke cycle involves intake stroke, compression stroke, power or expansion stroke and exhaust stroke. But in a six stroke internal combustion engine, two additional strokes are added that increase the work extracted per unit input of fuel energy. These additional strokes involve trapping & recompression of some of the exhaust from the fourth stroke, followed by a water injection and expansion of the resulting steam exhaust mixture. Energy from the trapped recompression exhaust gases is transferred to the liquid water, causing it to vaporize & increase the pressure. This added pressure then produce more work from another expansion process [27]. In six strokes internal combustion engine more work can be produced without any extra fuel injected into the cylinder, thus improving fuel economy of the engine. There are many patents awarded for designs of six stroke engine which are discussed in references [28 - 35]. Conklin and Szybist [27] believe that an engine cycle that utilizes water injection to absorb the heat directly from the exhaust gas is more practical than using the combustion chamber surfaces as the primary heat source.

1.3.4 Cogeneration and Tri generation technologies

Cogeneration and Tri generation technologies have emerged as the most effective techniques for achieving the goal of energy conservation and sustainability. In cogeneration system, most of the electric and heating demands are met simultaneously by a prime mover along with a heat recovery system, a heat storage system, etc. as shown in Fig.1.25.This is also known as combine heating and power (CHP) system. If some thermally activated technology is added to a CHP system to provide cooling effect, then the system is called a tri-generation system as shown in Fig. 1.26. This is also known as combined cooling, heating, and power (CCHP) system.

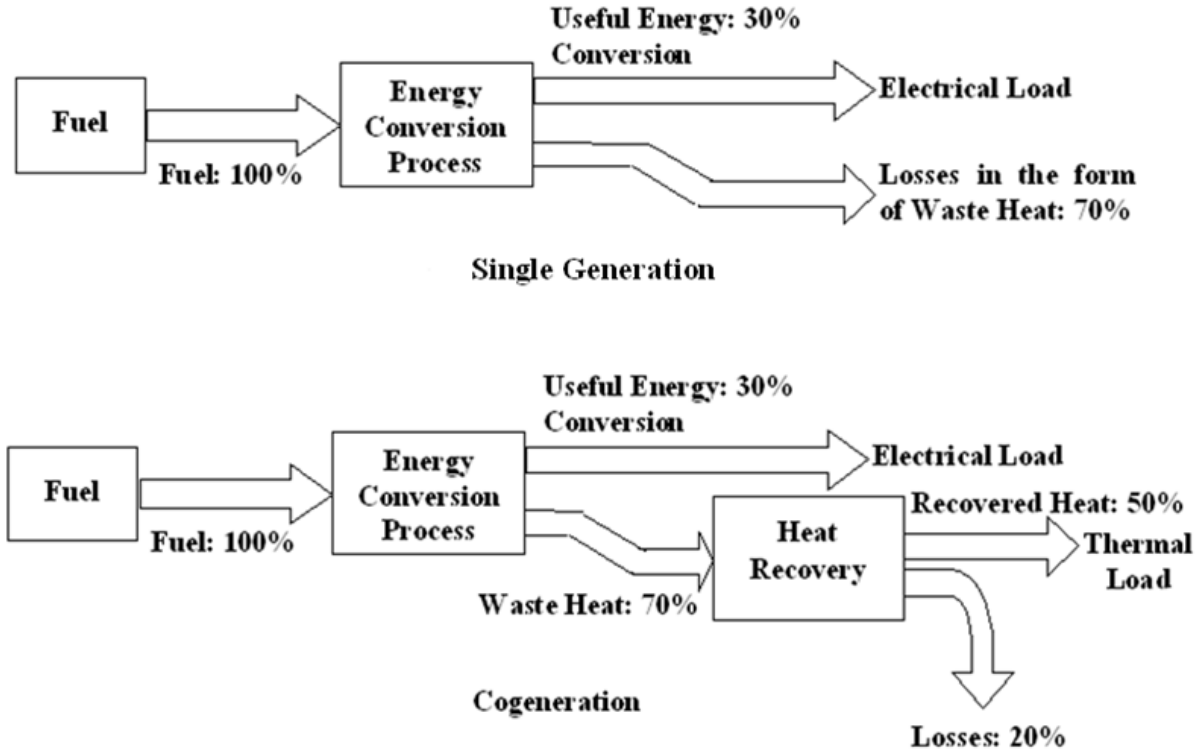

Fig. 1.25: Single Generation vs. Cogeneration [36]

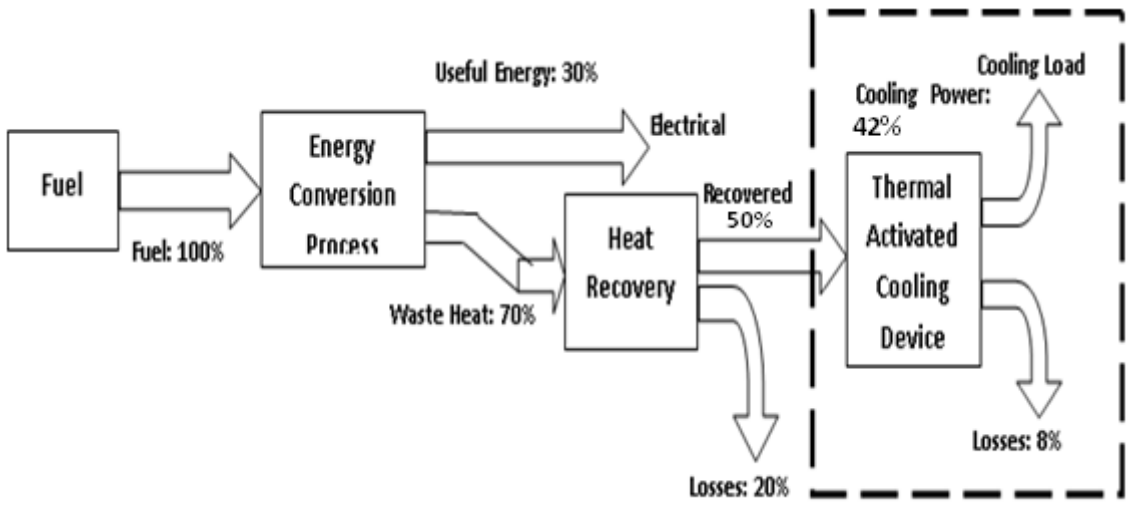

Fig. 1.26: Extending Cogeneration to Tri-generation [36]

Tri generation system requires a prime mover for producing mechanical or electrical power, a heat recovery device for heating and a thermally activated component for cooling or refrigeration. Tri-generation is one form of "Eco Generation." Eco Generation is defined as the optimization of economic and ecological benefits in the power generation process. Eco

generation produces huge savings for our environment through the reduction, or even elimination of pollution associated with power and energy generation. Eco generation of power and energy through an onsite tri-generation system is a sustainable energy system that benefits our environment in the short term as well as long term duration. Tri-generation system is the best technology available for reducing greenhouse gas emissions and other pollutants found in a typical power plant. It also is a means for conserving fuel and reducing our reliance on imported oil and energy supplies. Tri-generation system is accepted as the most energy efficient means of producing electricity. By implementing the heat recovery system, the CCHP system can collect the byproduct heat to feed the absorption/adsorption chillers and heating unit to provide cooling & heating energy respectively. No additional electricity needs to be purchased from the local grid to drive the electric chillers in summer but only the recovered heat is used. In winter, a CCHP system degenerates to a CHP system. The other benefit by the CCHP system is the reliability [36]. Reliability can be regarded as the ability of an energy system to secure the energy supply at a reasonable price. The CCHP system, which adopts the distributed energy technologies, can be resistant to external risks and has no electricity blackouts, because of its independency on electricity distribution. With the benefits of high system & economic efficiency and less GHG emissions, CCHP systems have been widely used in commercial sector as well as in industrial sector. Commercial sector utilizing tri-generation techniques include office buildings, hospitals, hotels, educational buildings, super markets, etc. The applications of tri-generation in industrial sector are widespread in chemical process industry, food processing, paper manufacturing, metal industry, etc.

Hence, in light of the above methods to conserve energy in internal combustion engines, this research work focused on analysis of cogeneration and tri-generation system for utilization of engine waste heat for heating and cooling purposes.

CHAPTER 2
LITERATURE REVIEW

Cogeneration and Trigeneration systems are proven technologies for efficient utilization of waste heat. Trigeneration systems require a prime mover for producing mechanical or electrical power, a heat recovery device for heating and a thermally activated component for cooling or refrigeration. The devices necessary for making a trigeneration system are described as follows:

2.1Prime movers

Prime movers obviously play the most crucial role in energy generation/conversion, they are the keystones of CCHP systems and to some extent. The qualities of good prime movers are low noise and vibrations, low maintenance, small size and low weight, reliable and simple operation, easy installation and low capital cost [37, 38]. Therefore, selecting a prime mover of a tri- generation plant is of major concern. Examples of the prime mover types are internal combustion engines, external combustion engines (Stirling engines), steam turbines, gas turbines and fuel cells.

2.1.1Internal Combustion Engine

There are two types of internal combustion engines currently in use. One is compression ignition (C.I.) engine running on diesel as well as other petroleum products, such as heavy fuel oil or biodiesel, vegetable oils, etc. Other is spark ignition (S.I.) engine running on natural gas, petrol, etc. Both these engine types are suited to CHP / CCHP systems, since the electrical output of a typical engine generating set is around 30 % of the fuel input, the rest being lost as waste heat, around 50 % of which is recoverable. Reciprocating engines are a proven technology, with a range of size and the lowest first capital costs, for all CHP / CCHP systems. In addition to the fast start up capability and good operational reliability, high efficiency at partial load operation gives the users a flexible power source, allowing for a range of different energy applications especially as emergency or standby power supply. Reciprocating engines are by far the most commonly used power generation equipments under 1 MW.

IC engines have some drawbacks e.g., high vibrations, more noise, frequent maintenance requirement, and short life [39, 40].Despite the limitations of IC engines as described earlier, they have a lot of advantages as well for using them as prime movers for trigeneration

systems. IC engines are inexpensive and reliable. The technology is mature and it has low operating cost, ease of maintenance, and wide service infrastructure. Many remote communities currently use these engines as their only source of electricity. Presently, the IC engines are the most widely used prime movers for trigeneration applications.

2.1.2Ranking cycle (RC) engine and micro gas turbines

The Ranking cycle systems are in the order of MW or above, but some small scale systems have capacity as low as 50 kWe [41]. The RC for micro CHP is less expensive than most other prime mover technologies. RC engines are not available in market as part of micro CHP systems and hence, sufficient data is not available to really evaluate this promising technology [41].

The major disadvantage of the RC engines is that the efficiency is quite low (around 10%). Micro gas turbines are small gas turbines up to an electric power output of 300 kWe [41]. The electric capacity of current micro-turbines, usually 25 kW or above, is too high to be in a residential micro-CHP unit. Research is ongoing for systems with capacities less than 25 kW, e.g. 1 and 10 kW which will be suitable for the single-family residential buildings [42, 43].Micro turbines offer a number of advantages to reciprocating internal combustion engines such as: fast response, compact size, low noise, low weight, and low NO_X emissions. Micro turbines can use natural gas, hydrogen, propane or diesel and other bio based liquid and gas fuels.

The high cost and relatively shorter life are the major disadvantages of this technology. The efficiency of micro turbines is not very high, although this is enough for residential micro CHP because of the high thermal/electric load ratio [44].

2.1.3 Stirling Engine

A Stirling engine is an external combustion engine, where combustion of the fuel takes place in an external boiler. Stirling engines can be used for primary power generation and as a bottoming cycle utilizing waste heat for power generation. Stirling engine can use low temperature energy sources since these engines have an ability to work at low temperatures. Stirling engine can also use all fossil fuels and biomass, to realize an environment friendly electricity production [41]. The noise and maintenance of the Stirling engine is lower than that of the IC engines. The combustion can be controlled relatively easily and the emissions are low. There are two main types of Stirling engines: kinematic Stirling engine and free-piston Stirling engine [45]. The major disadvantages of Stirling engines are their high cost

and lesser durability of certain parts, and also, that the engine needs a few minutes to warm up.

The Stirling engines are 15-30% efficient in converting heat energy to electricity. The total efficiency of a micro CHP with Stirling engine is 40% [46]. Stirling engine technology is still in its primitive stage and so no statistical data is available.

2.1.4 Fuel cell

Fuel cells are electrochemical energy converters similar to primary batteries [47, 48]. Fuel cell micro-CHP systems are either based on the low temperature proton exchange membrane fuel cell (PEMFC) which operate at about 80^0C, or are based on the high temperature solid oxide fuel cells (SOFC) working at around 800-1000^0C. Size range for PEMFC is 3-250 kW and for SOFC it is 1-10 MW [47, 49].

Fuel cells normally run on hydrogen, but can also be used with natural gas or other fuels by external or internal reforming [47]. Fuel cells have several benefits: higher efficiency (up to 60% electric), emissions are essentially absent producing negligible amounts of pollution, fuel cells are very quiet [47, 49, 42, 50]. Fuel cells are still in the R&D stage [51]. The major problem of fuel cells is the short lifetime of the membrane and their high cost [47, 50]. There are no fuel cell based micro-CHP systems commercially available at this moment [47].

Major parameters and performance of theses prime movers are shown in Table 2.1:

Table-2.1: Characteristics & performance of Prime Movers in CCHP System [52-57]

	Steam Turbines	**Diesel Engines**	**Spark Ignition Engines**	**Micro-turbines**	**Stirling Engines**	**Fuel Cells**
Capacity Range	50 kW-500 MW	5 kW-20 MW	3 kW-6 kW	15kW-300 kW	1 kW-1.5 MW	5 kW-2 MW
Fuel used	Any	Gas, propane, distillate oils, biogas	Gas, biogas, liquid fuels, propane	Gas, propane, distilled oils, biogas	Any (Gas, alcohol, butane, biogas)	Hydrogen and fuels containing hydrocarbons
Electrical efficiency (%)	7-20	35-45	25-43	15-30	~40	37-60
Overall efficiency (%)	60-80	65-90	70-92	60-85	65-85	85-90
Power to heat ratio	0.1-0.5	0.8-2.4	0.5-0.7	1.2-1.7	1.2-1.7	0.8-1.1
Exhaust Temperature (^{o}C)	Up to 540	A	A	200-350[b]	60-200	260-370
Noise	Loud	Loud	Loud	Fair	Fair	Quiet
CO_2 emission (kg/MWh)	C	650	500-620	720	672[d]	430-490
NO_X (kg/MWh)	C	10	0.2-1.0	0.1	0.23[d]	0.005-0.01

Availability (%)	90-95	95	95	98	N/A	90-95
Part load performance	Poor	Good	Good	Fair	Good	Good
Life cycle (Year)	25-35	20	20	10	10	10-20
Initial cost (dollar/kW)	1000-2000	340-1000	800-1600	900-1500	1300-2000	2500-3500
Operating and maintenance cost (dollar/kWh)	0.004	0.0075-0.015	0.0075-0.015	0.01-0.02	N/A	0.007-0.05

a- Up to a third of the fuel energy is available in the exhaust at temperatures from 370 to 540^{o}C; other rejected heat is low temperature, often too low for most processes (jacket cooling water at 80-95^{o}C, lubricating oil at 70^{o}C and intercooler heat rejection at 60^{o}C, none is good for use in CHP).

b- 650^{o}C without recuperator.

c- Emissions associated with a steam turbine are dependent on the source of the steam. Steam turbines can be used with a boiler firing any one or a combination of a large variety of fuel sources, or they can be used with a gas turbine in a combined cycle configuration. Boiler emissions vary depending on fuel type and environmental conditions.

d- Stirling engine emission characteristics / STM 4-260. Gas-fired distributed energy resource technology.

2.2 Thermally activated cooling

An important difference between cogeneration (CHP) systems and conventional systems (single generation – power only) is that CHP systems also include some heat recovery device like heat exchangers. Whereas, the important difference between tri-generation (CCHP) systems and conventional systems is that CCHP systems include some cooling components (in addition to heat recovery device) as well. The methods for producing cooling effect utilizing a heat source are called thermally activated cooling technologies. Thermally activated cooling technologies can be classified into heat transformation processes and thermo mechanical processes. The heat transformation processes are the most developed and used systems in which sorption cooling is dominated. Sorption may contain both absorption and adsorption: absorption is the process in which a substance in one phase is incorporated into another substance of a different phase (e.g. gases being absorbed by a liquid); adsorption refers to the use of a solid to adhere the molecules of another substance onto its surface.

Both absorption and adsorption are used to facilitate thermal compression of the refrigerant. Evaporation and sorption of a refrigerant generates a useful cooling effect in the evaporator. The main differences between adsorption and absorption are in the nature of the sorbent and the duration of the sorption cycle [58].

Thermally activated cooling systems have their own suitable working temperatures and hence, the real success of a CCHP system depends on the perfection of the match between the thermally activated cooling technologies and the prime movers. Absorption chillers can be divided into single effect, double effect and triple effect depending on the number of times the supplied heat is utilized within the chillers. E.g. if power source is gas turbine then since the heat source temperature is at 540^{o}C, the thermally activated cooling technology can be triple effect or double effect absorption system. Similarly for micro turbine and Stirling engine, the temperature of heat source is 320^{o}C & 90^{o}C respectively and thermally activated cooling for both micro turbine & Stirling engine are single effect absorption system. If SOFC & PEMFC fuel cells are used as prime movers in tri-generation system, then heat source temperature is 480^{o}C & 60^{o}C respectively and thermally activated cooling technology can be triple effect absorption system and desiccant cooling technologies respectively. For an IC engine as a prime mover providing exhaust gas temperature of 90^{o}C, single effect absorption is matching technology for cooling [59].

Amongst the technologies for thermally activated cooling, lithium bromide water absorption systems has been widely adopted as it is the most common and efficient method for air conditioning applications. Water ammonia vapor absorption machines are the most commonly used system for small sized residential or large capacity industrial refrigeration applications. Silica gel water adsorption system is widely used for commercial air-conditioning / refrigeration currently [60]. Areas where dehumidification is important, solid desiccant or liquid desiccant cooling is applied [61].

2.2.1 Absorption chiller using lithium bromide water

The most common working pairs in absorption refrigeration systems are lithium bromide-water and water-ammonia systems. The lithium bromide-water pair is widely used for air conditioning applications, with evaporation temperatures of about 5-10^{o}C; while the water-ammonia pair is mostly used when evaporation temperatures are below 0^{o}C. The basic principle of a lithium bromide-water single effect absorption chiller is shown in Fig. 2.1, which is the simplest and most commonly used design. In the absorption cycle, compressing refrigerant vapor is achieved by the combination of absorber, the pump and the generator. Water evaporated from evaporator (which outputs a cooling effect) is absorbed into a strong lithium bromide solution in the absorber, and the absorption process releases the heat of absorption to the atmosphere. After absorbing the water vapor, the lithium bromide solution becomes a weak solution which is then pumped to the generator. When heat is added to the generator using an external source, water will be desorbed from the solution in a vapor form. The vapor flows to the condenser, where it is liquefied and heat is rejected to the atmosphere. The pressure is reduced when the condensed water flows through the expansion device. The strong lithium bromide solution from the generator is then fed back to the absorber to absorb water vapor again. The entire cycle operates below atmospheric pressure, since water is used as the refrigerant.

The parameters & characteristics of LiBr–H_2O absorption chillers are as follows: the heat source temperature range for single effect, double effect & triple effect systems are 80-120^{o}C, 120-170^{o}C & 200-230^{o}C respectively. The COP range for LiBr–H_2O absorption technology is 0.5-0.7 for single effect, 1-1.2 for double effect and 1.4 -1.7 for triple effect. Cooling capacity varies from 35-7000 kW in single effect, 20-11630 kW in double effect, and 530-1400 kW in triple effect [60, 62, 63].

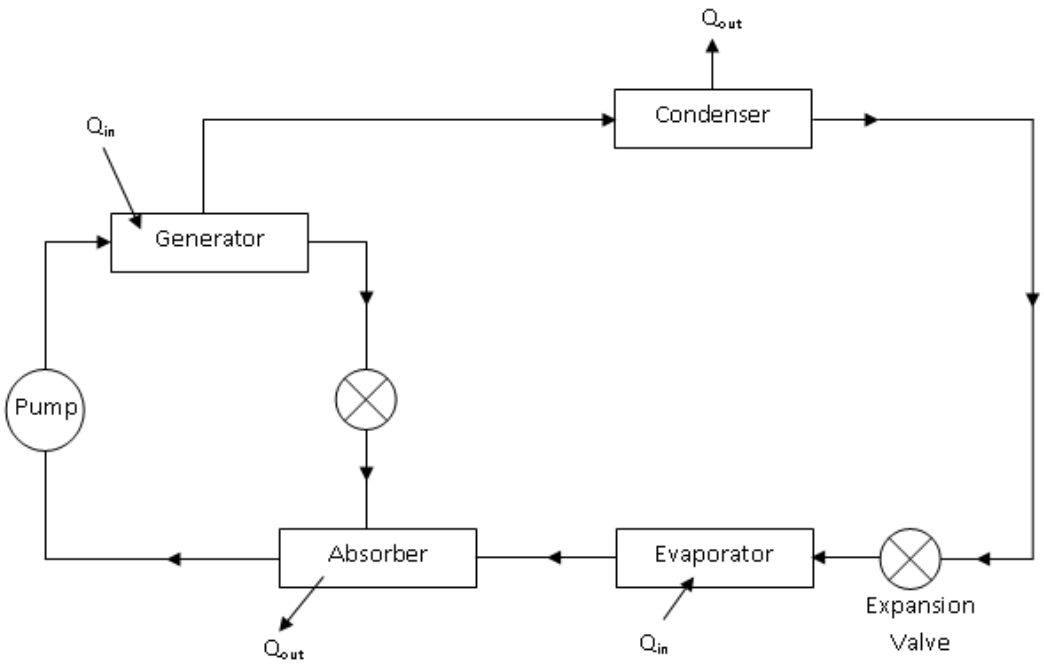

Fig.2.1: Basic single-effect LiBr-H2O absorption cycle

There are three main problems for lithium bromide-water absorption chillers: first is the corrosion due to Li-Br solution at higher temperatures. If this problem could be satisfactorily resolved, triple-effect Li-Br solution absorption chillers could be widely used. Second is the operation at vacuum pressures between 0.8 and 20 kPa , which could be a problem if the chiller is not well sealed. The third problem is the narrow concentration range of lithium bromide-water solution, which is limited by crystallization. Other problems are the high initial cost of absorption chillers especially for small residential use.

2.2.2 Absorption chiller using water-ammonia

The water-ammonia system is the oldest sorption refrigeration technology, but until recent times it was applied, primarily to large industrial refrigeration only, e.g. cold storage process for frozen food. The basic absorption cycle, and generator-absorber exchanger (GAX) absorption cycle, of a single-effect water-ammonia system are shown in Fig. 2.2 & 2.3 respectively, where the absorbent is water and the refrigerant is ammonia. Each system includes four main components: the generator (including the rectifier), the condenser, the evaporator and the absorber. A pump may or may not be used before the generator.

The rich solution of ammonia as solute in water is heated in the generator at about 100-120^{o}C to separate most of the ammonia in the form of vapor resulting in a weaker ammonia-water solution left behind. The ammonia vapor is then condensed to liquid ammonia in the condenser before

passing it through the throttle valve. Then the (vapor – liquid) mist of ammonia is evaporated in the evaporator, where the cooling effect is produced primarily due to the latent heat of vaporization. The evaporated ammonia is then absorbed by the weak solution coming back from the generator, to become a rich solution again. Now the rich solution is sent into the generator by a pump. Since both ammonia and water are volatile, the cycle requires an extra component called a rectifier to purify ammonia (separation from water vapor). Since ammonia has a lower vaporization temperature than water, rectification is necessary. COP of basic water-ammonia cycle is lower than that of lithium bromide-water cycle.

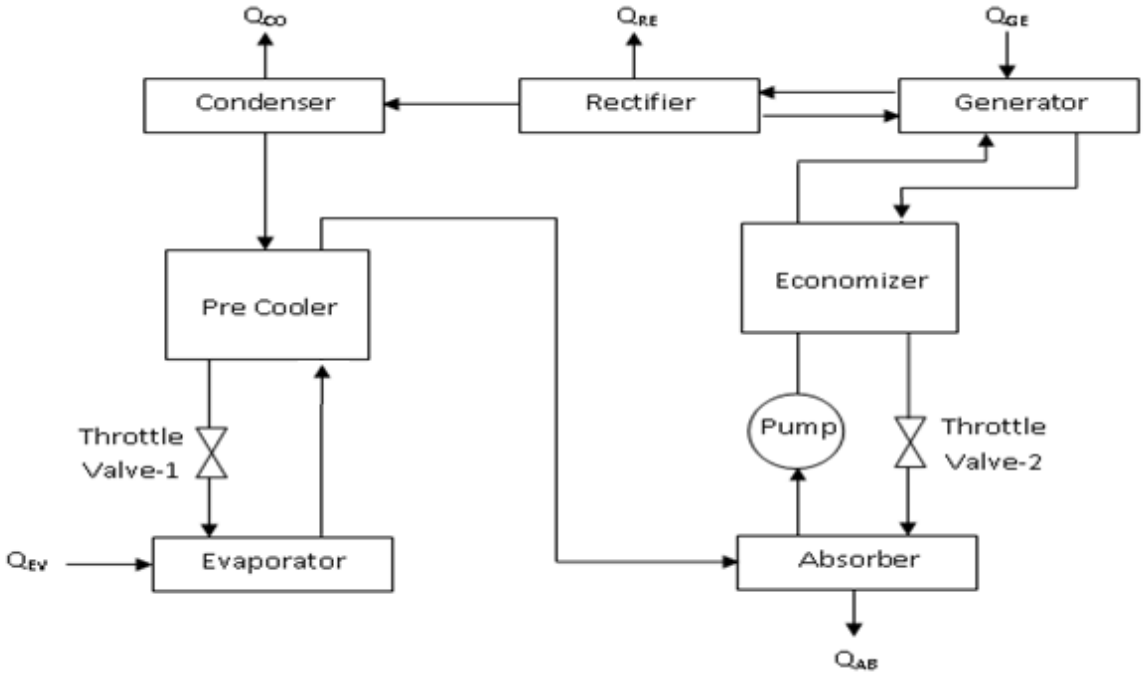

Fig.2.2: Working principle of single-effect water-ammonia absorption chillers: basic absorption cycle

The GAX system requires higher heat source temperatures (180-200^{o}C). In the GAX absorption cycle, there is a big concentration difference between the rich solution and the weak solution. It is possible that the temperature at some part of the absorber is even higher than the temperature of the generator; hence, an extra internal heat recovery sub-cycle may be added to use some of the heat of absorber to raise the temperature of generator. By adding this heat recovery sub-cycle, the thermal energy needed at generator is greatly reduced and hence, the COP_{th} is increased by 30% approx. [64, 65].

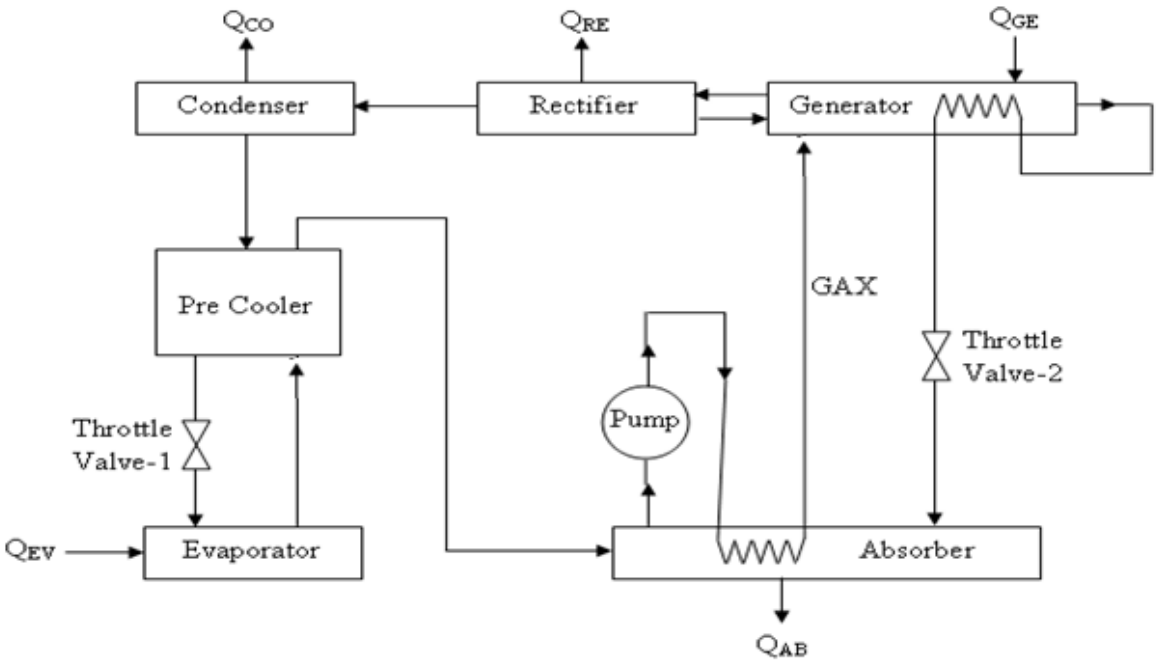

Fig.2.3: Working principle of single-effect water-ammonia absorption chillers: GAX absorption cycle

The advantages of water ammonia chillers over the more common lithium bromide-water systems are: a low freezing point of ammonia (–77.7^{o}C), resulting in lower refrigeration temperatures; with a low specific volume, making the unit more compact; and problem-free crystallization. The disadvantages of the water-ammonia system include the high operation pressure (1.5-2.0 MPa), which could cause the system to act as a pressure vessel, requiring strict safety precautions [68].

The parameters and characteristics of conventional water-ammonia absorption chillers are summarized as follows: for the single effect water ammonia absorption technologies, the heat source temperature is 100-200^{o}C and for GAX it varies from 160-200^{o}C. The cooling capacity for the single effect water ammonia absorption technology varies from 10 to 6500 kW and for GAX it varies from 10 to 90 kW. COP for the single effect water ammonia absorption technology ranges from 0.25 to 0.6 whereas, in case of GAX, it is more than 0.7 [62,66,67].

2.2.3Adsorption chiller

There are two types of adsorption refrigeration working pairs: (1) physical adsorption working pairs, such as zeolite -water, activated carbon-methanol, activated carbon-ammonia and silica gel-water; (2) chemical adsorption working pairs, which are mainly metal hydride-hydrogen and metal chloride-Ammonia (e.g. $CaCl_2$, LiCl, etc. with NH_3).

The basic cycle of adsorption refrigeration schematically is shown in Fig. 2.4 (a). During the adsorbent desorption process, the valve between the adsorber and the condenser is opened while the other valve is closed resulting in condensation of refrigerant in the condenser and heat is released to the environment. After the desorption process, the adsorber is connected to the evaporator through the valve. Then the adsorption process generates the cooling effect in the evaporator due to the evaporation of refrigerant. In basic adsorption refrigeration system the cooling power output is intermittent but for continuous output, two adsorbers, one condenser and one evaporator should be adopted, as illustrated in Fig. 2.4 (b). Thus, at least four valves should be employed in an adsorption chiller. Since a mass recovery process could greatly improve the performance of an adsorption refrigeration system, the two adsorbers could be connected with a valve and significant improvement of the COP_{th} could be achieved. In addition, heat recovery between the two beds should be considered to improve the COP_{th}.

(a)

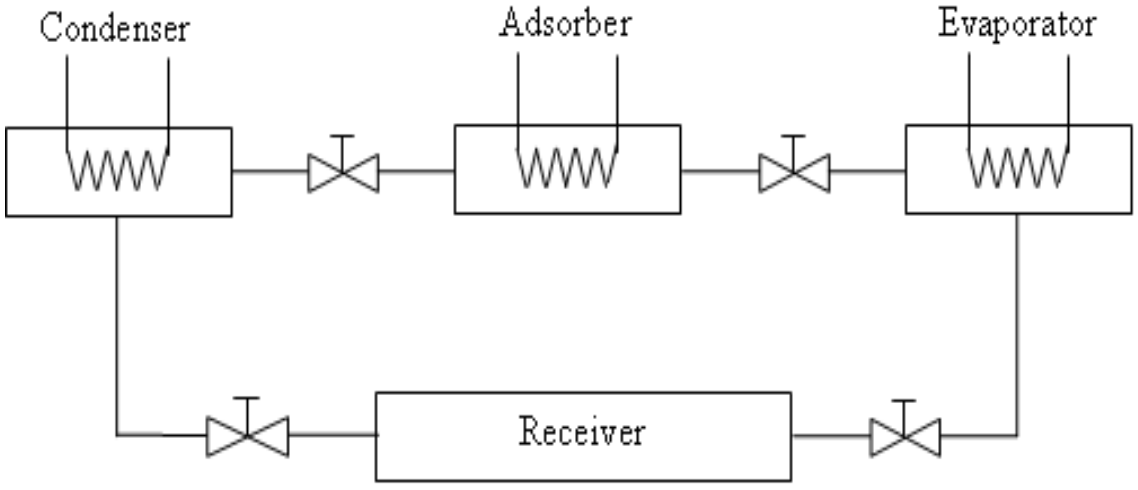

(b)

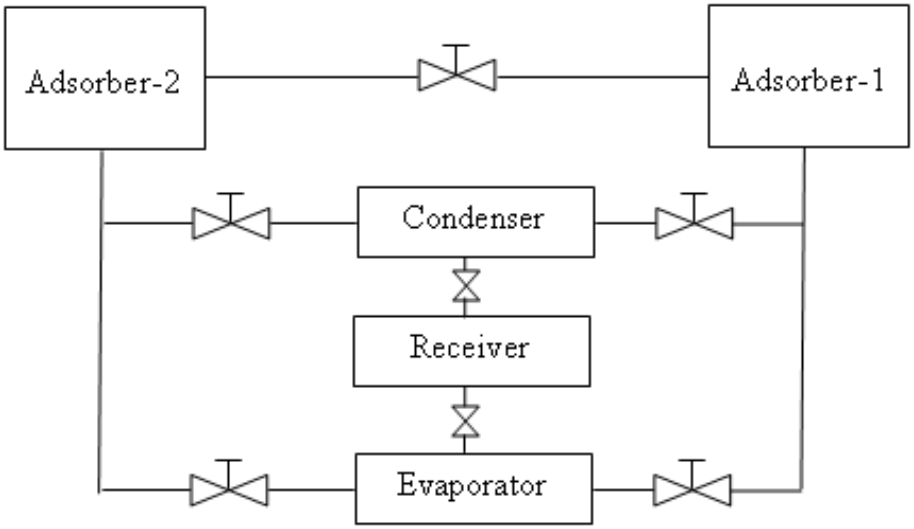

Fig. 2.4: Conventional adsorption refrigeration systems: (a) basic adsorption refrigeration system; (b) continuous adsorption refrigeration system

There are three main problems in adsorption refrigeration technology, one is the low thermal conductivity of the adsorbent; the second is the relatively low cycle mass of the working pair, and desorption phase is low; the third is that the heat exchanger cannot be applied to the adsorption cycle which limits the effective utilization of heat. These problems lead to low COP_{th} (0.4-0.5) and large volume of the chiller. The initial cost of the adsorption refrigeration system is high. If water or methanol is used as the refrigerant then operation at vacuum conditions may pose another maintenance problem [68].

2.2.4 Desiccant dehumidifiers

The desiccant process involves exposing the desiccant material (such as silica gel, activated alumina, lithium chloride salt or molecular sieves) to a moisture-laden process air stream, retaining the moisture of the air in desiccant and regenerating desiccant material via a heated air stream. Dehumidification technology is divided into two major types, solid desiccant dehumidifiers and liquid desiccant dehumidifiers; both are useful for the mitigation of indoor environmental quality and health problems and for humidity control in buildings. Liquid desiccant technologies—particularly those with air washing and biocide capabilities— are viewed as a critical path towards ensuring indoor environmental security under extraordinary circumstances and reducing indoor air pollution in general [69].

2.3 Heating Purpose

The heating technologies for trigeneration consist of the waste heat recovery from engine cooling system or from exhaust gases. The waste heat may be utilized for heating purpose like space heating, hot water production, preheating intake air and fuel, dryer, etc. Typical examples of use would be preheating of combustion air, space heating, or pre-heating of boiler feed water or process water, etc. There are various types of heat recovery devices available in the market. The common commercially available heat recovery equipments are recuperators, regenerators, heat wheels, heat pipes, shell and tube type heat exchangers, plate heat exchangers, run around coil heat exchangers, waste heat boilers, heat pumps and thermo compressors. The simplest configuration for a recuperator is the metallic radiation recuperator. A second common configuration for recuperators is called the tube type or convective recuperator. For maximum effectiveness of heat transfer, combination of radiation and convective design is used. These are more expensive than simple metallic radiation recuperators, but are less bulky. The principal limitation of metal recuperators is the reduced life of the liner at inlet temperatures exceeding 1100°C. In order to overcome the temperature limitations of metal recuperators, ceramic tube recuperators have been developed since these allow operation on the gas side at up to 1550°C and on the preheated air side at up to 815°C.The regenerator which has been widely used in glass and steel melting furnaces may be used as a waste heat recovery device. A heat wheel is finding increasing applications in low to medium temperature waste heat recovery systems. Its main area of application is where heat transfer is required between large masses of air having small temperature difference. Heat pipe exchanger is light weight compact waste heat recovery equipment, in which there are no moving parts to wear out and so, no need for mechanical maintenance. The main application of heat pipe exchanger is space heating. Run around coil exchanger is quite similar in principle to the heat pipe exchanger. The heat from hot fluid is transferred to the colder fluid via an intermediate fluid known as the heat transfer fluid. One coil of this closed loop is installed in the hot stream while the other is in the cold stream. Circulation of this fluid is maintained by means of circulating pump. The typical industrial applications of run around coil exchanger are ventilation, air conditioning and low temperature heat recovery.

In most micro-trigeneration applications, heat recovery is accomplished by ducting the exhaust gas from a prime mover to a heat exchanger to capture the thermal energy in the gas

stream. Generally, these heat exchangers are air-to-water heat exchangers, where the exhaust gas flows over a fin-tube heat exchanger surface and the heat is used to produce hot water, or in some cases, steam. For prime movers that include a cooling jacket which circulates engine coolant, a liquid-to-liquid heat exchanger can also be used to recover waste heat for hot water production. Depending on the amount of waste heat available and the emission concentration of the prime mover, air-to-air heat exchangers can be used for space heating of a building. If the house uses forced air heating, air will be heated by hot water coil. If a hydronic heating system is used, the hot water from the heat recovery equipment may be used directly.

2.4 Existing work in the field of micro trigeneration system

In terms of rated size, CCHP applications are categorized into micro, small, medium & large systems for the size range of less than 20 kW, from 20 kW to 1MW, from 1MW to 10 MW & more than 10 MW respectively [70, 71].From the research outcomes worldwide, different heat and power generating technologies have been considered as prime movers for trigeneration applications. These technologies could be divided into two categories, combustion based technologies and electro-mechanical based technologies. Stirling engine, gas turbine, Rankine cycle & reciprocating engines are combustion based technologies while fuel cells are based on electro-mechanical technology. Table 2.1 shows that reciprocating engines are better than other prime movers on techno-economic and market parameters. Reciprocating engines and gas turbine are commercially mature and widely available in the market whereas other prime movers are still in research and development stage. Prime mover drives a generator which produces electrical power. The waste heat from the prime mover is recovered and used to drive thermally activated components such as an absorption/adsorption chiller or desiccant dehumidifier, and to produce hot water, steam, warm air or other heated fluid through the use of heat exchangers. Various studies reporting either on the basis of real life installed systems such as hospitals [72], factories [73, 74], educational buildings [75], supermarkets [76] and hotels [77], or computer operated simulations have already shown the feasibility of tri-generation systems in excess of 50 kW [78]. The new frontier of tri-generation is in the residential and small commercial building sector. Applying tri-generation technology to small residential and small commercial buildings is an attractive option because of the large market potential. This section presents outcome of existing research on real life experimental models and the theoretically modeling techniques for IC engine operated micro trigeneration systems.

G. Angrisani et al. [79] carried out an experimental study at the Built Environment Control Laboratory of Seconda University, Italy. In the laboratory, a natural gas fuelled reciprocating I .C. engine was coupled with a thermal chemical absorption (T.C.A.) system and both micro cogeneration system and micro trigeneration system were experimentally investigated. The experimental data was analyzed from energy, economic and environmental point of view and the performance of the proposed system was compared with the conventional system. It was shown that the system produces 5.4 kWe allowing a reduction of 26% on CO_2 emissions and 30% on the operating cost.

Giovanni A.et al. [80] simulated the performance of micro trigeneration system which consisted of heat led micro-cogenerator with a desiccant based cooling system, equipped with a silica gel desiccant wheel. Simulation was performed using TRNSYS software to compare the thermal and economic performance of the system. A sensitivity analysis was performed on the proposed system to analyze total energy recovered depending on the share of cogenerated electricity.

Simon Paul Borg et al. [81] presented the results of high resolution performance analysis of micro trigeneration system in an energy efficient residential building under varying operating conditions. The whole building simulation tool was used to assess the performance of a grid connected micro trigeneration system. The combined deterministic and sensitivity methodology was adapted to study the effect. The results indicated that the use of residential micro trigeneration system reduces primary energy consumption by about 40% compared to that of single generation system.

Jian Deng et al. [82] analyzed a micro-trigeneration system using the exergy cost analysis method based on the structural theory of thermo-economics. The results reflected that structural theory of thermo-economics is a systematic and efficient tool that provides in depth information related to costs and efficiency of energy conversion processes.

J.Y.Wu et al. [83] experimentally investigated the micro-CCHP system which mainly consisted of an I. C. engine with a rated electrical output of 16 kW, an adsorption chiller, and a thermal management controller. Results show that this system can produce 17.7 kW of heating, 6.5 kW of cooling and 16 kW of electrical output. The primary energy ratio reached 0.765 in CHP mode and 0.56 in CCHP mode.

Y.Huangfu et al. [84] discussed the economic & exergy analysis of micro trigeneration system using a small IC engine with rated electrical power of 12 kW and an adsorption chiller with refrigeration capacity of 9 kW. Economic evaluation showed that the payback period for this micro-CCHP system was only 2.97 years with a very small initial cost. From the exergetic point of view, the electrical efficiency of the gas engine should be enhanced for an improved micro-CCHP system.

J.Godefroy et al. [85] described the design, testing and mathematical modeling of a small trigeneration system based on a gas engine with 5.5 kW electricity output and an ejector cooling system. Analysis showed that an overall efficiency of around 50% could be achieved.

X.Q. Kong et al. [86] described an experimental investigation of performance of a micro CCHP system. In this study, LPG and natural fired gas engine was used as a small generator set driven by a small adsorption chiller, which has a rated electric power of 12 kW, a rated cooling capacity of 9 kW and a rated heating capacity of 28 kW. The result showed that in comparison to large CCHP system, the small CCHP test facility provided better test rig platform for cooling, heating and power generation and micro CCHP system can save more primary energy than the conventional system.

Yaodong Wang et al. [87] examined the performance and emission characteristics of a household size trigeneration system based on a diesel engine generator fuelled with hydrogen and compared it with the performance and emission characteristics of single generation and cogeneration systems using ECLIPSE simulation software. The study showed that use of hydrogen as the fuel to run the domestic micro trigeneration system based on a diesel engine gen set was feasible. Results also indicated that trigeneration system produces zero emissions when fuelled with hydrogen.

Yaodong Wang et al. [88] studied the performance and emission characteristics of a trigeneration system based on a diesel engine generator fuelled with raw jatropha oil and compared it with the performance and emission characteristics of single generation and cogeneration systems using ECLIPSE simulation software. The results from the study showed that the overall efficiency of trigeneration system was higher and CO_2 emissions of trigeneration system were lower than that of single and cogeneration system.

Andre Aleixo Manzela et al. [89] conducted an experimental study of an ammonia water absorption refrigeration system using the exhaust of an internal combustion engine as energy

source. The impact of exhaust gas energy availability and the absorption refrigeration system on engine performance, exhaust emissions, and power economy were evaluated. The engine was tested for 25%, 50%, 75% and wide open throttle valve. The refrigerator reached a steady state temperature between 4^{o}C and 13^{o}C about 3hours after system start up. Exhaust hydrocarbon emissions were higher when the refrigeration system was installed in the engine exhaust, carbon monoxide emissions were reduced, while carbon dioxide concentration remained practically unaltered.

L. Lin et al. [90] had designed and realized in laboratory, a household size trigeneration system based on a small diesel engine - generator set. Experimental tests were carried out to evaluate the performance and emissions of the original single generation system and that of the whole trigeneration system. The test results showed that the total thermal efficiency of trigeneration system reaches up to 67.3% at the engine full load, compared to that of the single generation system at 22.1% only. Within the range of engine loads tested, the total thermal efficiency of trigeneration system varied from 205% to 438% higher than that of the thermal efficiency of single generation. The CO_2 emission per unit of useful energy output (kWh) from trigeneration was 0.401 kg CO_2/kW h at the engine full load, compared to that of 1.22 kg CO_2/kW h from single generation at the same engine load. Within the range of engine loads tested, the reduction of CO_2 emission per unit of trigeneration output (kWh) was from 67.2% to 81.4% compared to those of single generation. The experimental results showed that the innovative small trigeneration is able to generate electricity, produce heat and drive a refrigeration system, simultaneously from a single fuel (diesel) input.

2.5 Research Gap Identification

Due to the increasing energy demand, increasing energy cost, energy supply security and environmental concerns have emphasized the limited resources more effectively, efficiently and wisely. Among the several options, cogeneration and trigeneration are emerging as the fast growing techniques to increase efficiency and reduce emissions in small scale applications. Several researchers have conducted theoretical & experimental investigation on medium and large trigeneration system. Very little work has been done in real life cases for small residential or commercial level especially for space cooling.

Applying trigeneration technology to small scale residential & small commercial building is an attractive option because of large market potential. On the basis mentioned above, we could only find twelve research papers of different researchers on IC engine base Micro-

trigeneration systems. Out of these twelve, seven were on theoretical work and the remaining five involved experimental studies but on large capacity engines. In none of the studies Micro-trigeneration has been tried for space cooling. **No work has been reported on micro trigeneration or micro cogeneration for space cooling purpose.** It was thus proposed to develop a micro trigeneration system using single cylinder CI engine for power, heating, and space cooling. It was envisaged that through this system the efficiency and reliability of the engine can be improved and the GHG emission can be reduced. This system would also find application in rural areas and semi urban areas where power outage hours are long.

2.6 Objectives

Following are major objectives of the proposed research work:

- To develop a real sized micro trigeneration system using single cylinder C.I engine for power, heating and space cooling.
- To analyze performance & emission characteristics of micro trigeneration system developed.
- To experimentally optimize the trigeneration system developed.
- To develop a mathematical model to predict the performance of Micro-trigeneration system for power, heating and space cooling.

2.7 Research Methodology

The work was carried out for design and development of trigeneration system by utilizing the waste heat from the exhaust and engine coolant. The work was divided into the following phases:

- Detailed literature review regarding the CI engines operated micro trigeneration system.
- Compilation of information of formation of design guidelines for trigeneration system.
- Procurement and installation (on the test bed developed for the engine) of a new Kirloskar AV1 water cooled C.I. engine.
- Design, development and installation of load bank, fuel storage system and air box.

- Engine test runs with the developed and modified system for its accuracy, reliability, and durability and leak-proof requirements. Further improvement/modification, wherever required, in the developed system.
- Evaluation and comparison of engine exhaust emission (CO, HC, smoke and NO_x) at various loads.
- Experimental evaluation of engine performance with diesel fuelling, including determination and comparison of various parameters such as thermal efficiency, specific fuel consumption, exhaust gas temperature, etc.
- Selection and modification of the heat exchanger for heating water by utilizing the waste heat of coolant and exhaust gases.
- Design and development of the vapor absorption system for space cooling.
- Fabrication of the cabin for air conditioning.
- Installation of demonstration plant for displaying all stages involved in trigeneration system, on real life scale. This included the engine, heat exchanger, VA system, cabin, etc.
- Insulation of cabin and VA system to achieve optimal performance.
- Experimental evaluation of micro trigeneration system's performance and its comparison with the conventional system (single generation).
- Experimentally optimizing the trigeneration system.
- Modeling of the proposed trigeneration system.
- Documentation of the research work.

CHAPTER 3

EXPERIMENTAL SET UP

3.1 Introduction

Experimental set-up for micro-trigeneration system mainly consisted of a diesel engine coupled with electric dynamometer, a heat exchanger for heating water and a combination of four units of vapor absorption refrigeration system for space cooling. Air box arrangement was used to determine the air flow rate. Fuel supply system consisted of a burette method to measure the volumetric fuel consumption. Rotameter and an analog type water flow meter were mounted in the pipeline to measure the flow rate of water. AVL DiGas 4000 Light 5-Gas Analyzer was used to measure CO, CO_2, HC, NO_x and O_2 in exhaust gas. Smoke percentage in the exhaust gas was measured using AVL 437 smoke meter. The detailed description of the instruments used is discussed in this section.

3.2 Details of experimental set up

3.2.1 Diesel Engine and dynamometer

A Kirloskar make single cylinder diesel engine (AV1) was chosen as the prime mover of the micro-trigeneration system. This engine is stationary single cylinder 4-stroke constant speed water cooled direct injection diesel engine. The detailed specifications of the engine are listed in Table 3.1.

A diesel engine was chosen as a prime mover for this study because it has a lot of advantages. I.C. Engine is inexpensive and reliable. The technology is mature and it has low operating cost, high ease of maintenance and wide service infrastructure. Another reason for choosing diesel engine as a prime mover in tri-generation system is the easy availability of engine. It is the most versatile engine widely used for agricultural purpose as well as for electricity generation in India.

Power star make electric dynamometer was used to determine the brake power. It consisted of an alternator to which electric bulbs were connected to apply load. The load was varied by switching on the desired number of electric bulbs. The electrical load bank with control panel is shown in Fig. 3.1 and the specifications of the dynamometer are given in Table 3.2.

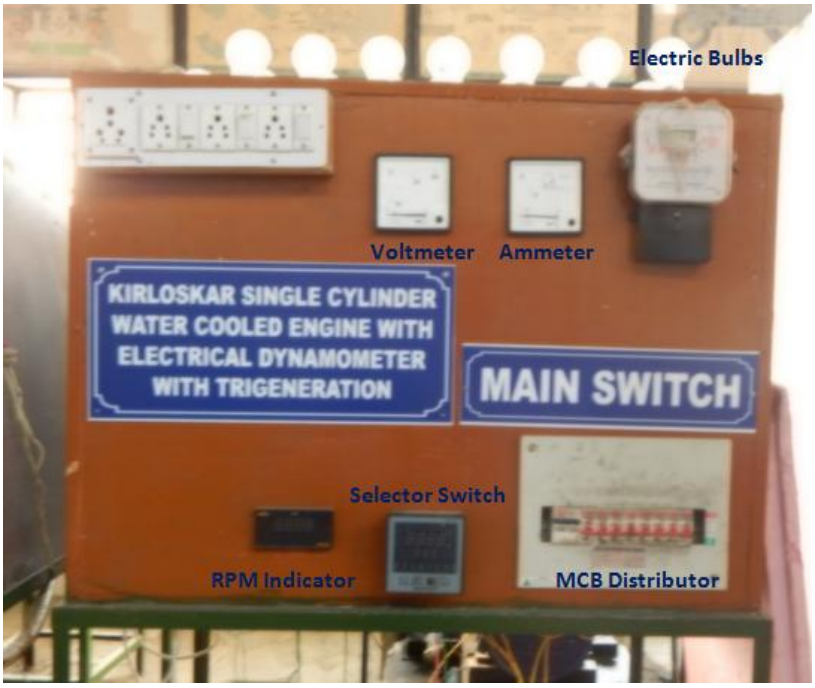

Fig. 3.1 Electric Load bank

Table 3.1: Specifications of the engine [91]

S. No.	Component	Unit	Description
1.	Type of engine	-	Vertical, four stroke cycle, single acting, totally enclosed, high speed C.I. engine
2.	No. of cylinders	-	1
3.	Power at 1500 rpm	kW(bhp)	3.7 (5.0)
4.	Bore	Mm	80
5.	Stroke	Mm	110
6.	Compression Ratio	-	16.5 : 1
7.	Recommended fuel specification	-	Diesel as per IS:1460
8.	Maximum permissible back pressure	kPa (bar)	2.59 (0.025)
9.	SFC at rated hp per 1500rpm		245 g/kWh (180 g/bhp/hr)

Table 3.2: Specification of the dynamometer [91]

S. No.	Particular	Description
1.	Make	Power star
2.	kVA	5
3.	Voltage	230 Volt
4.	Current	21.7 A
5.	Frequency	50 Hz
6.	Rating	Continuous
7.	PF	1.0

3.2.2 Air flow measurement

Air box was used to measure airflow. It also dampens the pulsation of air. At the entrance of one side wall of air box, an orifice (diameter=25mm and coefficient of discharge, C_d =0.6) was fitted. The outlet of the air box was connected to air filter mounted on engine. During operation, pressure inside the box was less than atmospheric pressure outside the box. The pressure inside the air box was measured with the help of U-tube manometer. Air induced per second is given by:

$$\text{Air induced/second } (m^3/s) = C_d \times A_{orifice} \times \sqrt{\frac{2gh_w\rho_w}{\rho_a}}$$

Where, C_d = 0.6

$A_{orifice}$ = 0.00038553 m^2

h_w = Manometer reading in m

ρ_w = Density of water= 1000kg/ m^3

ρ_a = Density of air = 1.15 kg/m^3

Mass flow rate of air can be calculated using the following equation:

Mass flow rate of air = Air induced/second (m^3/s) * Density of air (kg/m^3).

3.2.3 Fuel flow measurement

Fuel flow measurement is an important step for quantitative determination of BSFC. Volumetric fuel flow rate was measured by burette method. A glass burette with calibration marks was connected to fuel tank and the engine through a tee valve. Initially, fuel line was connected to the engine and burette, so as to fill the burette with the fuel, while the supply of fuel to the engine was not interrupted. In order to measure the fuel consumption the valve was adjusted so that the fuel started flowing from the burette to the engine. The time taken by the engine to consume a fixed volume of fuel was measured with the help of stopwatch. This volume divided by the time gave the volumetric flow rate.

3.2.4 Water flow measurement

A digital water flow meter in conjunction with acrylic rotameter was used to measure the flow rate of water flowing in the cooling jacket circuit and through the heat exchanger. Rahul make domestic water meter was mounted in the pipeline carrying cooling water through engine block. Although digital water flow meter alone can measure flow rate of water but by using rotameter the flow rate was cross-verified and was calibrated for error in flow measurement, if any. The detailed description of rotameter and digital water flow meter is shown in Table 3.3 and 3.4 respectively. Figure 3.2 shows the water cooling arrangement of engine.

Fig.3.2 Water cooling arrangement showing water flow meter and rotameter.

Table 3.3 Technical specifications of rotameter [92]

Meter body	Acrylic
Float	SS-316, SS-304 PTFE, PVC
Wetted Parts	SS-316, SS-304 SS, PTFE, PVC & PP
O Rings	Neoprene, PTFE, Silicon, Viton
Scale	Engraved on body
Temp. Rating	70^0 C
Full Scale	10:1
Repeatability	0.5%

Table 3.4 Technical specifications of digital water flow meter [93]

Size	Length body (Max.) – 165 mm Overall length incl. nipples (Max.) 250 mm Thread length on body- 10 mm Overall width- 100 mm
Class	B Type
Flow rate	Maximum 3 kl/h Nominal 1.5kl/h Transitional 120l/h Minimum 60l/h
Accuracy	Metering accuracy (Max.) ± 2% Metering accuracy (Min.) ± 5%

3.2.5 Exhaust Emission Analysis

AVL make DITEST (AVL DiGas 4000 light) 5 gas analyzer was used to analyze the exhaust emission from the engine. The exhaust emission included NO_x, CO, HC, CO_2 and O_2, out of which, CO, HC andCO_2 were measured by NDIR Technique and NO_x and O_2 were measured by electrochemical sensors. It gives HC and NO_x emissions in PPM and that of other gases in percentage. Smoke in exhaust was measured with the help of AVL 437 smoke meter. Detailed specification of exhaust gas analyzer and smoke meter is shown in Table 3.5 and 3.6 respectively.

Table 3.5: Specifications of 5-Gas analyzer [94]

Type	AVL DiGas 4000 light
Object of measurement	CO, HC, CO_2, NO_x
Measurement Principle	CO, HC, CO_2 = Infrared NO_x = Electrochemical
Range of measurement	CO = 0……..10 % by vol. CO_2 = 0…….20 % by vol. HC = 0……...20000 ppm by vol. NO_x = 0…….4000 ppm by vol.
Resolution	CO = 0.01 % by vol. CO_2 = 0.1 % by vol. HC = 1ppm by vol. NO_x = 1ppm by vol.
Warm up time	15 min. (self) at 20^0C
Speed of response time	Within 15 s for 90 % response
Weight	17.7 kg
Dimensions	470 mm x 431 mm x 230 mm
Power draw	150 VA
Operating Voltage	195…253 V, 47….63 Hz

Table 3.6: Specifications of smoke meter [95]

Type	AVL 437 smoke meter
Measuring value output	Opacity N [%] or absorption k [m^{-1}]
Measuring range	N = 0 ... 100% or k = 0 ... 99.99 m^{-1}
Resolution of displayed values	0.01 % opacity or 0.0025 m^{-1}
Limit of detection	0.1 % opacity
Zero stability	{0.1 % or 0.0025 m^{-1}}/30 min. (drift with zero gas)
Exhaust gas temperature	0 ... 600°C (800°C with high pressure option)
Exhaust gas pressure	-100 mbar ... + 400 mbar(including pulsation peaks) 0 mbar ... +3000 mbar with high pressure option
Calibration	Automatic (Self calibration immediately after switch on or at the press of key)
Dimensions	501mm x 200mm x 330mm (Control Unit) 520mm x 255mm x 455mm (Sensor Unit)
Weight	16 kg (Control Unit) 21 kg (Sensor Unit) 6 kg (Trolley)
Power Consumption	600 W (Overall equipment) 500 W (Measuring Chamber Equipment)
Storage Temperature	-30^{o}C to +65^{o}C
Power Supply	190…..240 V AC, 50….60 Hz, 2.5 A, 11.5….. 36 V DC

3.2.6 Temperature measurement

J-type thermocouples were installed at required points on the engine to measure temperature of intake air, exhaust gas and cooling water. These thermocouples are available in the range

of-40°C to 750°C. Standard and special limits of error of this thermocouple were from ± 2.2°C or ± 0.75% and ± 1.1°C or ± 0.4% respectively. Sensitivity and power consumption of the thermocouple is about 55μV/^{0}C& 3 mW respectively.

Same type of thermocouple was used to measure temperatures at different VA units' generators and evaporators.

3.3 Vapor Absorption Refrigeration System (VARS) for Space Cooling

Combination of four units of Electrolux vapor absorption system, each with a capacity of 51 liters and heat input of 95 Watts, was used for space cooling. This type of cooling system is also called three fluids absorption system. The three fluids used in the system were ammonia, hydrogen and water. Ammonia was used as refrigerant because it possesses most of the desirable properties for refrigerant. Hydrogen being the lightest gas was used to increase the rate of evaporation of liquid ammonia passing through the evaporator. Water was used as a solvent because it has the ability to absorb ammonia readily. Figure 3.3 and Fig. 3.4 show the working of Electrolux type refrigerator and the schematic setup of vapor absorption system respectively.

The vapor absorption system cycle is as follows. The ammonia liquid leaving the condenser flows downward under gravity to the evaporator where it meets hydrogen gas. The hydrogen gas which is being fed to the evaporator permits the liquid ammonia to evaporate at a low pressure and temperature according to Dalton's principle. The mixture of ammonia and hydrogen passes to the absorber. In absorber, weak ammonia solution in water is also added coming downward from water separator with gravity flow. Water absorbs ammonia in absorber and hydrogen returns upwards from absorber to evaporator. Hence, strong solution of ammonia in water passes from absorber to the generator where it is heated and ammonia vapor with traces of water vapor rises off to the water separator. Water is separated out from ammonia in water separator and a weak solution of ammonia is returned downward to the absorber with gravity flow. The ammonia vapor rises from the separator to the condenser where it is condensed to ammonia liquid, hence, completing the cycle.

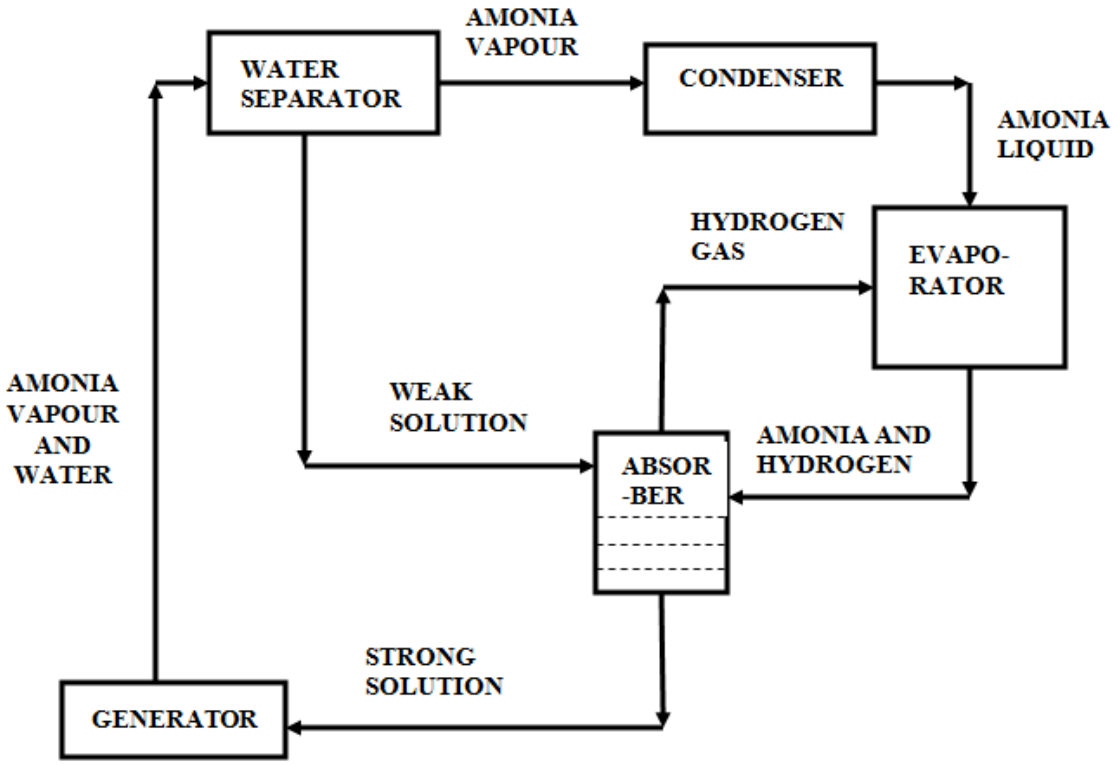

Fig.3.3 Electrolux type vapor absorption refrigeration system

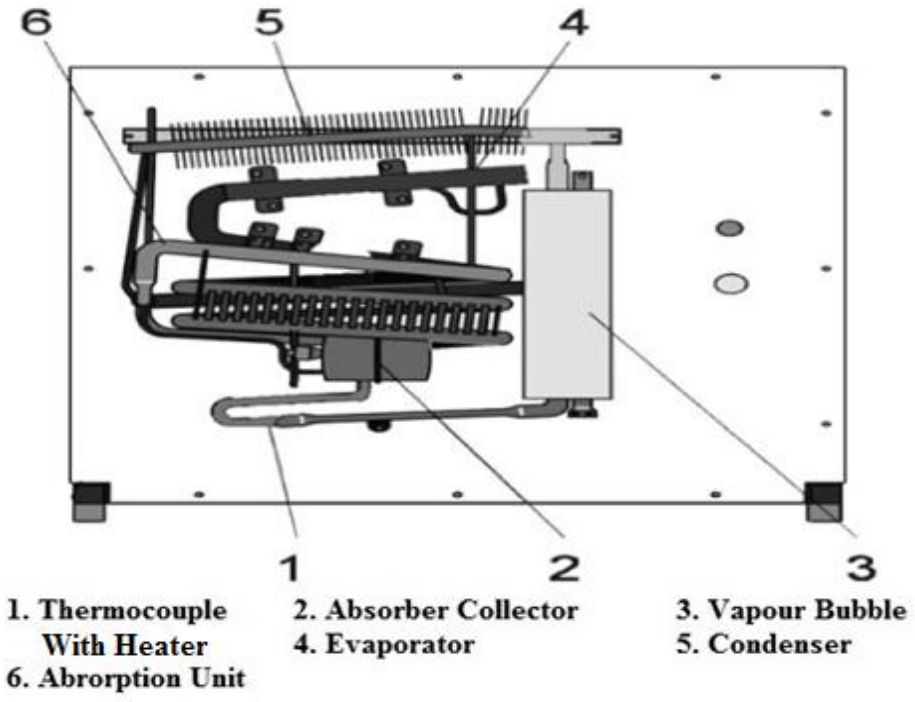

Fig.3.4 Schematic setup of vapor absorption refrigerator system in the laboratory [96]

Total heat available from exhaust gas coming from engine was little more than 2 kW at full engine load. However, VARS can't be installed near the engine because engine heat may

affect the performance of VARS, and there would be considerable heat losses before the exhaust gas enters the generator of vapor absorption unit if it is away from engine. Hence, the system was put at an optimal distance from the engine.

The VAR systems available in the market are either very small (41 – 51 liter) or too large (600 TR). To properly utilize the waste heat in the current experimental set-up, approximately 200 liter capacity VAR system was required. Since 51 liter VAR system was not sufficient to produce desired amount of refrigeration effect for space cooling of the experimental cabin; and bigger capacity VARS systems available in market are for large industrial purposes only, which could not be run using the exhaust heat available in this case. Hence, to resolve the problem, four units of 51 liter VARS systems were used.

3.3.1 Fabrication of complete VA system

Four identical VA units were arranged in rectangular pattern with two rows and two columns consisting of two VA units each. Henceforth, the four VA units will be addressed as top left, top right, bottom left and bottom right VA units according to their position shown in Fig. 3.5 while looking from the front of the VA system. The heat inputs to the generators of all VA units were from the same engine exhaust. The exhaust gases from engine were feed as input to distributor unit. The distributor unit supplies the gases to generator of 4 different VA units through different pipes. G.I. pipes were used to transfer exhaust gases from distributer to generator of VA units separately. There were two solenoid valves that are used to control temperatures at generator exit of two different VA units separately. One solenoid valve was used to control outlet temperatures of generators of top left and bottom left VA units collectively. And other one was used for two set of VA units placed at top right and bottom right. The exhaust gases after supplying heat to generator was flown out by a pipe to atmosphere.

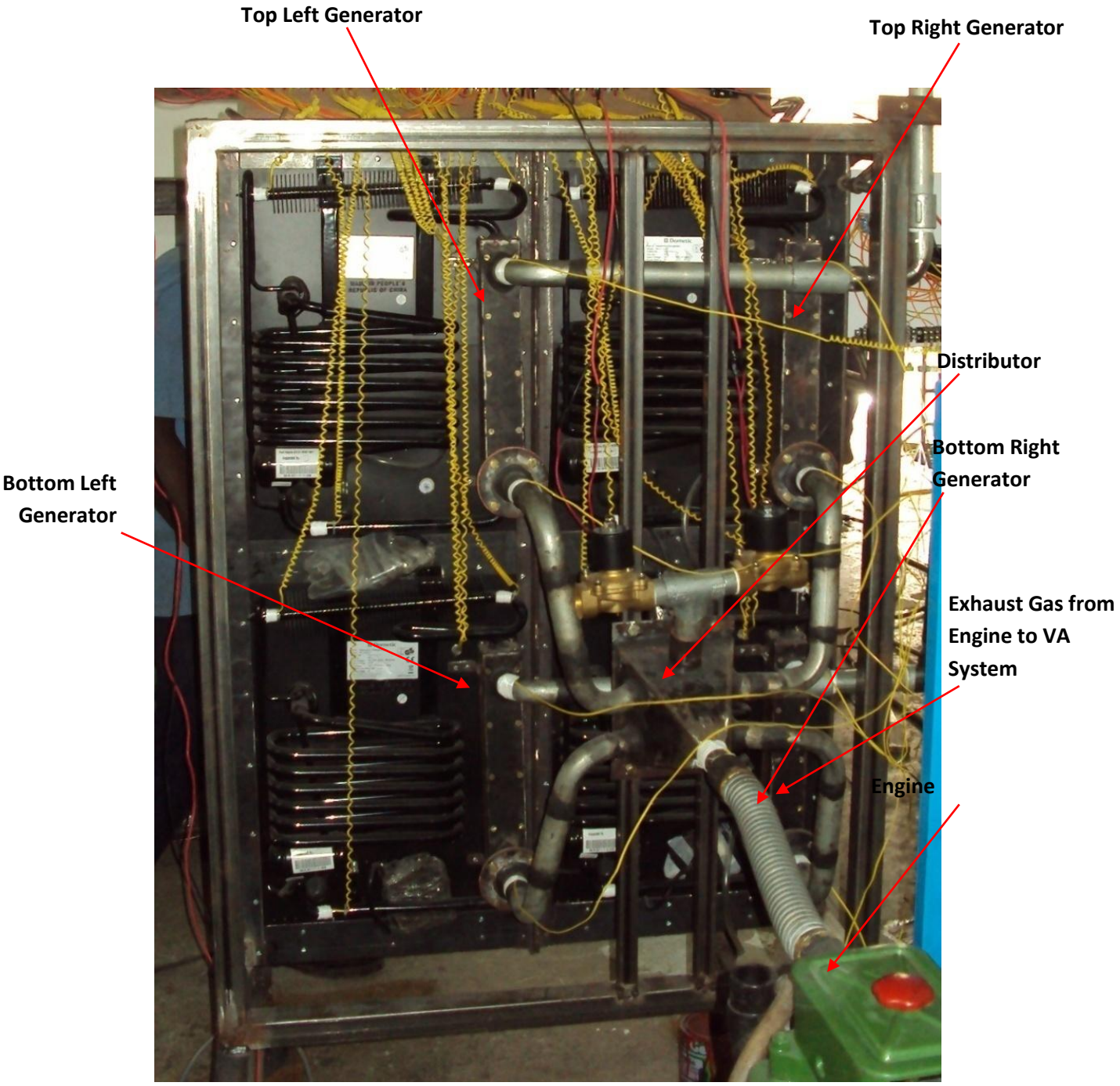

Fig. 3.5 Fabrication of VA system showing four VA units separately

To measure temperatures at different locations of complete VA set up, a number of thermocouples were used. After observations, it was found that only 12 thermocouples were sufficient to indicate the temperatures at desired locations. The locations were as given in Table 3.7.

Table 3.7: Location of different thermocouples showing different temperatures in VA system

S. No.	Temperature	Location of thermocouple
1	T1	Temperature of engine exhaust gases at entrance of VA system
2	T2	Temperature of refrigerant at exit of bottom right generator
3	T3	Temperature of refrigerant at exit of bottom right evaporator
4	T4	Temperature of refrigerant at exit of bottom left generator
5	T5	Temperature of refrigerant at exit of bottom left evaporator
6	T6	Temperature of refrigerant at exit of top right generator
7	T7	Temperature of refrigerant at exit of top left generator
8	T8	Temperature of refrigerant at exit of top right evaporator
9	T9	Temperature of refrigerant at exit of top left evaporator
10	T10	Temperature of exhaust gases after passing through generator at exit to atmosphere
11	T11	Cabin Temperature
12	T12	Atmospheric Temperature

The solenoid valve output was connected to digital indicator to show the temperatures of generators' exits shown in control panel. Different thermocouple temperatures are indicated by digital temperature indicator by rotating the knob of indicator. Fig. 3.6 shows the control panel and different indicators. Top left and bottom left VA units were connected to one solenoid valve whereas the top right and bottom right VA units were connected to the other solenoid valve.

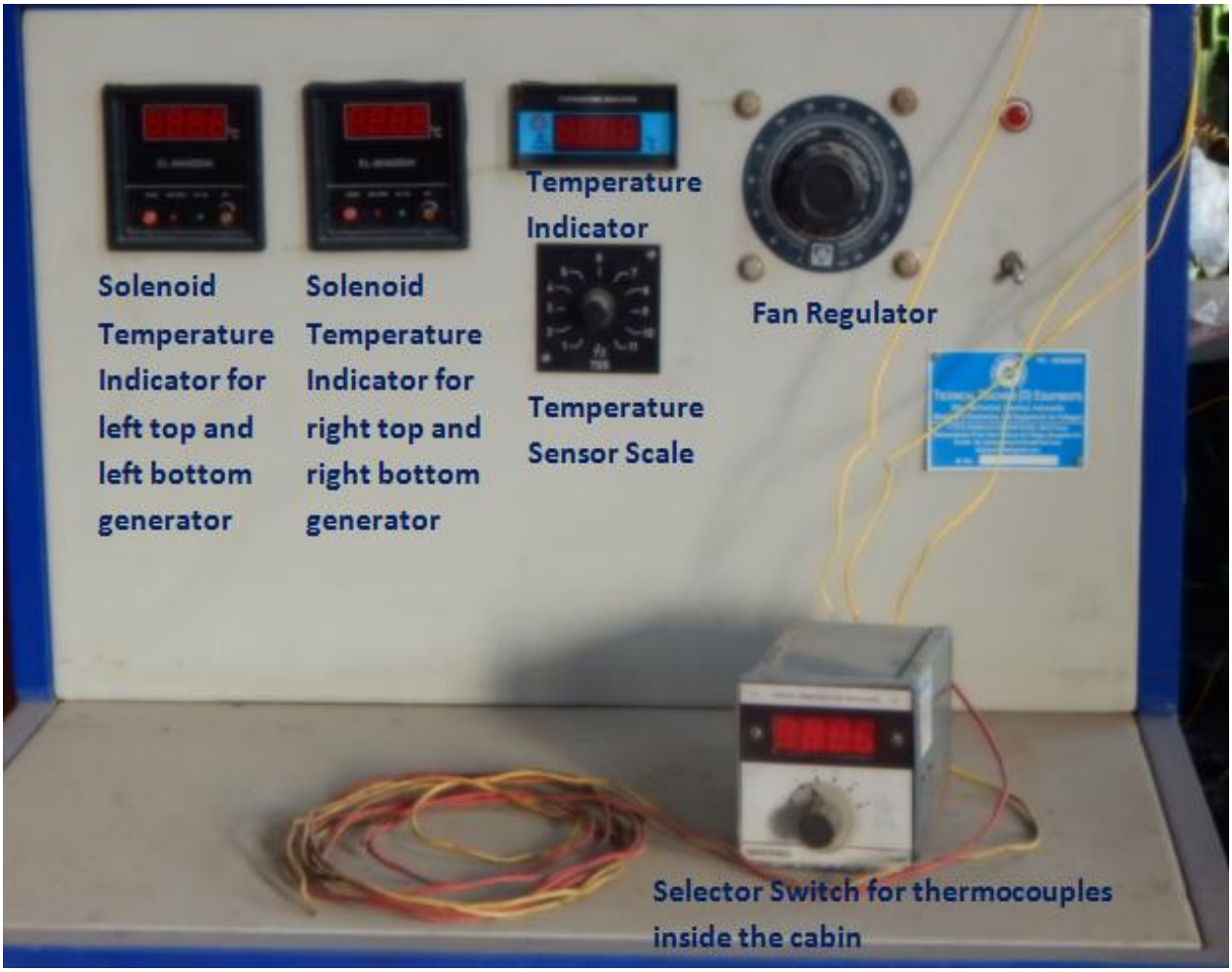

Fig. 3.6 Control panel of VA system

Hence, the test set-up was ready for the observations. So, the engine was started and the exhaust gases were fed to the distributor unit of VARS. From distributor the gases were directed to all the 4 generators of the 4 VA units through different pipes. The heat supplied to different generator units was utilized to produce cooling effect to cool the 4 evaporator coils as per the theory of VARS system. However, it was observed that the amount of exhaust heat sent to the 4 generators simultaneously was not able to produce the desired cooling effect. This was the biggest problem faced during the trial stage of observations. To solve this problem, another set of observations was planned. The details of the same are as discussed below:

It was then planned to supply the heat to generators of VA units one by one in a rational order. The order was planned based on the observations and limitations of the various system parts. Each connection to generators was then fitted with individual valves to regulate exhaust

gas flow. At first, heat was supplied to the top left generator, keeping all other valves closed. The aim was to produce a temperature of 110^0C at generator as per the requirement of Electrolux VA unit to produce refrigeration effect. After running the engine for some time and achieving the desired generator temperature of top left generator, valve for top right generator was opened to supply heat to another unit; valve for top left unit was closed. This was to take care that the two units, associated with same solenoid valve, should not be operated together at this stage. This way, all the four VA units were operated one by one by opening and closing the valves (as required) of the individual VA units from time to time. To achieve the desired effect from all four VA units, different permutations and combinations of valves was to be operated upon depending on each VA unit's generator temperature. At full engine load and when all the VA units' generator temperatures were at 110^0C, all four valves were opened. With this arrangement and valve provisions to supply heat to all VA units, the evaporator temperature of each VA unit reached 12^0C-15^0C, hence giving an appreciable cooling effect. To observe further improvement in evaporator temperature, the pipes carrying exhaust gases from engine to VA generators were insulated using asbestos rope. It was seen that the temperature of evaporator further dropped down to 8-10^0C. The valve arrangement at entrance of all VA units' generators is shown in Fig. 3.7 with pipes properly insulated by asbestos ropes. So with all the arrangements described as above, the preliminary objective of fabrication of VARS system (comprising of 4 VA units) to produce required amount of evaporator temperature was fulfilled.

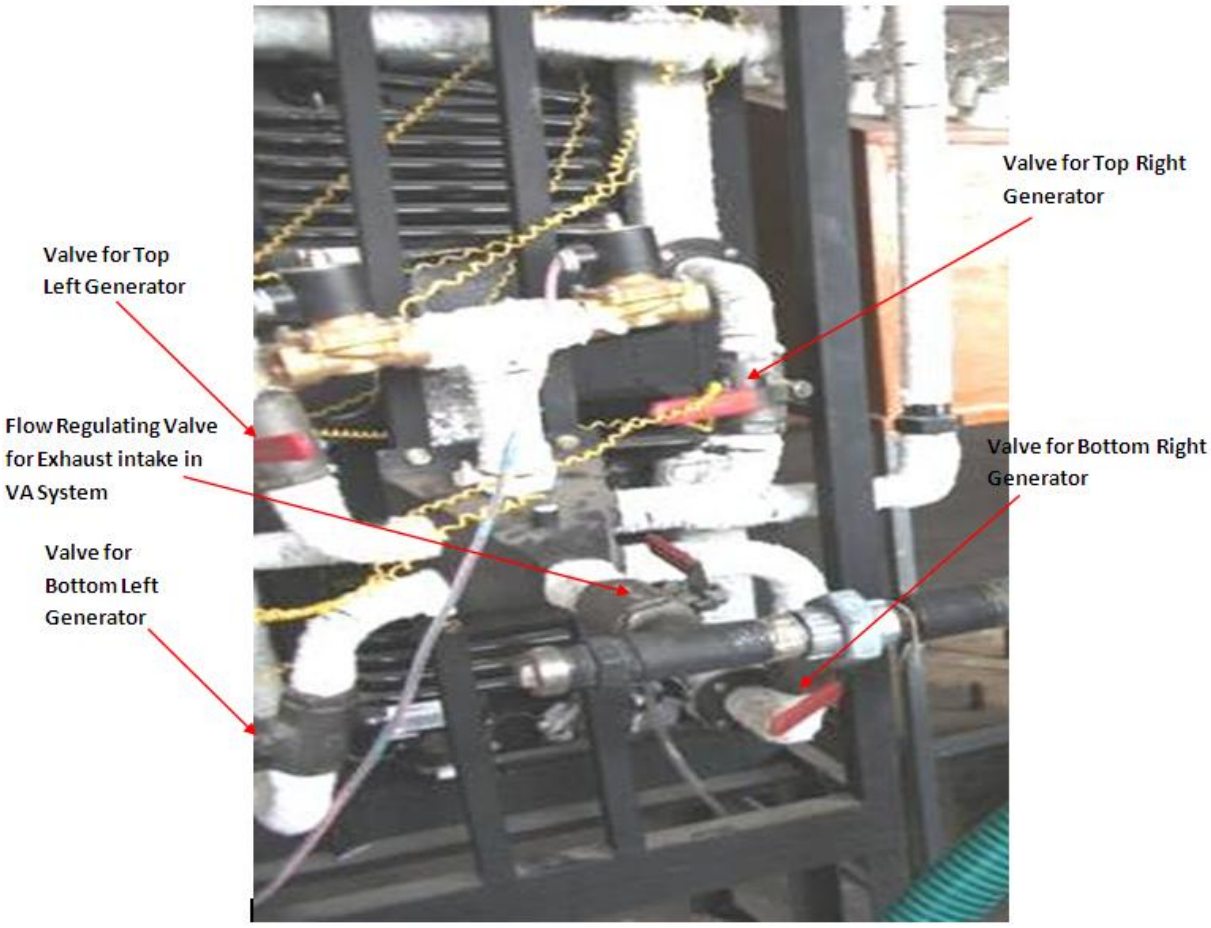

Fig. 3.7 Flow regulating valves for different VA units

3.3.2 Fabrication of experimental cabin/cooling space:

The objective of the research was to cool a 5'×5'×6'space (closed cabin) using the VA system developed and described as above. Before connecting the cabin in the flow, it was established that the evaporators of VA system (comprising of four VA units) were at 8^{o}C – 10^{o}C when the ambient temperature was 35^{o}C and hence, this temperature gradient could be utilized for space cooling. Following the usual air-conditioning principles, if air is passed to the cabin after being in contact with the evaporator coils, it should produce the space cooling effect. Hence, air was force pushed into the confined space and it was found to be effective for space cooling. The cabin was fabricated near the engine by using ply sheets of 19 mm thickness as shown in Fig. 3.8. During fabrication of the cabin, a provision of door-shifting was provided to change the size of the cooling space. Most of the VA system was placed on the back side of the cabin and evaporator coils of all the 4 VA units of the VA system were placed inside the cabin so as to maximize the cooling effect inside the cabin. Six air circulating fans were used between VA system and cabin to suck the cold air from evaporator

coils and deliver it into the cabin. The specifications of the air circulating fans were as follows: Stranger make, model 80/80/25, 220V, 50Hz, 0.7amp impedance protected. The power required to run the fans (i.e. 100 Watt for four fans) was supplied by the engine generator set.

(a)

(b)

(c)

Fig. 3.8 (a) Cabin for space cooling (b) Inside view of cabin with six circulating fans (c) Back side of cabin with VA system and its control panel

3.3.3 Experimental run of VA system

After complete fabrication of VA refrigeration unit into an air-conditioning system working as one complete unit, it was expected that the VA system would sufficiently cool the cabin space. The desired temperature at evaporators was achieved after 3-4 hours of continuous running of engine from idle to full load with a number of different valve combinations applied to run different VA units in specific order as was found feasible. However, it was observed that during this period of stabilization, some heat was also being rejected by the 4 condensers of the VA system, and that heat was being transferred to the cooling space producing an adverse effect. Similarly, due to continuous flow of exhaust to the 4 generator units, the pipes were also rejecting heat continuously. Also, one side of the cabin was adjacent to the electrical load (bulbs) and this was also heating the cabin space. Hence, all the above sources of heat were nullifying the effect of cooling within the cabin space and hence, the system was not able to fulfill the requirement of space cooling. The space provided for cooling inside the cabin was initially of 5'×5'×6' and it was a greater volume to be cooled by the provided facility. For proper cooling of the cabin space, the size of cabin was reduced to 3'×5'×6' by provision of shifting the door inside as discussed earlier section. After reducing the cabin space, it was decided to properly insulate the cooling space and the VA system so as to minimize the loss of cooling effect.

For proper insulation of the cabin, nitrile rubber was used on the rear wall of the cabin, over which a glass wool layer was used and further on the top of glass wool layer, aluminum foil was pasted, giving the cabin rear a three layer firm insulation cover. The thickness of nitrile rubber, glass wool and aluminum foil layers of insulation was10 mm, 25 mm and 2.5 mm respectively as shown in Fig. 3.9 (a). Figure 3.9 (b) shows the side wall of the cabin which was adjacent to the engine and was provided with thermal insulation by 3 layers of 1 inch thick thermocol sheets making it a 3 inch insulating layer of thermocol. The inner wall just opposite to the thermocol layers as in Fig. 3.9 (c) was covered with 2 inch thick Formula R extruded polystyrene insulated sheet with R value of 5 per inch and exceptional moisture resistance capability. The higher the R value, greater the resistance will be to heat flow, i.e., higher R value means higher insulation capacity. The cabin roof was provided with one layer of 1 inch thick thermocol sheet above the ply wood ceiling. The other two walls did not need insulation as those were away from the engine. Two fans were used to reduce the excessive heat from top left and top right condensers as shown in Fig. 3.9 (d).

There was another factor for heat gain i.e., convection of generator heat to the refrigerated space and that in turn reduces cooling effect in the cabin. This resulted in reduction of cooling effect between ambient and cabin space just to 2^{o}C against an expectation of 5 to 10^{o}C. To increase the cooling effect inside cabin, the heat was restricted to enter inside refrigerated space by insulating the space using glass wool and aluminum foil as shown in the Fig. 3.9 (e). The reason behind this insulation was to avoid the heating of air inside the refrigeration space due to heat transfer from VA system generators. To provide sufficient amount of fresh air inside the refrigerated space, the space was provided with vents from the top and side by drilling holes on the side walls of VA system at uniform distance as in Fig. 3.9 (g).

Initially, the cold air produced in refrigerated space was sucked into the cabin space by using 6 small capacity fans, as described earlier. However, 6 fans were not sufficient to suck the proper amount of air and also their motors produced ample amount of heat. To avoid the heat from fans and to improve air circulation from evaporator space to the cabin, only two (instead of 6) circulating fans (Make: Crompton Greaves, sweep=150mm, 230V, 1750rpmand 20W) were used as shown in Fig. 3.9 (f).The power required to run the fans was supplied by the engine generator set. The fans were used to force the air inside the cabin from the bottom evaporators' side of the VA system. After proper insulation of the cabin from all sides, the system was allowed to run and observations were made.

(a)

(b)

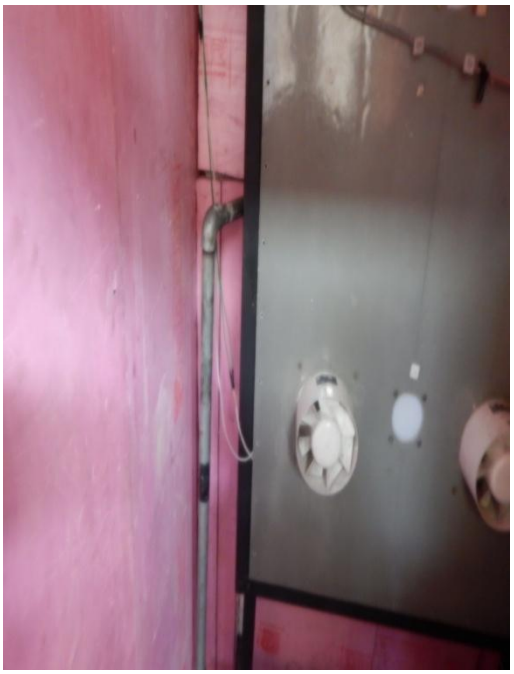

(c)

(d)

(e)

(f)

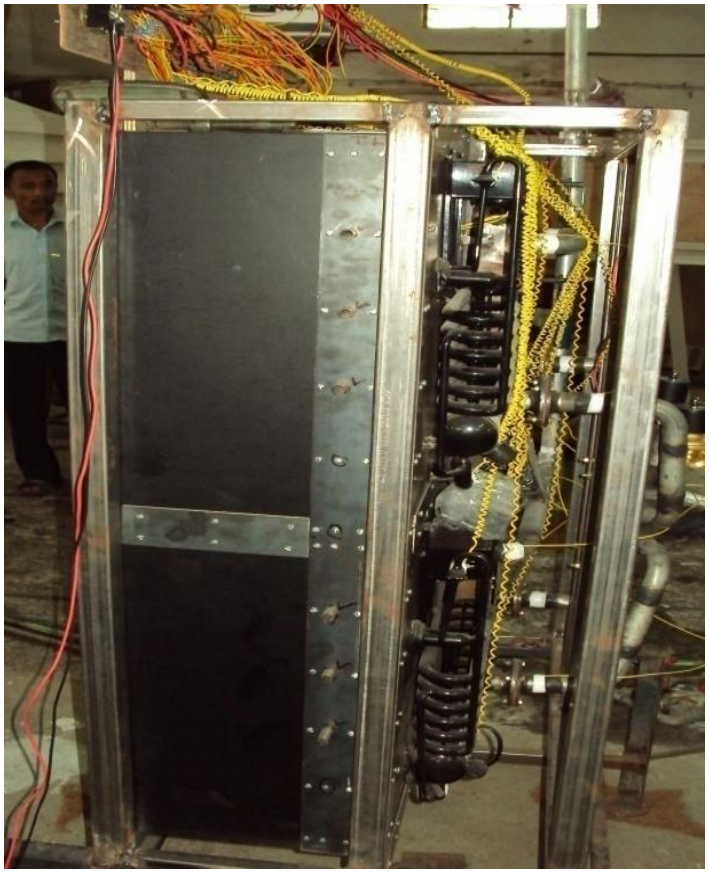

(g)

Fig.3.9 (a) Insulation of back side of VA system and cabin (b) Insulation of side wall of cabin (c) Insulation of inner wall of cabin (d) Cooling fans installed above top left and top right condensers (e) Insulation in refrigerated space (f) Suction fans installed between rear of VA system and cabin (g) Side holes provided for ventilation.

3.4 Design of heat exchanger for hot water production

A heat exchanger was designed and fabricated for producing hot water. Heat transfer area was the major factor in designing the heat exchanger. A special and important class of heat exchanger was used to achieve a very large heat transfer surface area per unit volume termed as compact type heat exchanger. Compact type heat exchangers have dense areas of finned tubes or plates and are typically used when at least one of the fluids is a gas, and hence is characterized, by a small convection coefficient. There are two types of compact type heat exchanger:

1) Plate heat exchanger
2) Tube-Fin heat exchangers. These are further divided into three categories:
    a) Flat fins with round tubes
    b) Flat fins with flat tubes
    c) Louvered fins with flat tubes

Compact type heat exchangers can be used as waste heat recovery devices for diesel engine. It can have either louvered fin or flat fins. But, in general, louvered fins have large heat transfer area and induce turbulence in flow, but due to unavailability of desired specifications, fabrication of louvered fin type heat exchanger could not be possible. So flat fin heat exchanger was selected to move forward with.

3.4.1 Design Parameters for flat fin heat exchanger

For designing of flat fin heat exchanger, at first the data related to the properties of engine exhaust and cooling water from engine block were observed and calculations made. Here, for calculation purpose, some of the properties of exhaust gases like viscosity, Prandtl number, etc. were taken for air because air is the major constituent of exhaust gas and the data for air was easily available in property Tables. Table 3.8 shows the various properties of hot fluid (exhaust gas) and cold fluid (water).

Based on heat balance test at full load, the exhaust heat available was calculated as follows:

Mass flow rate of exhaust gas = mass flow rate of fuel + mass flow rate of air (Eq. 3.1)

Mass flow rate of fuel, m_f =1.005 kg/hour

Mass of air sucked, $m_a = \rho_{air} * V_a$

$V_a = A_{orifice} * C_d \sqrt{(2g * h_{air})}$ (Eq. 3.2)

Take $c_d = 0.6$, $A_{orifice} = 314\ mm^2$

$h_{air} = (\rho_w / \rho_{air}) * h_w$ (Eq. 3.3)

$= 1000/1.2 * 5.5/100$

$= 45.83$ m of air

$V_a = 20.32\ m^3$/hour

So, $m_a = 24.39$ kg/hour

Mass flow rate of exhaust gas = 24.39 + 1.005

= 25.395 kg/hour

Mass flow rate of water, m_w = 1lt/min

= 1 kg /min

= 60 kg / hour

Temp of exhaust gas, $T_{h\,i} = 360^oC$

Temp of outlet, $T_{ho} = 180^oC$ (assumption to avoid condensation)

Water inlet, $T_{c\,i} = 70^oC$

Water outlet, $T_{c\,o}$ =will be calculated using energy balance

Energy balance equation can be applied for both fluids

$$q = m_h c_{ph}(t_{h\,o} - t_{hi}) = m_c c_{pc}(t_{co} - t_{ci}) \quad \text{(Eq. 3.4)}$$

Table 3.8: Properties of exhaust gases and water

Properties	Hot fluid (exhaust gases)	Cold fluid (water)
m (kg/hr)	25.399	60
T_{inlet} (^oC)	$T_{hi=}360$	$T_{ci}=70$
T_{outlet} (^oC)	$T_{ho=}180$	T_{co}(by energy balance)

c_p (kJ/kg-K)	1.1	4.18
μ	$20*10^{-6}$	$32*10^{-5}$
P_r	0.7	2.2
ρ	1.2	1000
r_n	0.0002	0.003

The value of UA was calculated with the help of Effectiveness (ε) using NTU method. For that heat capacity, rate of hot fluid (C_h) and heat capacity rate of cold fluid (C_c) were determined by the following expressions;

$$C_h = m_h c_{ph} \quad (3.5)$$

$$C_c = m_c c_{pc} \quad (3.6)$$

The expression for maximum heat transfer rate (q_{max}) was obtained by the following expression;

$$q_{max} = C_{min} (T_{hi} - T_{ci}) \quad (3.7)$$

Where, C_{min} is equal to C_c or C_h, whichever is smaller. The effectiveness for the heat exchanger was determined as the ratio of actual heat transfer rate to the maximum possible heat transfer rate i.e.

$$\varepsilon = q/q_{max} \quad (3.8)$$

$$\varepsilon = c_h(t_{hi}-t_{ho})/c_{min}(t_{hi}-t_{ci}) \quad (3.9)$$

The ratio of minimum and maximum heat capacity rate is defined as Capacity Ratio (C), which is given by the following formula:

$$C = C_{min}/C_{max} \quad (3.10)$$

For any heat exchanger it can be shown that the effectiveness is function of NTU and C i.e.

$$\varepsilon = f(NTU, C) \quad (3.11)$$

From the above relationship available in the form of NTU- ε chart as shown in appendix B, the value of NTU was calculated.

The number of transfer units (NTU) is a dimensionless parameter, which is widely used for heat exchanger analysis and is defined as

$$NTU = UA/C_{min} \quad (3.12)$$

From the above relationship, UA value was calculated.

This value was verified with the help of another method in which, heat transfer coefficient of gas and water side were determined. In this method, a chart of Stanton number and friction factor for surface (11.32 – 0.737-SR) was used which is shown in appendix C. The method of calculation is presented as given below:

From the help of chart, for the surface of finned flat tube (11.32–0.737-SR), the flow parameters of exhaust gas side and of that of water side were taken as shown in Table 3.9 & Table 3.10 respectively.

Table 3.9: Flow parameters of exhaust gas side

Parameter	Value	Description
$(r_{hi})_a$	$0.878*10^{-3}$m	Flow passage hydraulic radius
A/V or α_a	886 m^2/m^3	Total gas side transfer area/total volume
A_f/A	0.845	Fin area/Total area
Acc/A_{fr} or σ_a	0.780	Free flow area/ frontal area
Δ	$0.1*10^{-3}$m	Fin metal thickness
L_f or ½(distance between tubes)	$5.71*10^{-3}$ m	Fin length

Exhaust gases were passed through the fins perpendicular to the tubes, so Reynolds number (R_{ed}) was calculated by an expression as given below,

$$R_{ed} = \rho V d_h / \mu \quad (3.13)$$

From graph at appendix C of radiator surface 11.32-0.737-SR, the value of $StPr^{2/3}$was calculated for obtaining the value of Reynolds number. From this Stanton number i.e., modified Nusselt number was calculated. Then, heat transfer coefficient for exhaust gas was calculated using.

$$h_{ex} = St*G*C_p \quad (3.14)$$

Where, G is the mass velocity and is given by

$$G = \rho v \quad (3.15)$$

Similarly, the value of heat transfer coefficient on water side was calculated. According to the dimension of tubes of selected surface, following parameters were calculated by taking the area of cross section and perimeter of one tube as shown in appendix C.

Table 3.10: Flow parameters of water side

Parameter	Value	Description
$(r_{hi})_w$	$0.933*10^{-3}$m	Flow passage hydraulic radius
A/V or α_w	138 m^2/m^3	Total gas side transfer area/total volume
Acc/A_{fr} or σ_w	0.129	free flow area/ frontal area

The value of heat transfer coefficient of water side was calculated similarly by calculating Reynolds number and Stanton number. Then, for finding out the value of UA the following equation was used:

$$UA = (1/\eta_{oex}A_{ex}h_{ex} + 1/\eta_{ow}A_w h_w)^{-1} \quad (3.16)$$

Where, η_{oex} and η_{ow} are the overall fin effectiveness of exhaust gas side and water side respectively.

The value of UA from above relationship came out approximately equal to the value of UA from ε-NTU method which confirmed the accuracy of the calculations.

With the help of this, different parameters of heat exchanger were calculated and are shown in Table 3.11.

Table 3.11: Different parameters of flat fin heat exchanger

Parameter	**Calculated value**
Heat transfer area	0.474 m^2
Core height	0.340 m
Core width	0.300 m
Core thickness	0.050 m
No. of tubes	100
No. of fins	152
Tubes pitch	0.010 m
Tubes depth	0.010 m

Figure 3.10 (a) and (b) show the basic configuration of the developed cross flow heat exchanger. Figure 3.11 (a) shows the front view of the heat exchanger. The major problem in designing the heat exchanger was to get the exhaust on the frontal area uniformly. To overcome this problem, it was needed to design a diffuser to get the exhaust gas uniformly on its frontal area and to get the gas expanded to reach every corner of frontal area of the heat exchanger uniformly. Similarly, in the outlet of heat exchanger, a converging section was designed, which was connected to a pipe to let the gas pass through to the environment [38]. Figure 3.11 (b) shows the heat exchanger with converging-diverging ducts. The length of different parts of the duct are shown in Fig. 3.12, and dimensions of the duct were determined which are shown in Table 3.12.

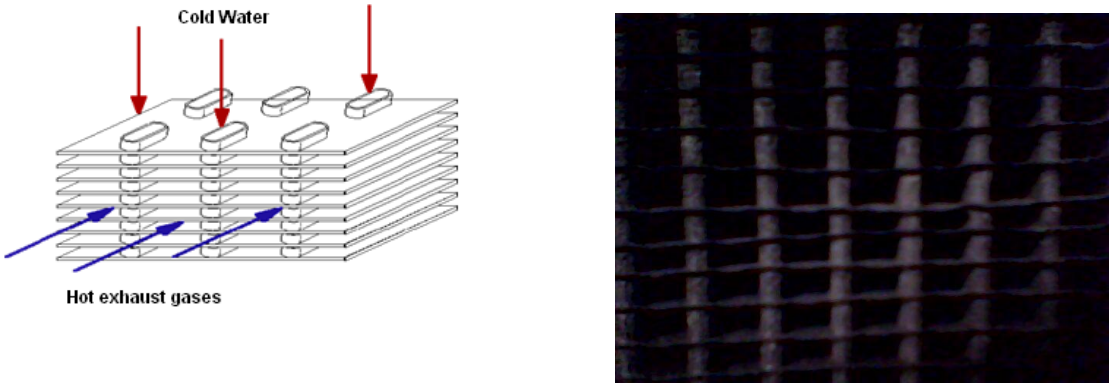

(a) (b)

Fig. 3.10 Basic configuration of crossflow heat exchanger (a) Flow in flat tube-plate fin heat exchanger (b) Photograph of a part of the tube fin arrangement in the heat exchanger

(a) (b)

Fig.3.11 Photograph of heat exchanger (a) View perpendicular to exhaust flow (b) Heat exchanger with diverging- converging duct

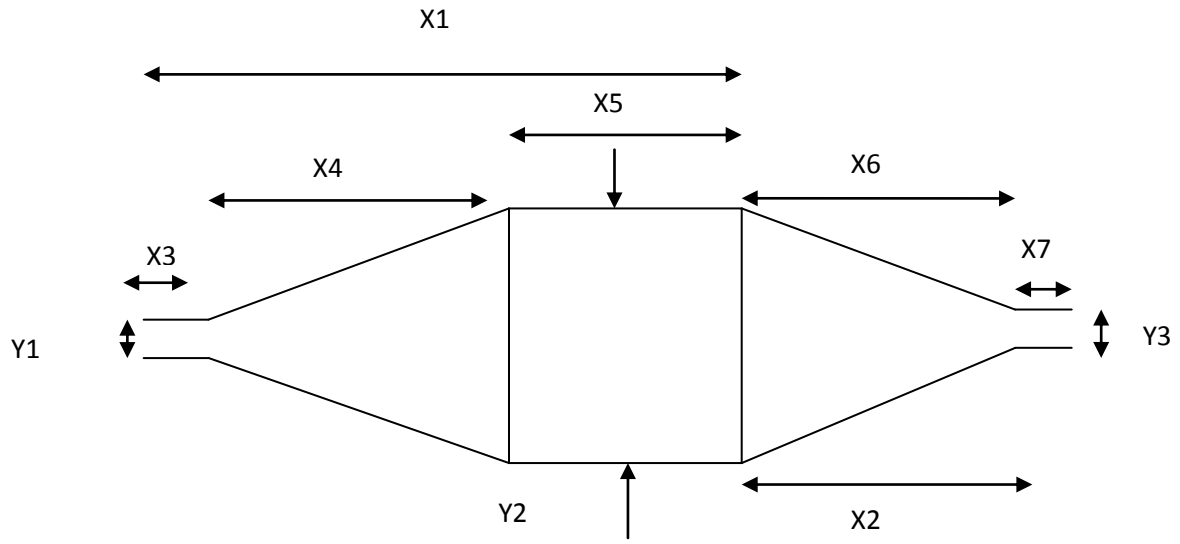

Fig.3.12 Divergent and convergent sections [38]

Table 3.12: Dimensions of divergent and convergent sections [38]

X1	0.398 m	X6	0.350 m
X2	0.345 m	X7	0.050 m
X3	0.090 m	Y1	0.020 m
X4	0.345 m	Y2	0.340 m
X5	0.050 m	Y3	0.020 m
Z1	17^o	Z2	17^o

3.5 Design procedure for calculation of effectiveness and heat transfer rate of generator:

The generator of the refrigerator used in this study was modified to utilize the waste heat of exhaust gases. For the above purpose, a counter flow, double pipe type heat exchanger was designed, fabricated, installed and commissioned. The heat exchanger for the generator was counter flow, double pipe type, taking the generator tube as the inner tube and a steel pipe as the outer pipe. Several types of arrangements for making this heat exchanger were tried and finally the outer pipe was cut and inserted through the generator tube to make a pipe in pipe heat exchanger as shown in Fig.3.13. The length of the outer pipe of heat exchanger was fixed according to the maximum vertical length available at the generator but the diameter of the outer pipe was varied within the restricted space, available between the generator tube and evaporator chamber in order to adjust the effectiveness of the heat exchanger which could provide the required heat transfer rate at the generator. The method of design procedure with calculation for effectiveness and heat transfer rate at generator is presented as following [97]:

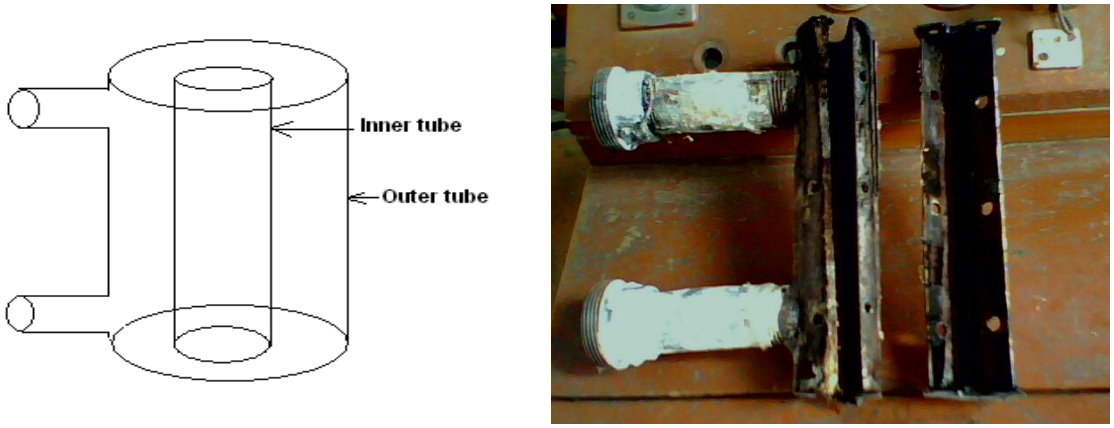

Fig. 3.13 Heat exchanger for generator: (a) schematic showing two concentric tubes (b) photograph of two parts of outer tube

The flow cross sectional area (A_c) was calculated using following equation,

$$A_c = A_{outer\ pipe} - A_{inner\ pipe} \quad (3.17)$$

and the flow wetted perimeter (P) was calculated using following equation,

$$P = \pi\, d_{\text{outer pipe}} + \pi\, d_{\text{inner pipe}} \quad (3.18)$$

The hydraulic diameter (D_h) was calculated by using following relation,

$$D_h = 4A_c/P \quad (3.19)$$

The value of Reynolds Number (R_e) was determined by the following expression,

$$R_e = \rho V D_h/\mu \quad (3.20)$$

The calculation of the friction factor (f) was done using the following expression,

$$f = 0.046R_e^{-0.2} \quad (3.21)$$

Knowing the Prandtl Number (Pr) for this application to be Pr=0.7, the Colburn equation for turbulent heat transfer in smooth pipes was used to obtain the value of Nusselt number (N_u) as given below [18]:

$$Nu = (f/2)\, R_e\, Pr^{0.33} = 0.023R_e^{0.8}\, Pr^{0.33} \quad (3.22)$$

Using convection correlations for non-circular tubes the convective heat transfer coefficient (h) was calculated using following expression:

$$Nu = hD_h/k \quad (3.23)$$

The major heat transfer resistance was due to the generator tubes. This resistance was calculated by neglecting the thermal resistance inside the inner tube using the following equation,

$$R_t = 1/\pi d_{\text{inner pipe}}\, lh \quad (3.24)$$

From the value of R_t as mentioned above, the value of UA was calculated by the following equation,

$$UA = 1/R_t \quad (3.25)$$

Number of transfer units (NTU) was calculated using the above value of UA and taking the minimum capacity rate (C_{min}) using the following expression,

$$NTU = UA/C_{min} \quad (3.26)$$

Here, the value of C_{min} (C = m*c) was obtained for the hot fluid and value of maximum capacity rate (C_{max}) was obtained for cold fluid. Then, the value of effectiveness (ϵ) was calculated by knowing the value of capacity ratio ($C = C_{min}/C_{max}$) using following equation,

$$\varepsilon = \frac{1-\exp\{-NTU(1-C)\}}{1-C\exp\{-NTU(1-C)\}} \quad (3.27)$$

The heat transfer rate through generator (Q_g) was calculated by the following formula,

$$Q_g = \epsilon C_{min}(T_{hi} - T_{ci}) \quad (3.28)$$

CHAPTER 4
EXPERIMENTAL PLAN AND PROCEDURE

Experimental test plan and performance parameters are discussed in this chapter. The experimental investigation of the performance of the trigeneration system was divided in various steps to suit the conditions of single generation, combined cooling and power (CCP), combined heating and power (CHP) and combined cooling, heating and power (CCHP) modes. In the first step, a series of tests were carried out to evaluate the engine generator performance when it was to be run on a single generation system. In the second step, a series of tests were conducted to evaluate the performance of CCP system mode. In the third step, a series of tests were conducted to evaluate the performance of CHP mode. In the fourth and final step, a series of tests were conducted to evaluate the performance of CCHP mode.

4.1 Performance of engine generator working on single generation system

A number of tests were performed on single generation system to determine the engine generator performance and emissions. While varying the engine load between idle to full load, various performance parameters were recorded e.g. power output, fuel consumption, exhaust temperature and emissions (CO, CO_2, NO_x, HC and Smoke) at optimum injection timing and injection pressure. As per the schematic flow diagram of the whole set up as shown in Fig. 4.4,valves A and E only were opened and rest of the valves were kept closed for single generation system. Exhaust gases coming from engine were passed to atmosphere through valve A while the hot water from engine was discharged to sink through valve E. The power produced by engine was measured using electrical dynamometer. The schematic diagram of experimental set up for testing of single generation system is shown in Fig.4.1.

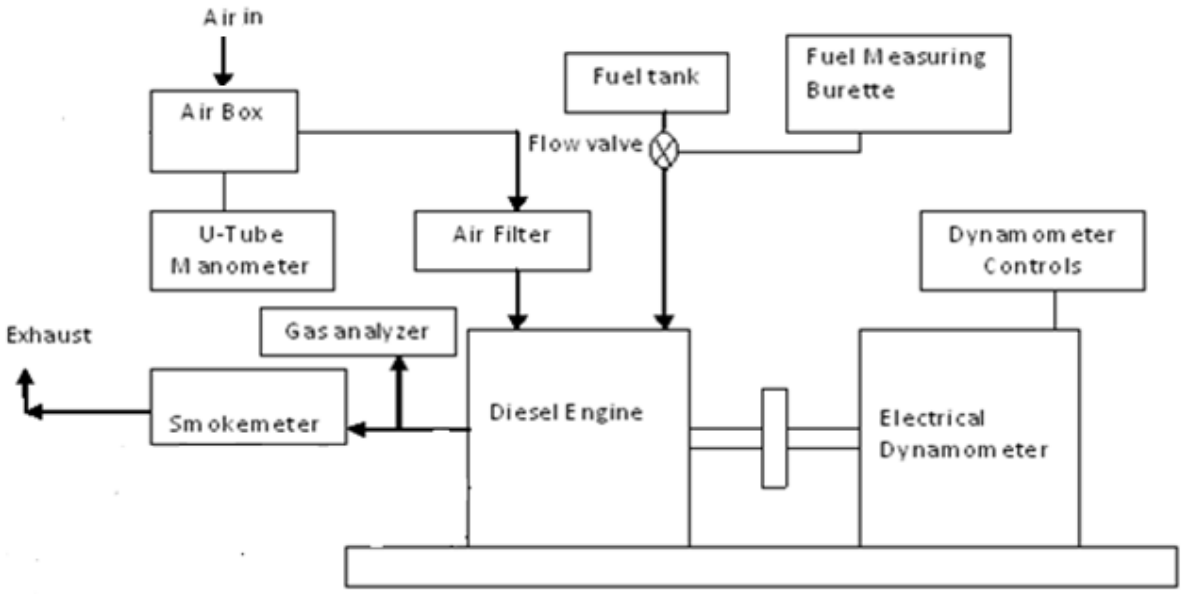

Fig. 4.1 Schematic diagram of single generation system

4.2 Performance of cogeneration system

(a) Combined cooling and power (CCP)

In the combined cooling and power (CCP) mode, it was planned to pass exhaust gases from engine to VA system generators for space cooling before exhausting to atmosphere. As per the schematic flow diagram for the whole set up as shown in Fig. 4.4, valves B, C and E were kept opened, while rest of the valves were kept closed. Exhaust gases passed through valve B into VA system (comprising of 4 VA units) and all the four VA units were operated one by one by opening and closing the valves (as required) of the individual VA units' generators (valves of each separate VA unit are shown in Fig. 3.10). To achieve the desired effect from all the four VA units, different permutations and combinations of valves were to be operated upon, depending on each VA unit's generator temperature. The four separate VA units were run in various combinations to produce the desired cooling effect at evaporator coils. The cold air around evaporators was sucked and thrown to the designed space for cooling. The exhaust gases after being utilized in VA units were passed to the atmosphere through valve C. Valve E was kept open to discharge hot water coming from engine after cooling. In this way, the same engine was used to produce the power as well as space cooling and hence, fulfilled the condition of cogeneration. The various parameters collected and recorded are as follows:

- Engine generator power output, BSFC and BTE
- Heat input to generators of VA system
- Refrigeration effect generated in the VA system
- The coefficient of performance (COP) of the VA system
- Exhaust emissions of cogeneration system.

The schematic diagram of experimental set up for testing of combined cooling and power generation system is shown in Fig. 4.2.

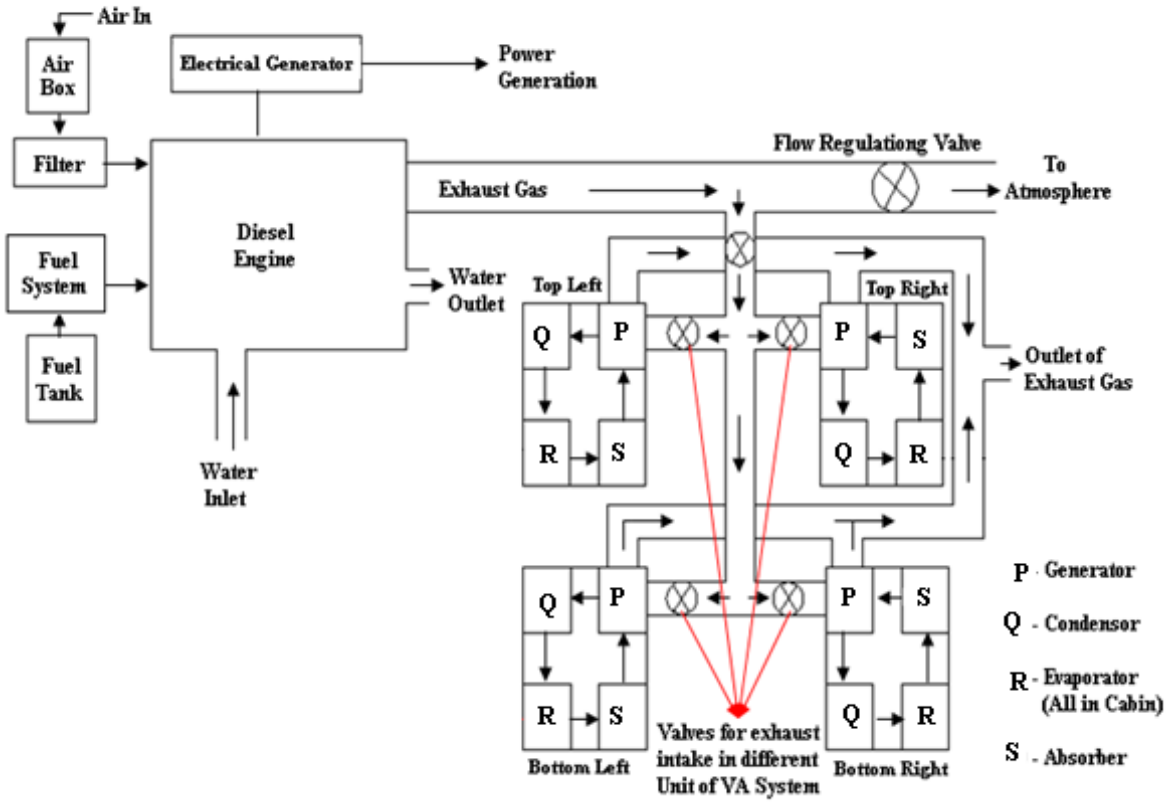

Fig. 4.2 The schematic diagram of experimental set up for CCP mode

(b) Combined heating and power (CHP)

In the combined heating and power (CHP) mode, exhaust gases from engine were passed through valve D to a compact type heat exchanger. The cooling water from engine was also passed to this heat exchanger through valve F, as shown in schematic diagram at Fig. 4.3. Rests of the valves (like E, A and B, etc.) were kept closed. Since the engine is water cooled, the water,

after gaining heat from the engine block, was passed through the heat exchanger (as cold fluid to further gain heat) developed for extracting heat from the engine exhaust gases (as hot fluid) coming through valve D. While varying the engine load between idle to full load, various parameters were recorded e.g. power output, fuel consumption, temperatures of cooling water at entry and exit points of both, engine and heat exchanger, water flow rate and emissions (CO, CO_2, NO_x, HC and Smoke).

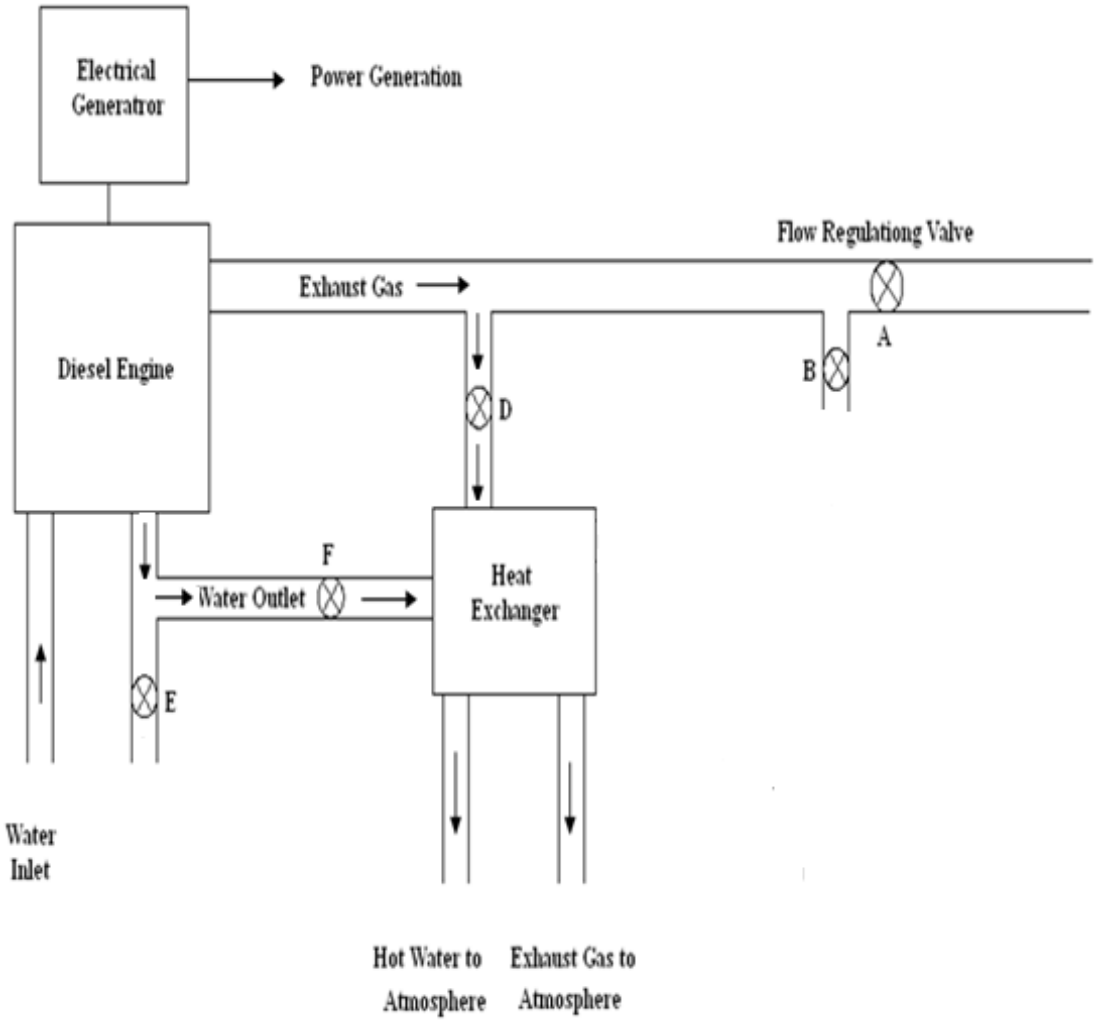

Fig. 4.3 The schematic diagram of experimental set up for CHP mode

4.3 Performance of combined cooling, heating, and power (CCHP)

In the CCHP mode, exhaust gases are first passed to VA system through valve B as shown in schematic diagram of the whole set up at Fig. 4.4. Valve G was kept open to pass the exhaust gases, coming out from VA system generators, to the heat exchanger. Cooling water after extracting heat from engine block was passed to the heat exchanger, through valve F. In all the

above conditions, the valves C, D and E were kept closed. The system was utilized to produce the following effects:

- Power was produced by engine that is measured by electrical dynamometer.
- Refrigeration/cooling effect was produced by VA system, using exhaust gases as the source of heat, and was used to cool the designed cabin.
- Hot water production, first by the engine block, and further by extracting heat from engine exhausts gases using the heat exchanger.

The system was used to produce three simultaneous effects using same fuel input. Therefore, CCHP is also known as a trigeneration system. Various parameters were recorded to determine the total useful energy output (power + heat recovered by coolant and from exhaust + refrigeration effect), total thermal efficiency, SFC, COP of VA system and emissions while varying the engine load between idle to full load. While performing the tests, for single generation, CCP, CHP and CCHP modes, the positioning of different valves were changed as shown in Table 4.1.

Table 4.1: Positioning of different valves in different test modes.

Test Mode	Valve A	Valve B	Valve C	Valve D	Valve E	Valve F	Valve G
Single Generation	On	Off	-	Off	On	Off	-
CCP	Off	On	On	Off	On	Off	Off
CHP	Off	Off	-	On	Off	On	-
CCHP	Off	On	Off	Off	Off	On	On

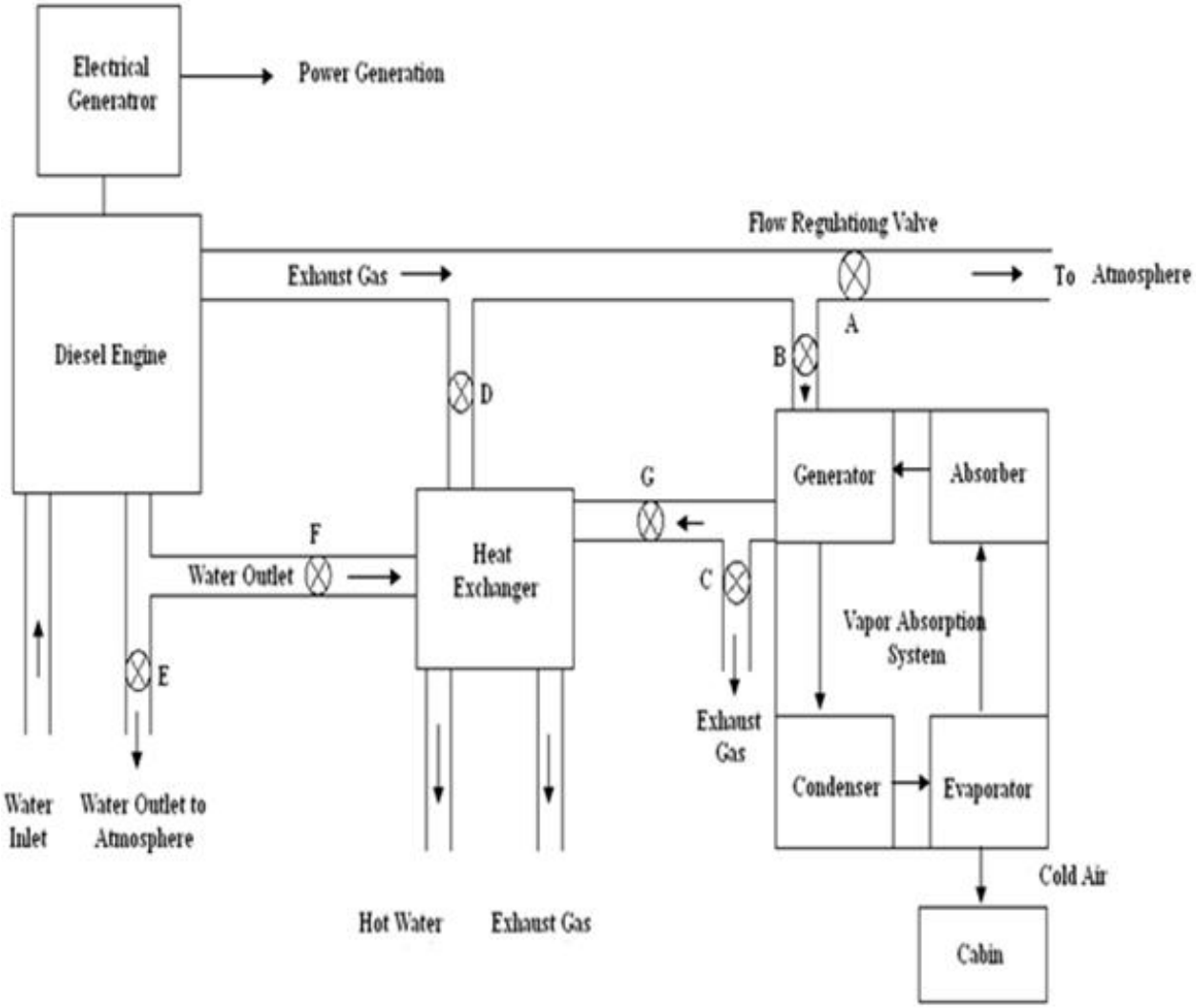

Fig.4.4 The schematic diagram of the whole experimental set up for CCHP mode

4.4 Thermodynamic Energy and Exergy Analysis

The energy & exergy analysis of the diesel engine operated single generation system, cogeneration system and trigeneration system is explained in this section. The principles of mass or energy conservation and the Second Law of Thermodynamics were applied. The exergy analysis is carried out for steady flow steady state condition. For the exergy analysis, the atmospheric pressure and temperature were taken as 1 atm & 40^0C (313K) respectively as the reference state.

The following performance parameters were calculated for the system developed under single generation, cogeneration and trigeneration modes based on the energy principle:

(a) Brake power (B.P.): Brake power of the engine was measured as the electrical load applied by switching on the bulbs with particular rating.

(b) Brake specific fuel consumption (BSFC): BSFC is defined as the ratio of fuel consumed in kg/h to the brake power and the expression of BSFC is given as

$$\text{BSFC} = \frac{\text{fuel consumed in kg/h}}{Brake\ power\ in\ kW}\ \text{kg/kWh} \tag{4.1}$$

(c) Heat supplied or thermal energy contained in fuel: Heat supplied was calculated by:

$$E_f = \dot{m}_f * LCV\ kW \tag{4.2}$$

Where LCV is lower calorific value of diesel in kJ/kg and $\dot{m}_f$ is mass flow rate of fuel in kg/sec.

(d) Brake thermal efficiency (BTE): BTE of the engine was calculated by the following relation:

$$\text{BTE} = \text{B.P.}/E_f \tag{4.3}$$

(e) Thermal energy carried by the exhaust gas: It is determined by the following equation:

$$E_{ex} = \dot{m}_{ex} C_{p_{ex}} \{T_{eng.ex.gas} - T_{ambient}\}\ kW \tag{4.4}$$

(f) Thermal energy recovered by engine cooling and exhaust gases: Total thermal energy recovered from engine cooling and engine exhaust system is the sum of the heat recovered from the run through cooling water system in engine block and extracted heat from the engine exhaust gases through the heat exchanger as given by the following equation:

$$E_{cw} = \dot{m}_w C_{p_w} \{T_{eng.ex.water} - T_{eng.inwater}\} + \dot{m}_w C_{p_w} \{T_{H.E.ex.water} - T_{H.E.inwater}\} kW \tag{4.5}$$

(g) Thermal Energy recovered by VA system: It is also known as refrigeration effect produced by VA system. The expression is as given below:

$$E_{ref} = UA\{T_{ambient} - T_{cab}\}kW \quad (4.6)$$

(h) Total useful energy for combined heating & power: Total useful energy output of CHP system is calculated as the summation of electrical output and heat recovered from engine cooling and engine exhaust gases as given below:

$$E_{tCHP} = Electric\ output + E_{cw}kW \quad (4.7)$$

(i) Total useful energy for combined cooling & power: Total useful energy output of CCP system is calculated as the summation of electrical output and heat recovered (or refrigeration effect)by VA system:

$$E_{tCCP} = Electric\ output + E_{ref}kW \quad (4.8)$$

(j) Total useful energy for combined cooling, heating & power: Total useful energy output of CCHP system is calculated as the summation of electrical output, heat recovered from engine cooling and engine exhaust gases and heat recovered (or refrigeration effect)by VA system.

$$E_{tCCHP} = Electric\ output + E_{cw} + E_{ref}kW \quad (4.9)$$

(k) Thermal energy efficiency for combined heating & power: Thermal energy efficiency for CHP system is the ratio of total useful energy output in CHP system to the heat supplied or thermal energy contained in fuel, i.e.:

$$\eta_{CHP} = \frac{E_{tCHP}}{E_f} \quad (4.10)$$

(l) Thermal energy efficiency for combined cooling & power: Thermal energy efficiency for CCP system is the ratio of total useful energy output in CCP system to the heat supplied or thermal energy contained in fuel, i.e.:

$$\eta_{CCP} = \frac{E_{tCCP}}{E_f} \quad (4.11)$$

(m) Thermal energy efficiency for combined cooling, heating & power: Thermal energy efficiency for CCP system is the ratio of total useful energy output in CCP system to the heat supplied or thermal energy contained in fuel, i.e.:

$$\eta_{CCHP} = \frac{E_{tCCHP}}{E_f} \tag{4.12}$$

(n) Total Energy supplied to the generators of VA system: The heat supplied to the generators of the VA system was calculate using the formula:

$$E_{gen} = \epsilon C_{\min}(T_{hi}\text{-}T_{ci}) \text{ kW} \tag{4.13}$$

Where, ϵ is the effectiveness of the heat exchanger of the VA system generator. C_{min} is the minimum heat capacity and T_{hi} and T_{ci} are the temperatures of the hot fluid and cold fluid at inlet respectively.

(o) COP of VA System: COP of VA system was calculated by the following equation:

$$COP_{VA} = \frac{E_{ref}}{E_{gen}} \tag{4.14}$$

The following performance parameters were calculated for the systems developed under single generation, cogeneration and trigeneration modes based on the second law of thermodynamics:

Kotas [101] examined the ratio of input exergy to input energy (e_f/E_f) for hydrocarbons and found it to be constant and that the proportionality constant between fuel exergy and fuel energy is 1.04.

(i) The input exergy to the diesel engine is given by:

$$e_f = 1.04E_f \; kW \tag{4.15}$$

Exergy lost in exhaust gas without cooling & heating (single generation) is given by:

$$e_{ex} = \dot{m}_{ex}[C_{p_{ex}}\{T_{eng.ex.gas} - T_{ambient}\} - T_O\{S_{eng.ex\ gas} - S_{ambient}\}]kW \tag{4.16}$$

(ii) Exergy recovered for engine cooling and exhaust is given by:

$$\boldsymbol{e_{cw} = \dot{m}_w C_{p_w}[\{T_{H.E.ex.water} - T_{H.E.inwater}\} - \mathbf{T_o} \ln(\frac{T_{H.E.ex.water}}{T_{H.E.inwater}})]} + \boldsymbol{\dot{m}_w C_{p_w}[\{T_{eng.ex.water} - T_{eng.inwater}\} - \mathbf{T_o} \ln(\frac{T_{eng.ex.water}}{T_{eng.inwater}})]\ kW} \quad (4.17)$$

(iii) Exergy recovered by VA system is given by:

$$e_{ref} = \dot{m}_{ex} C_{p_{ex}}\left[(T_{eng.ex.gas} - \mathrm{T_{ex.VA}}) - \mathrm{T_o} \ln(\frac{T_{eng.ex.gas}}{T_{ex.VA}})\right] k \quad (4.18)$$

(iv) Total useful exergy for combined heating & power is given by:

$$e_{tCHP} = Electric\ output + e_{cw} \quad (4.19)$$

(v) Total useful exergy for combined cooling & power is given by:

$$e_{tCCP} = Electric\ output + e_{ref} \quad (4.20)$$

(vi) Total useful exergy for combined cooling, heating & power is given by:

$$e_{tCCHP} = Electric\ output + e_{cw} + e_{ref} \quad (4.21)$$

(vii) Exergy efficiency of diesel engine (only power) is given by:

$$\eta_p = \frac{Electric\ output}{e_f} \quad (4.22)$$

(viii) Exergy efficiency for combined heating & power is given by:

$$\eta_{CHP} = \frac{e_{tCHP}}{e_f} \quad (4.23)$$

(ix) Exergy efficiency for combined cooling & power is given by:

$$\eta_{CCP} = \frac{e_{tCCP}}{e_f} \tag{4.24}$$

(x) Exergy efficiency for combined cooling, heating & power is given by:

$$\eta_{CCHP} = \frac{e_{tCCHP}}{e_f} \tag{4.25}$$

(xi) Maximum possible coefficient of performance is given by:

$$COP_E = \left(1 - \frac{T_o}{T_{gen}}\right)\left(\frac{T_{eva}}{T_o - T_{eva}}\right) \tag{4.26}$$

(xii) Exegetic efficiency for VA system is given by:

$$\eta_{ex} = \frac{COP}{COP_E} \tag{4.27}$$

CHAPTER 5
EXPERIMENTAL RESULTS AND DISCUSSION

In this section, various performance parameters defined in the previous chapter such as BSFC, BTE, emissions (CO, HC, NO_x, CO_2 and Smoke), exhaust gas temperature and recovered heat were evaluated for single generation, cogeneration (CCP & CHP) and trigeneration modes at different load conditions i.e. zero load to full load. Three sets of readings were taken for all cases. Error analysis is discussed at Appendix A. The following sections show the test results of average values of the three tests for each parameter. Optimum fuel injection pressure and fuel injection timing for the diesel engine with diesel fuel were determined by operating the engine at different injection pressures and injection timings. With the change of shim quantity, engine injection timing changes. Experimental data shows that the **Kirolsker AV1** water cooled diesel engine, which was used for research, has 23° crank angle as optimum injection timing and 195 kgf/cm^2 optimum fuel injection pressure for neat diesel and it was verified with results obtained in an earlier research on the same engine setup and the engine manual of **Kirolsker AV1** water cooled diesel engine. At this optimum injection pressure and optimum injection timing, the engine produces maximum brake thermal efficiency and minimum brake specific fuel consumption [38].

5.1 Engine generator performance for single generation, cogeneration and trigeneration systems

5.1.1 Brake thermal efficiency (BTE)

Brake Thermal Efficiency (BTE) is an important parameter, as it provides a measure of net power developed by the engine, which is readily available for use at the engine output shaft. The variation of brake thermal efficiency with different loads (0, 1000, 2000, 3000 & 3700 watts) with single generation, cogeneration (CCP & CHP) and trigeneration system is shown in Fig. 5.1.The brake thermal efficiency was vary from 14.47% at 1000 watts load to 31.31% at full load in single generation while in trigeneration, it was vary from 14.75% at 1000 watts load to 29.22% at full load. In cogeneration system (CCP & CHP) the BTE was same at full engine load i.e. 30.26%. The results show that BTE of single generation, cogeneration (CCP & CHP) and trigeneration systems are nearly the same. It can be seen by results that the performance of engine generator is not influenced adversely by addition of VA system and/or heat exchanger to the engine generator.

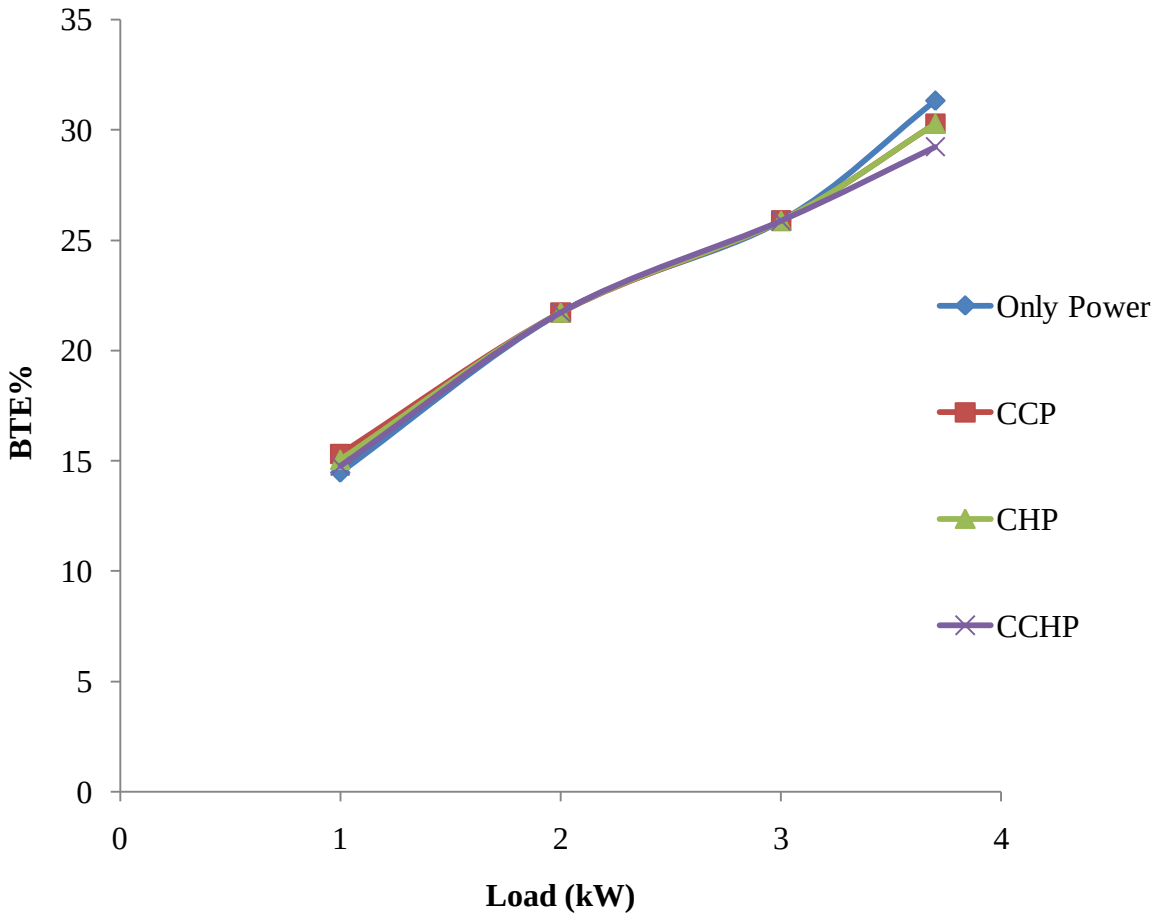

Fig.5.1 Variation of brake thermal efficiency with load for different operation modes

5.1.2 Brake specific fuel consumption (BSFC)

Specific fuel consumption is a comparative parameter that shows how efficiently an engine is converting energy of fuel into work. BSFC is ratio of fuel consumed in kg/h to the brake power. For the determination of fuel consumed in kg/h, volumetric flow rate of diesel was measured by burette method and then it was multiplied by the density of diesel. Figure 5.2 shows the variation of brake specific fuel consumption for different operation modes (single generation, cogeneration & trigeneration) at no engine load to full engine load. The difference in BSFC in case of single generation, cogeneration and trigeneration was negligible. It means performance of engine generator was not influenced adversely by addition of VA system and/or heat exchanger to the engine generator.

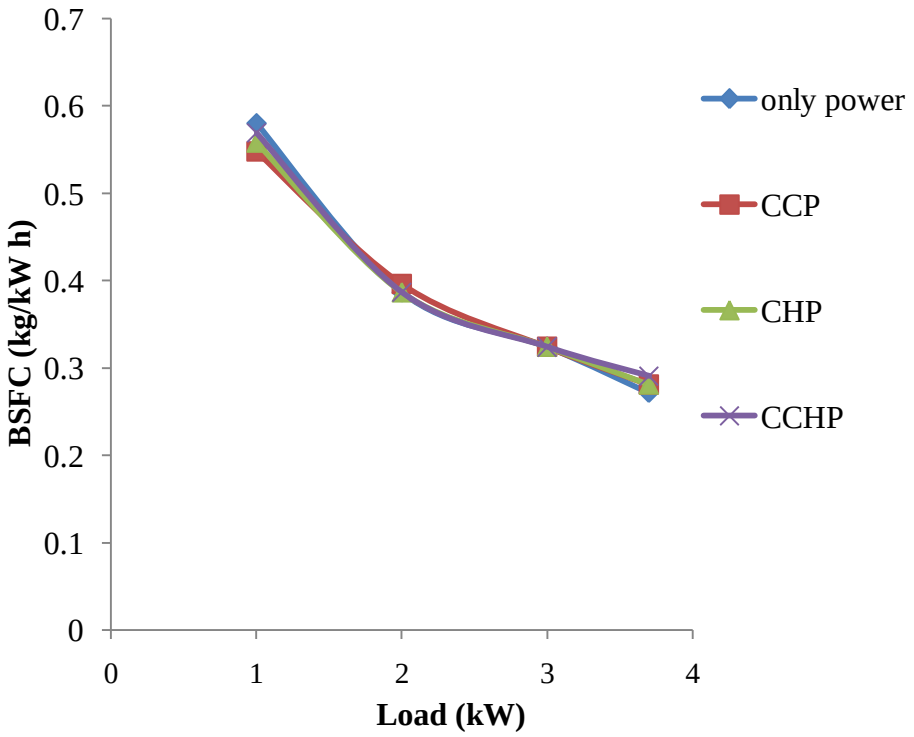

Fig.5.2 Variation of brake specific fuel consumption with load for different operation modes

5.2 Emissions' analysis for single generation, cogeneration and trigeneration modes

The emission of CO, HC, NO_x, CO_2 and smoke from single generation, cogeneration and trigeneration systems at various loads are describe in this section. The aim of these tests was to do a comparative analysis of engine exhaust emissions of single generation, cogeneration and trigeneration systems. The results show that the emissions from the engine on single generation, cogeneration and trigeneration systems are nearly the same at the same load and this proves that integration of vapor absorption system and/or heat exchanger does not adversely effect the performance of engine generator.

5.2.1 NO_x emissions

Among the gaseous pollutants emitted by diesel engines, NOx is the most significant. NOx formation is mainly due to high in-cylinder temperature, excess oxygen availability and duration of combustion. As the load increases, in-cylinder temperature increases, producing more NO_x. Due to increased back pressure in cogeneration and trigeneration mode the available oxygen in cylinder would be less as compared to single generation which results in reduced NOx emissions in cogeneration and trigeneration as compared to single generation.

Figure 5.3 shows the variation of NO_x with engine load for comparison between single generation, cogeneration (CCP &CHP) and trigeneration systems.

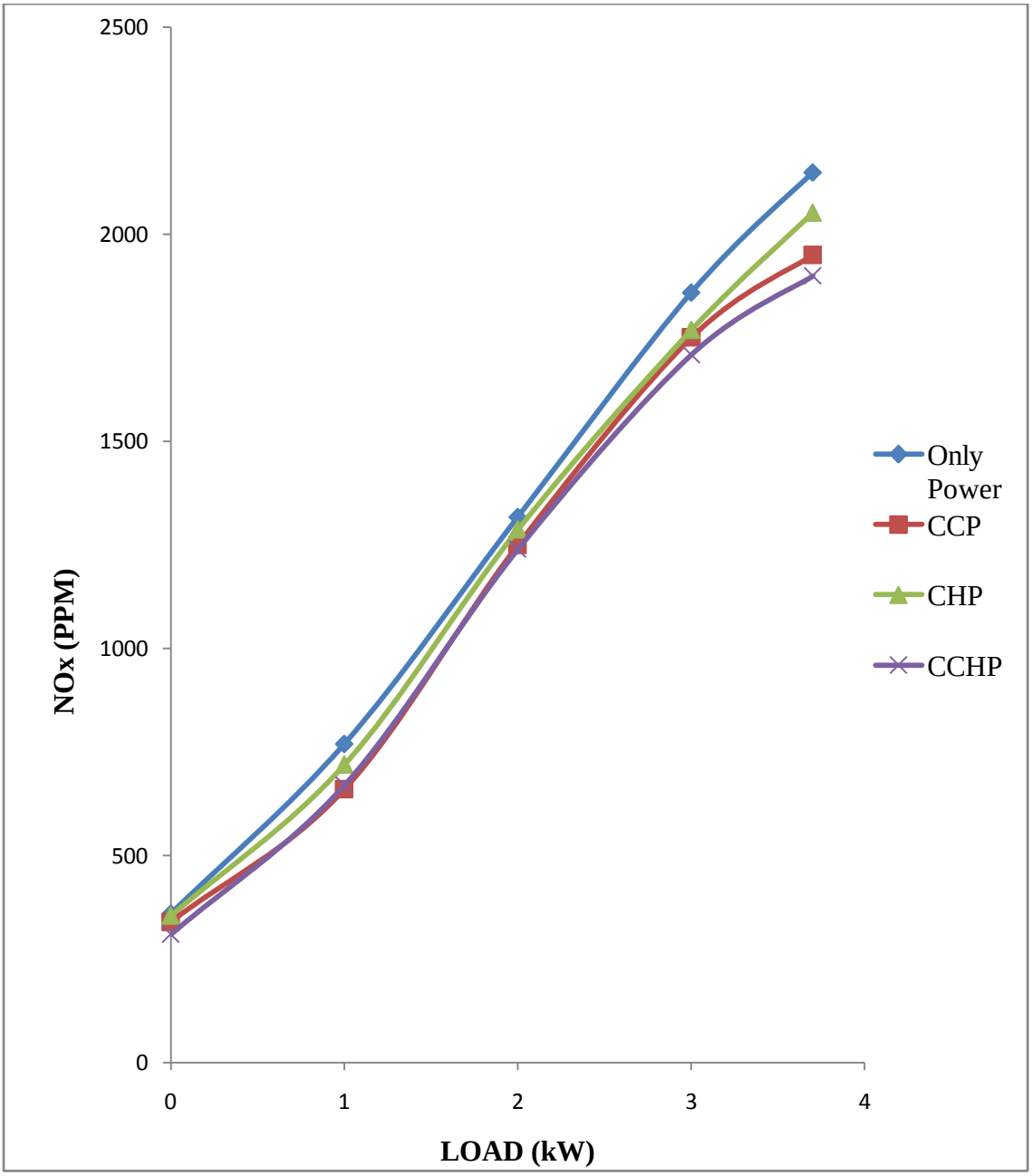

Fig.5.3 Variation of NOx emissions with engine loads for different operation modes

5.2.2 Smoke

Smoke from exhaust is a visible indicator of the combustion process within the engine. As the load of the diesel engine increases, larger fuel injection combined with lack of oxygen in the cylinder contribute to a very quick rise in smoke emission [98].

Fig. 5.4 shows the variation of smoke with engine load for comparison between single generation, cogeneration (CCP &CHP) and trigeneration systems. In single generation system, value of smoke varied from 10.5% at zero load to 30% at full load while in trigeneration, it varied from 8.5% to 25.2% at the same load conditions. The exhaust gas temperature obtained in CCP, CHP and CCHP mode was found less than single generation which indicates that the combustion temperature in single generation is more than CCP, CHP and CCHP. Lower combustion temperature results in reduced thermal cracking thus less smoke is produced in CCP, CHP and CCHP as compared to single generation.

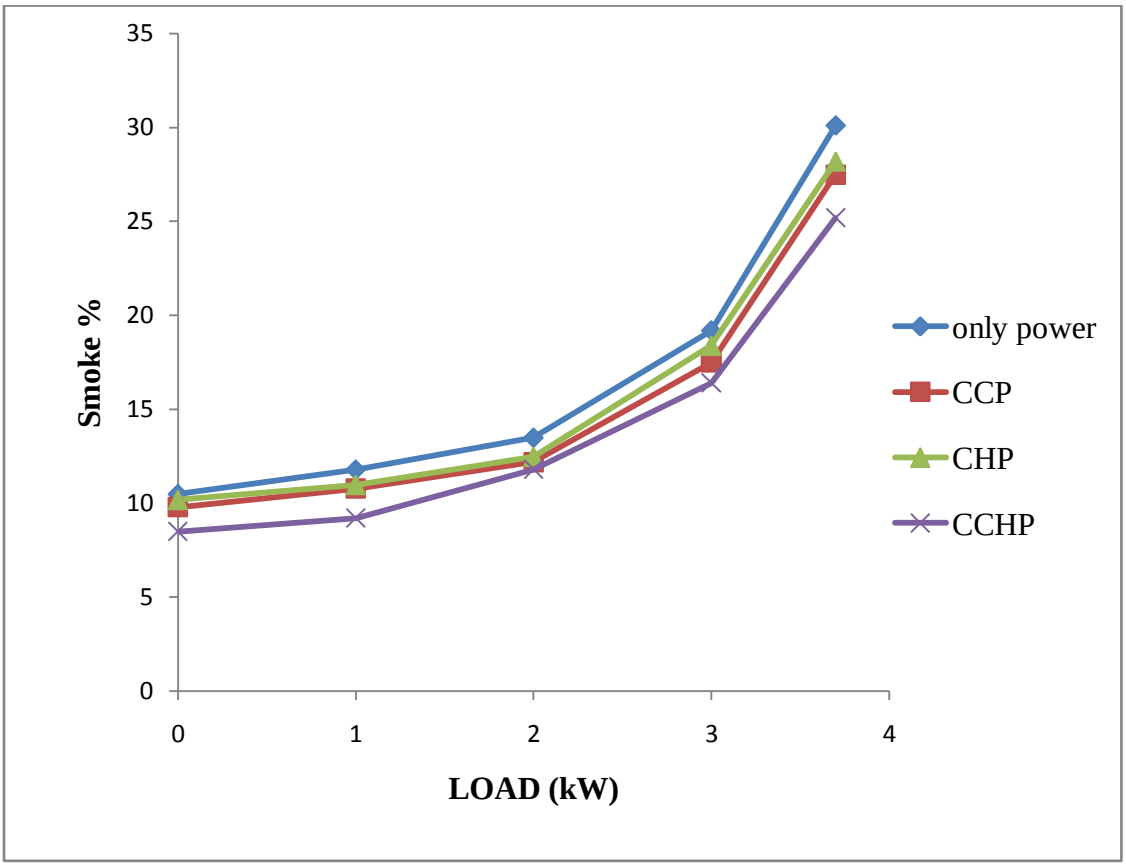

Fig.5.4 Variation of smoke emission with engine load for different operation modes

5.2.3 CO emission

CO is formed due to incomplete combustion of fuel. From Fig.5.5 it is clear that at idle or low load conditions CO emission was high due to low operating temperatures and incomplete combustion of fuel. With the increase in load, both, the operating temperature and mixing of fuel increases, resulting in reduction of CO emissions. But at high loads, the available oxygen for combustion becomes lesser (lean air-fuel ratio), resulting in increased CO emissions. The

concentration of CO in exhaust at idle engine load was 0.05%, 0.04%, 0.04% and 0.04% for single generation, CCP, CHP and CCHP modes respectively.

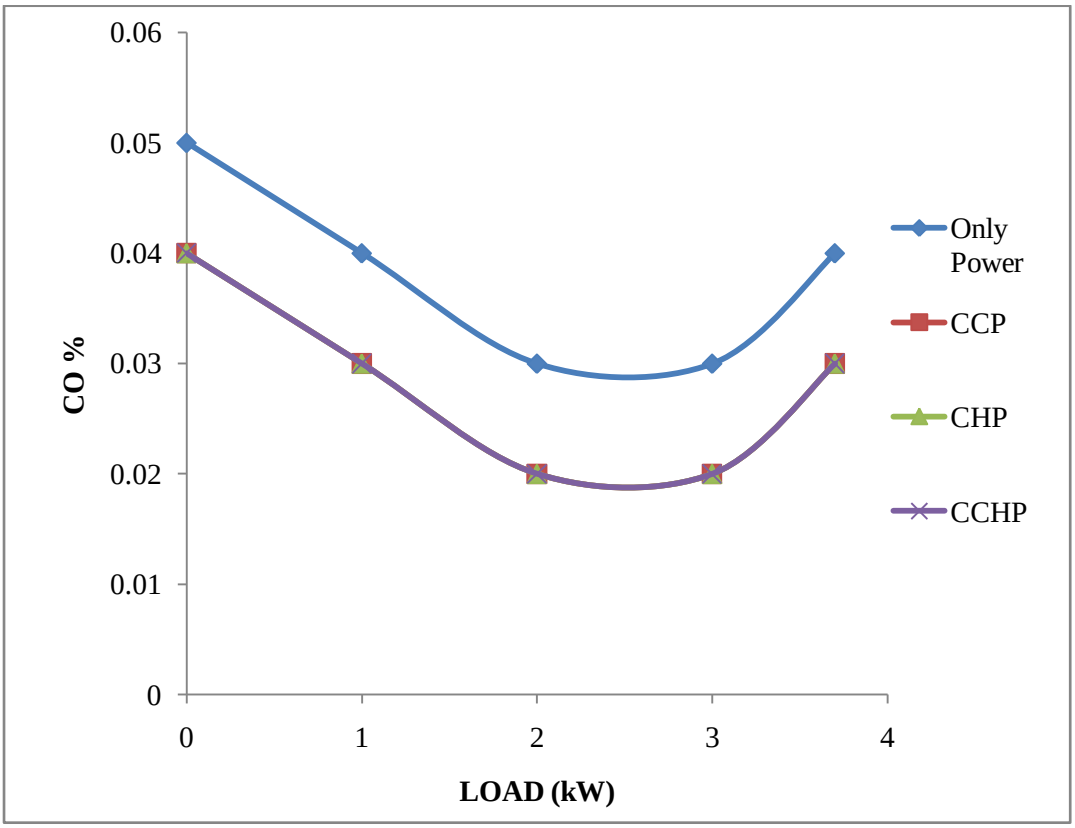

Fig.5.5 Variation of CO emission with engine loads for different operation modes

5.2.4 HC emission

Figure 5.6 shows the variation of unburned hydrocarbon with the load for comparison between single generation, cogeneration (CCP & CHP) and trigeneration (CCHP) systems. It was observed from Fig.5.6 that at full engine load condition, HC emission in PPM was 58, 51, 55 and 49for single generation, CCP, CHP and CCHP modes respectively. In cogeneration/trigeneration the pressure drop during the exhaust was taking place gradually because of longer length of pipe, which resulted in improved scavenging during exhaust. This resulted in improved combustion and hence, HC got reduced [99].

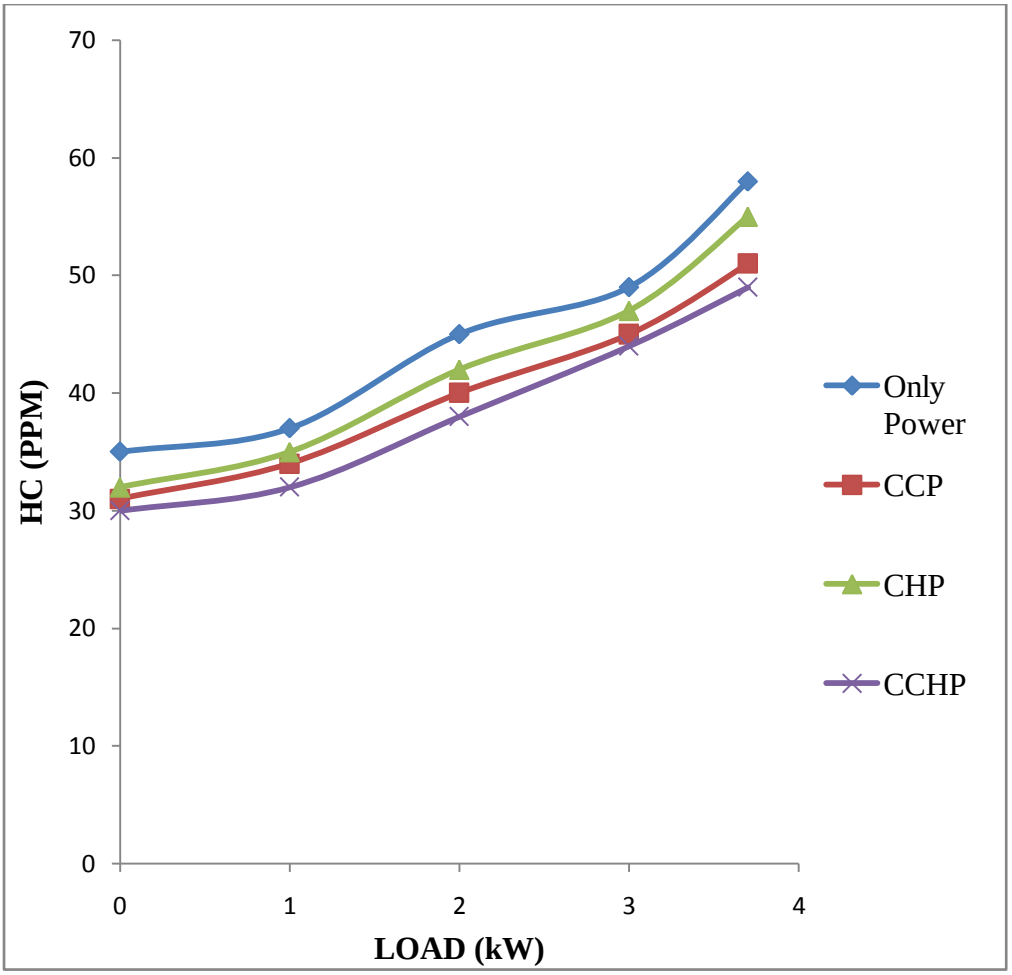

Fig.5.6 Variation of HC emission with engine load for different operation modes

5.2.5 CO_2 emission

CO_2 emission increased with the increase of engine load in all modes. It was observed from Fig.5.7 that CO_2 emission was more in case of single generation compared to that in cogeneration and trigeneration modes. In single generation mode CO_2 emission varied from 3.2% to 10% at zero load to full load. While in trigeneration mode, CO_2 emission varied from 2.9% to 8.5% at zero load to full load conditions.

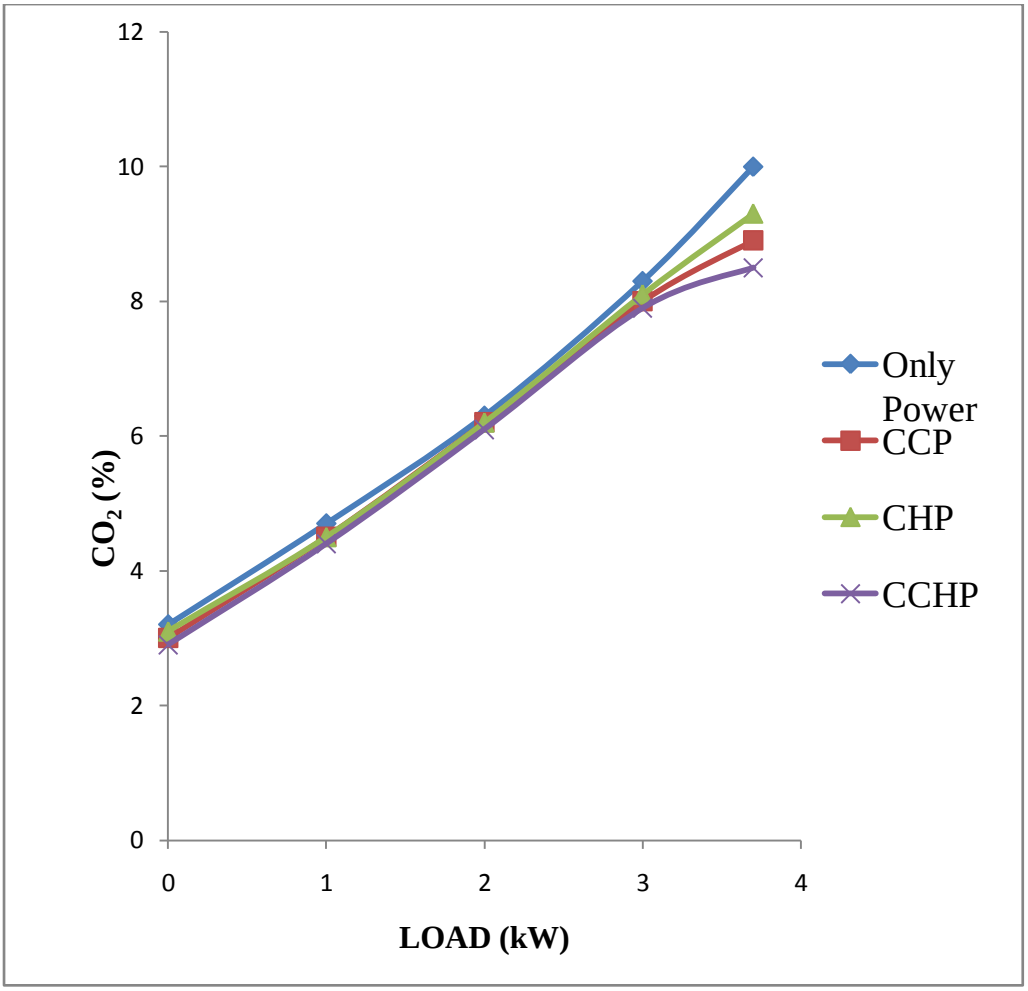

Fig.5.7 Variation of CO_2 emission with engine load for different operation modes

5.3 Temperature of exhaust gas when vented out to atmosphere in different modes

5.3.1 Temperature of exhaust gas when vented out to atmosphere in single generation

In single generation mode, temperature of exhaust gas vented to atmosphere was the same as at the engine exhaust. Figure 5.8 shows the variation of temperature of exhaust gas when vented out to atmosphere with the engine load. It was observed that with the increase in load, engine exhaust gas temperature also increased. The exhaust gas temperature for single generation varied from 170^{o}C at zero load to 360^{o}C at 3700 watt (full load).

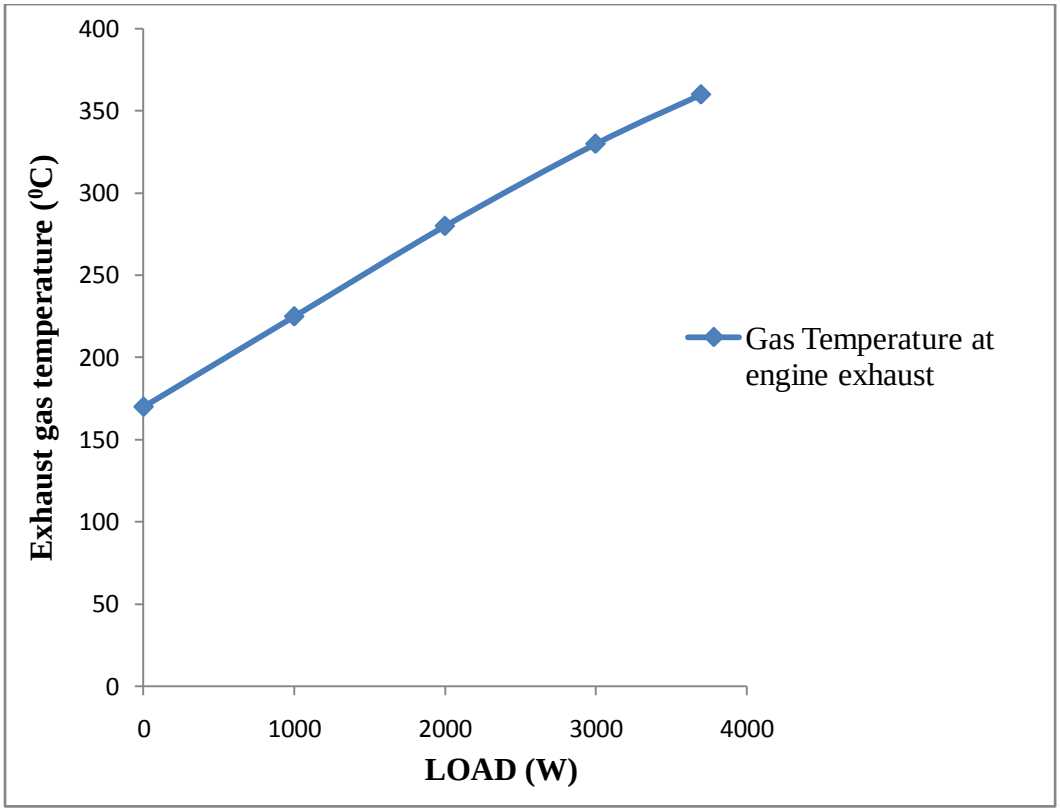

Fig.5.8 Variation of exhaust gas temperature with load for single generation

5.3.2 Temperature of exhaust gas when vented out to atmosphere in CCP mode

In the CCP mode, gases coming from engine exhaust were passed to VA system. So, in CCP mode, temperature of exhaust gas when vented out to atmosphere was the temperature at the exit of VA system. Figure 5.9 shows the variations of exhaust gas temperature in CCP mode with the engine load when one, two, three and all four VA units were in operation. More number of VA units was put to operation and more reduction of exhaust gas temperature after the VA system was observed. Hence, it was observed that the temperature of exhaust gas at exit from VA system was lower when all four units were in operation as compared to when only one, two or three VA units were in operation. The exhaust gas temperature in CCP mode (when only one unit on VA system was in operation) varied from 86^0C at zero load to 230^0C at 3700 watt (Full load). Whereas, the exhaust gas temperature varied from 75^0C at zero load to 210^0C at full load, 70^0C at zero load to 200^0C at full load and 65^0C at zero load to 185^0C at full load when two, three and four units of VA system were put in operation respectively.

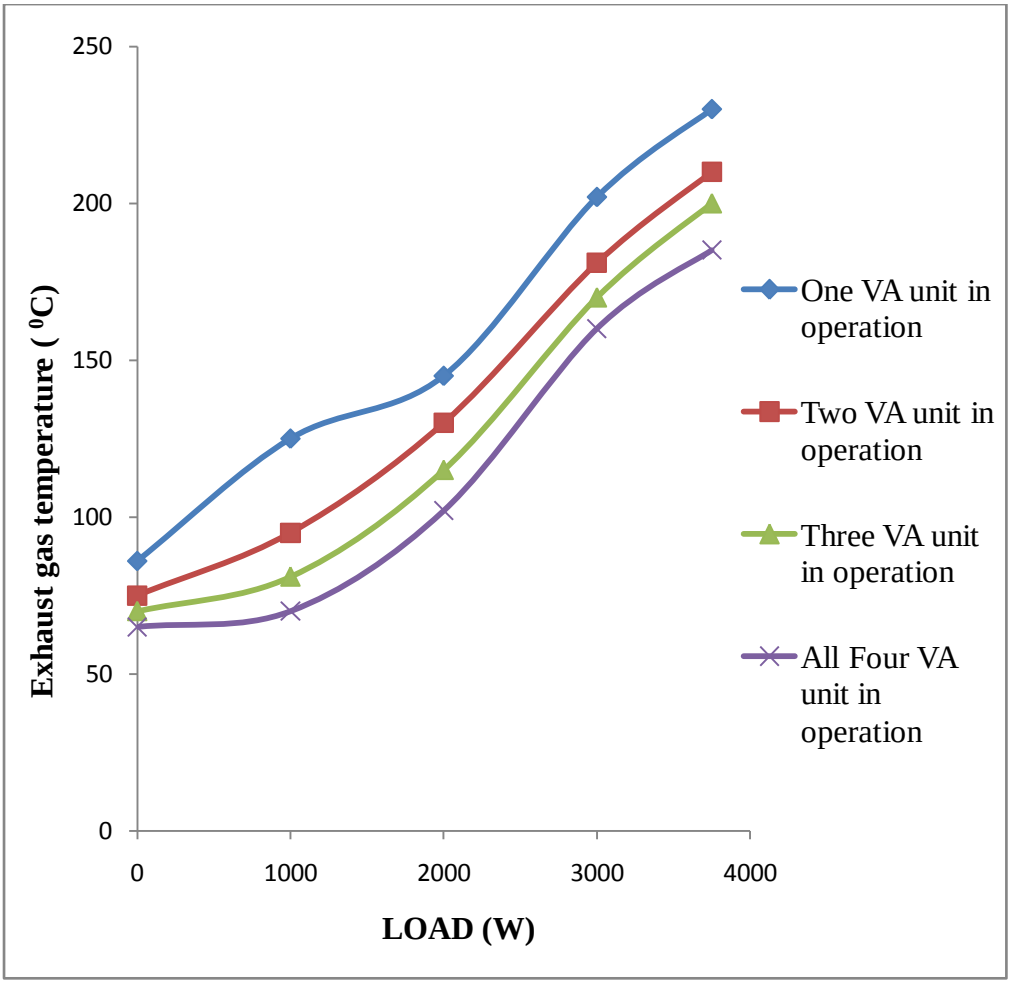

Fig.5.9 Variation of exhaust gas temperature at exit of VA system with engine load for CCP

5.3.3 Temperature of exhaust gas when vented out to atmosphere in CCHP and CHP modes

In the CCHP mode, exhaust gases from engine were passed to VA system for space cooling. Then exhaust gases, coming out from VA system generators, were passed to the heat exchanger for hot water production. Whereas, in CHP mode, exhaust gases from engine were directly passed to the heat exchanger (hence, skipping the VA system). In both, CCHP and CHP modes, the temperature of exhaust gases measured was the temperature of gas at the exit of heat exchanger. Figure 5.10 shows the variation of exhaust gas temperature in CCHP/CHP mode with the engine load and it was observed that the exhaust gas temperature at exit of heat exchanger in CHP mode was higher than that in CCHP mode. The exhaust gas temperatures in CCHP mode varied from 52^0C at zero load to 78^0C at 3700 watt (full load). Similarly, in CHP mode, temperature of exhaust gas varied from 57^0C at zero load to 90^0C at 3700 watt (full load).

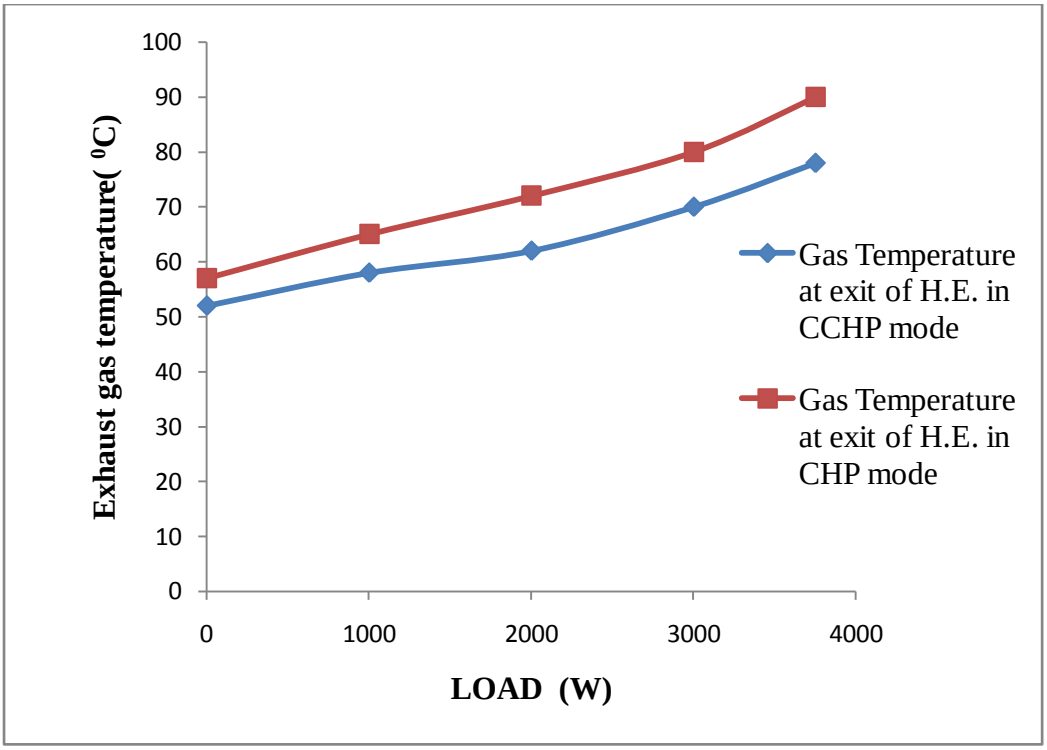

Fig.5.10 Variation of exhaust gas temperature at exit of heat exchanger with engine load in CHP and CCHP modes

5.4 Performance of vapor absorption system

Combination of four units of Electrolux vapor absorption system, each with a capacity of 51 liters and heat input of 95W, was used for space cooling. Different parameters of vapor absorption system were recorded and the performance of vapor absorption system was evaluated during the working of cogeneration/trigeneration system on different engine loads. Four flow regulating valves were provided for regulating the flow of exhaust coming out from the engine to the generators of each unit. Heat was to be provided to generators of the four vapor absorption units for each unit to provide cooling effect. The exhaust flow was directed towards the four VA units one by one by opening and closing the valves (as required) of the individual VA units. In the beginning only the top left generator was operated keeping the rest of the generator valves closed. When the temperature of top left generator reached 100^{o}C, then the valve of top right generator of VA system was opened. In that condition, both, top left and top right units were in operation. Similarly, different permutations and combinations of valves were operated upon depending on the temperature of each VA unit's generator. There were total 15 combinations for operation of VA units. If G_1, G_2, G_3 and G_4 are considered as the top left, top right, bottom left and bottom right generators respectively and similarly E_1, E_2, E_3 and E_4 are considered as the top left, top

right, bottom left and bottom right evaporators respectively, then the observed sequence of operation of VA units is given in Table 5.1.The generator and evaporator temperatures of each VA unit were recorded in each sequence of operation and a graph between generator temperature and combination of VA units was plotted. Similarly, a graph between evaporator temperature and combination of VA units was also plotted. Figure 5.12 and Fig. 5.13 show the variation of generator & evaporator temperature of each VA unit with the combination of VA units respectively.

Table 5.1Sequence of operation of VA units with all 4 units to reach steady state condition

S. No.	1	2	3	4	5	6	7	8	9	10	11	12	13	14	15
Sequence of operation	G_1	G_1, G_2	G_2	G_2, G_3	G_3	G_3, G_4	G_4	G_1, G_3	G_2, G_4	G_1, G_4	G_1, G_2, G_3	G_2, G_3, G_4	G_1, G_3, G_4	G_1, G_2, G_4	G_1, G_2, G_3, G_4

5.4.1 Variation of generator and evaporator temperature with different combinations of VA units

From the graphs at Fig.5.11 & 5.12, it was observed that when the top left unit of VA system was in operation, then generator and evaporator temperature of this unit reached 106^{o}C & 7^{o}C respectively. In that condition, generator temperature of top right unit also increased due to conduction and reached 40^{o}C but still there was no change of evaporator temperature of other units of the VA system. The target was to reach and maintain a steady state condition i.e., to bring the generator temperature of each VA unit to approx. 105^{o}C (as per the specifications of the Electrolux VA system, the generator temperature should lie between 100 and 130^{o}C to obtain the refrigerating effect in evaporator).

Using different combinations of VA units, the required generator temperature was attained by opening different valves as per the prescribed sequence. With combination at s. no. 12, 13, and 14 of Table 5.1, when three valves were operated, evaporators of corresponding VA units reached the temperature of10^{o}C but the evaporator temperature of the remaining one VA unit for which the valve remained closed, was observed to be above 10^{o}C, which was not desirable situation. At this stage, although the cooling effect was produced in the cabin as seen from the plot of cabin

temperature difference vs. combination of VA units (as shown in Fig. 5.13), but the result obtained was not optimum and steady state was not obtained inside the cabin.

At full engine load, all four valves were opened and all VA units' generators' temperatures were found to be at 110^{o}C. In the experimental set-up, it took approximately 4 hours to reach the desired steady state condition. In that condition, generator and evaporator temperatures of the top left, top right, bottom left and bottom right VA units were recorded as 110^{o}C, 110^{o}C, 109^{o}C and 110^{o}C; and 7^{o}C, 7^{o}C, 8^{o}C& 6^{o}Crespectively. Figure 5.11 and 5.12 show the variation of generator temperature and evaporator temperature for different combinations of VA units respectively.

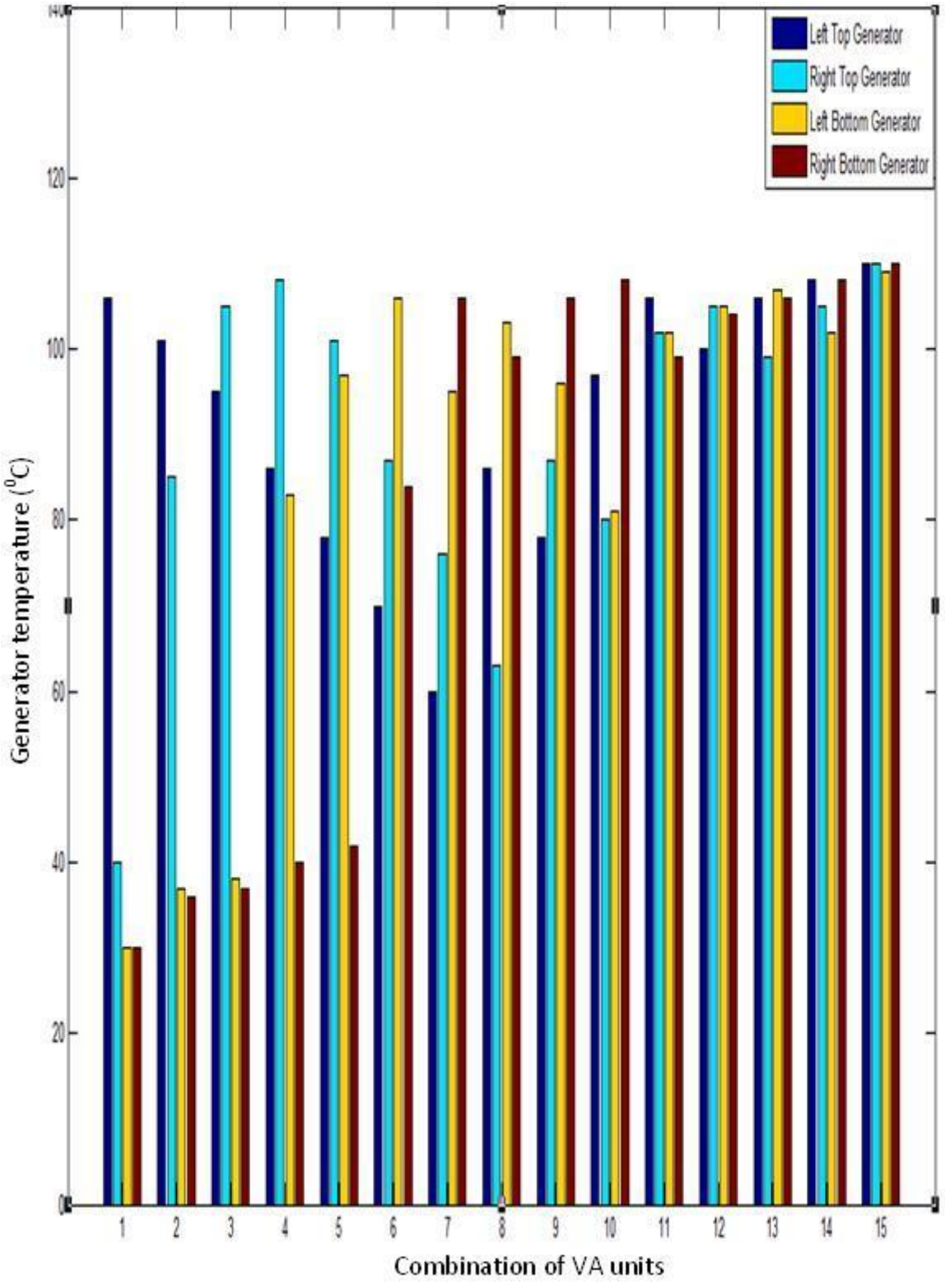

Fig.5.11 Variation of generator temperature with combination of VA units

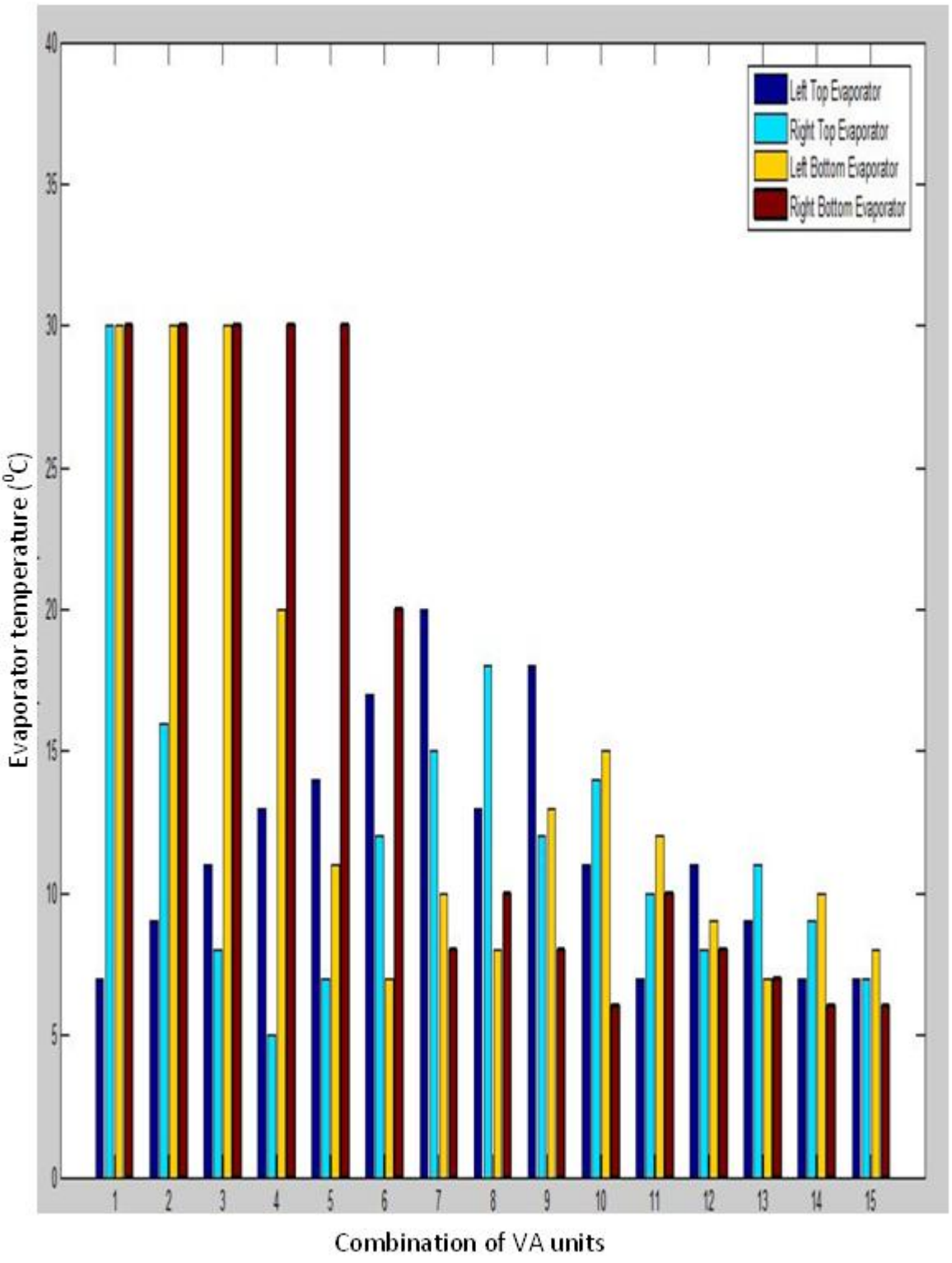

Fig.5.12 Variation of evaporator temperature with combination of VA units

5.4.2 Variation of temperature difference of cabin and ambient

Figure 5.13 shows the variation of temperature difference (cabin and ambient) with respect to time. Since the temperature of cabin at different heights was different, 3 thermocouples were placed in the cabin at a height of 0 mm, 900 mm and 1750 mm from the ground, and the average of these three temperatures was considered as $T_{cab,}$ to measure space cooling effect. The operation of VA system was same as described in previous section. Initially, there was no temperature difference between ambient and the cabin. After an hour of operation and following the sequence of operation of each VA unit as discussed before, temperature difference of 1.3^0C was observed between the cabin and ambient and it increased slowly but consistently. When the temperature of all the evaporators reached around 7^0C after 4 hours from engine start up time, the temperature difference between the cabin and ambient was found to be around 4^0C. However, the desired cooling effect could not be produced unless the sequence of operation was rigidly followed as mentioned in Table 5.1 at full load. Hence, at full engine load and when all four valves were opened following the right sequence, remarkable temperature difference between ambient and the cabin was obtained i.e. 6.5^0C, after approx. 6 hours from engine start up time. However, further drop in temperature was not achieved in the cabin, thus balancing the cooling effect from VA system with the heat gain from the atmosphere and the equipments.

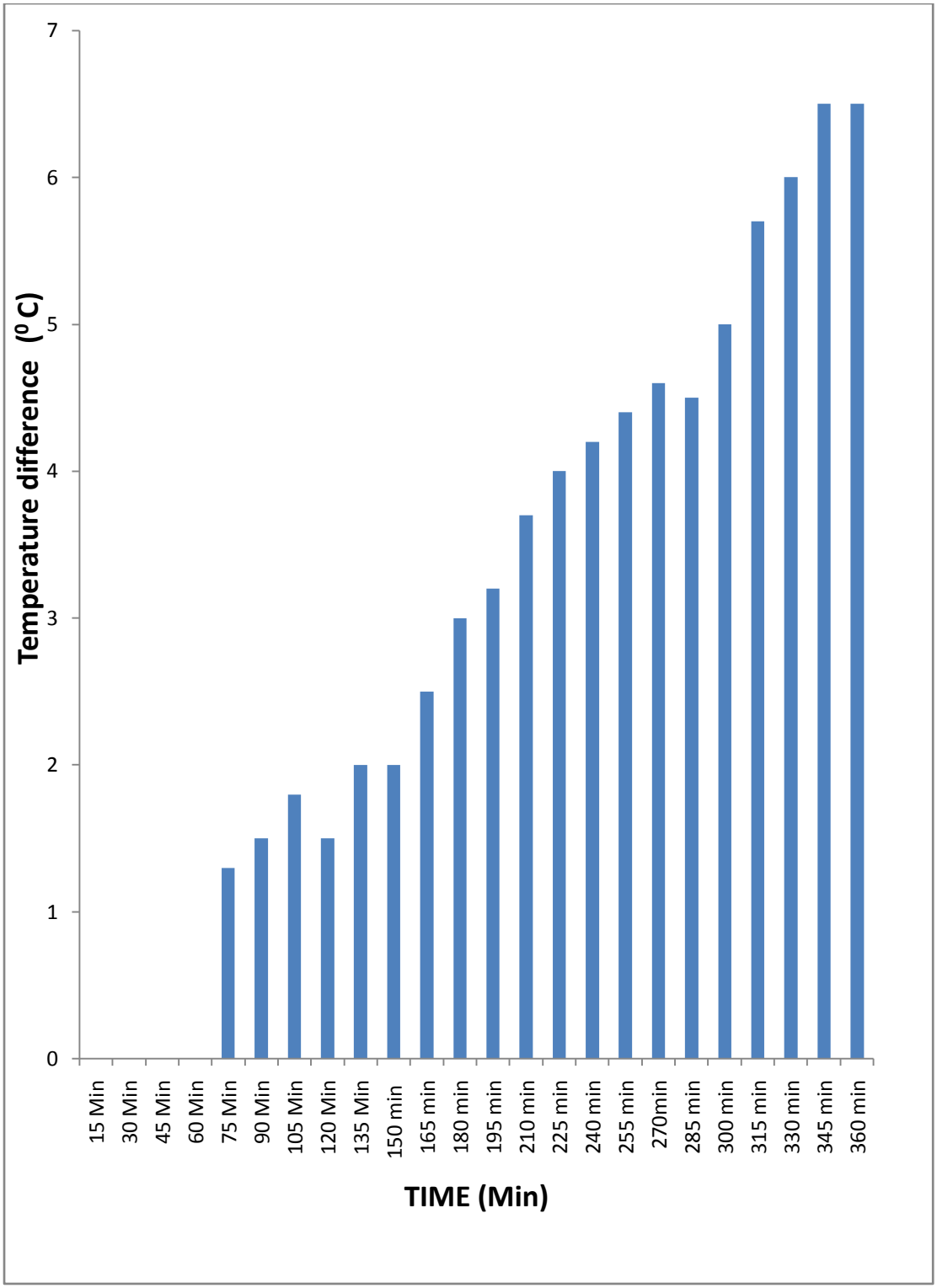

Fig.5.13 Variation of temperature difference (between cabin space and ambient)

5.5 Heat recovered from cooling water and engine exhaust in CCHP and CHP modes

In this section, heat recovered from engine cooling water and engine exhaust is discussed in CCHP and CHP modes. In the CCHP mode, cooling water, after extracting heat from engine block, was passed through the heat exchanger as cold fluid. Whereas, exhaust gases coming from engine, after passing through the VA system generators for space cooling, were passed through the heat exchanger as hot fluid for further heating the water i.e., the cold fluid, for raising its temperature further. While in CHP mode, cooling water after extracting heat from engine block was passed through the heat exchanger and exhaust gases coming from engine were directly passed through the heat exchanger for hot water production. Experiments on CCHP and CHP systems were performed and the data of the heat, collected from engine exhaust and engine cooling system (run through system in engine block),were recorded to evaluate the amount of heat energy obtained from the trigeneration (CCHP) and cogeneration (CHP) systems.

Figure 5.14 (a, b) show the variation of heat from engine coolant and engine exhaust with respect to engine load in CCHP and CHP modes respectively. In case of CCHP mode, the heat recovered from engine exhaust with heat exchanger varied from 243.83 W at no load to 1463 W at full load, whereas, the heat obtained from engine cooling system varied from 487.67 W at no load to 2727.16 W at full load. Hence, the total amount of heat obtained from CCHP system varied from 731.5 W at no load to 4190.16 W at full load.

In case of CHP mode, the heat recovered from engine exhaust with heat exchanger varied from 243.83 W at no load to 1950.67 W at full load, whereas, the heat obtained from engine cooling system was the same as in CCHP mode i.e., 487.67 W at no load and 2727.16 W at full load. Thus, the total amount of heat obtained from CHP system varied from 731.5 W at no load to 4677.83 W at full load.

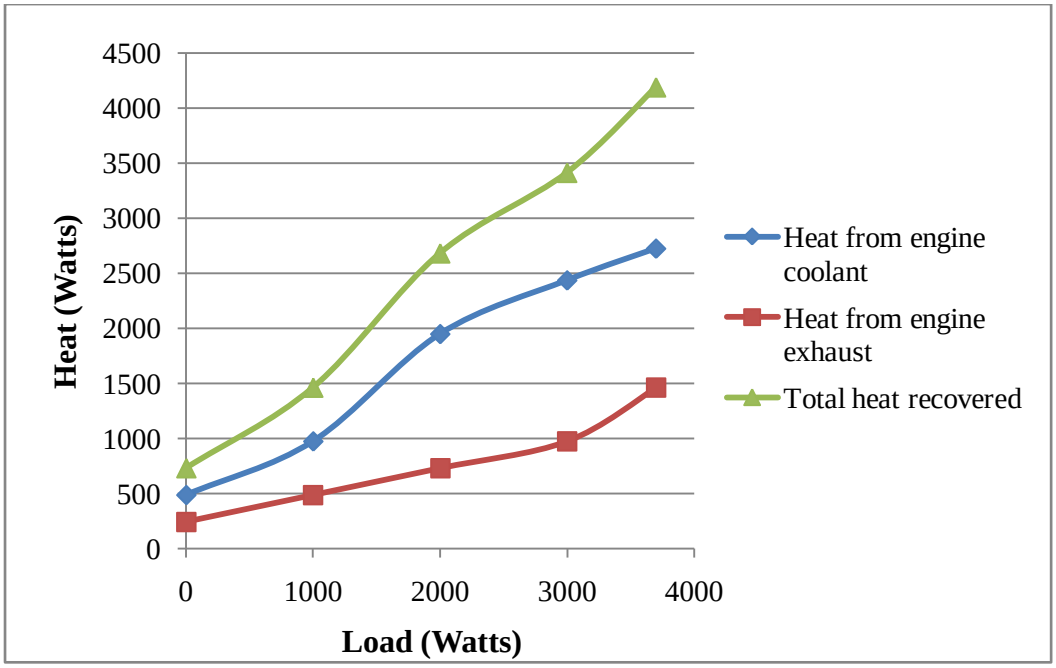

(a)

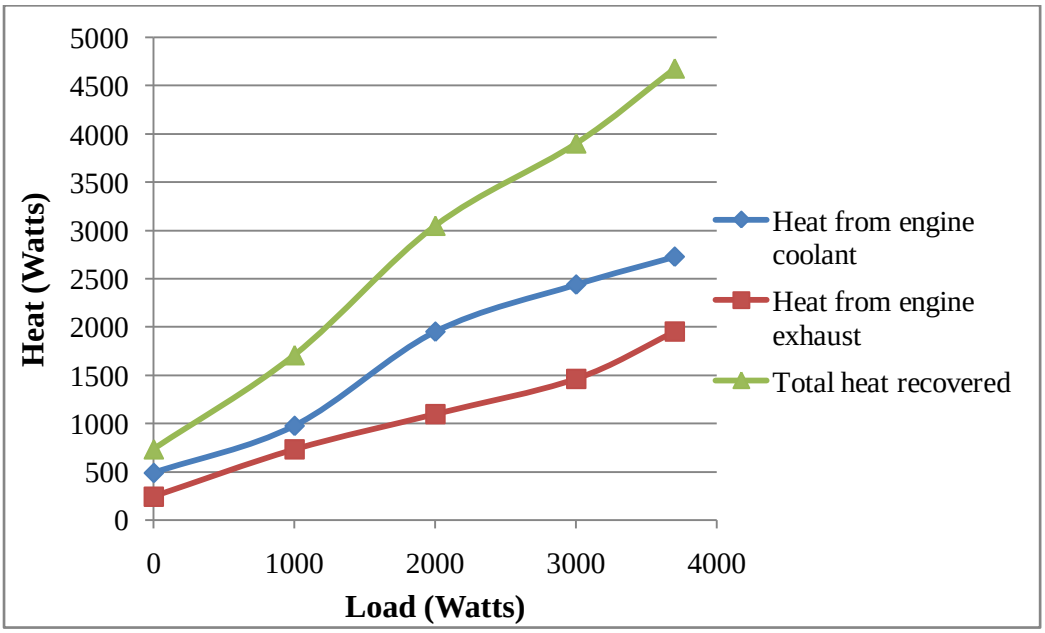

(b)

Fig.5.14 Variation of heat from engine coolant and engine exhaust with engine load in (a) CCHP mode and (b) CHP mode

5.6 Performance of trigeneration system compared to that of single generation and cogeneration systems

Various performance parameters such as overall useful energy output, total thermal efficiency, specific fuel consumption and CO_2 emission in kg/kWh for various modes of operation are discussed in this section. Various graphs in this section show the comparison of overall useful energy output, total thermal efficiency, specific fuel consumption and CO_2 emission in kg/kWh between CCHP, CHP, CCP and single generation systems at full load.

The test results were compared and verified with the results of experimental study on a small household size trigeneration carried out by various researchers mentioned at [86, 90,101]. It was found that the range of values for the performance parameters obtained from the test results were matching satisfactorily with the results from the above mentioned references.

5.6.1 Useful energy output

The useful energy output for CHP varied from 2.70 kW at 1000 watt load to 8.38 kW at 3700 watt (full load) compared to 1000 watt to 3700 watt (full engine load) for single generation system. However, in CHP (0.975 kW) and CCHP (0.731 kW) systems, energy was available in the form of exhaust heat even when the engine was in idling (no load) condition. The increase in useful energy output was from 170% at 1000 watt to 119.72% at 3700 watt. The useful energy output for CCHP system varied from 2.46 kW at 1000 watt to 8.135 kW at 3700 watt. Hence, the increase in useful energy output is from 146% at 1000 watt to 119.86% at 3700 watt. In CCP system, refrigeration effect was obtained only at 3700 watt i.e. full engine load. So, in CCP mode, useful energy output varied from 1000 watt to 3990 watt compared to 1000 watt to 3700 watt for single generation system. The increase in useful energy output was from 0% at 1000 watt to 7.83% at 3700 watt. Figure 5.15 shows the comparison of useful energy output for various modes of operation at full engine load.

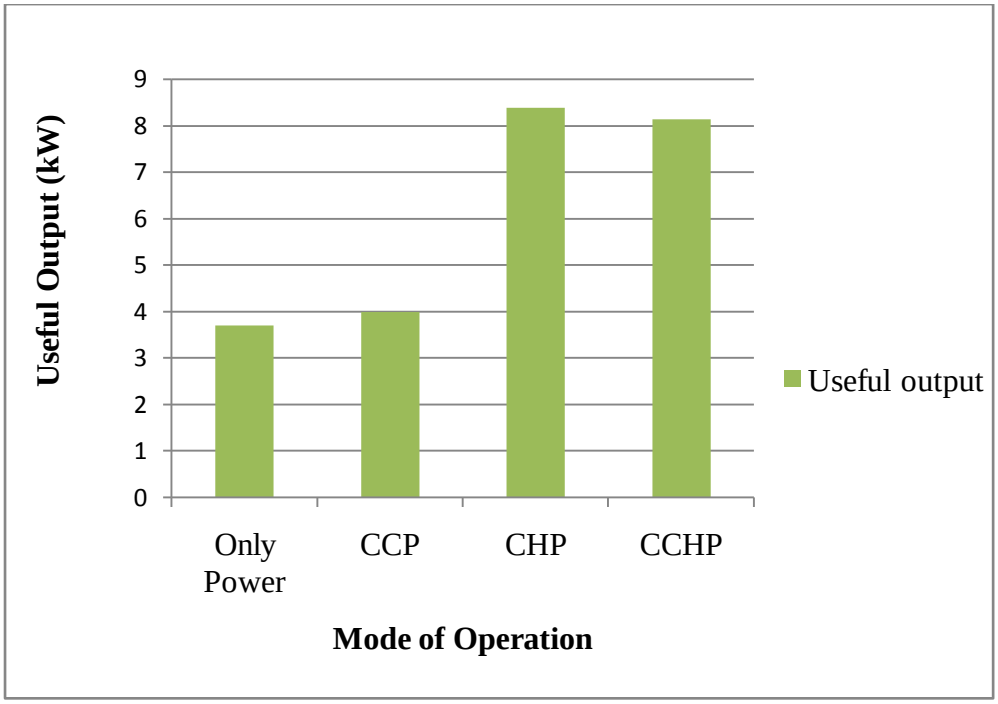

Fig.5.15 Comparison of useful energy output for various modes at full engine load

5.6.2 Total thermal efficiency

The total thermal efficiency for CHP varied from 40.61% at 1000 watt load to 65.61% at 3700 watt (full engine load) compared to 14.47% and 30.85% respectively for single generation system. Hence, the increase in total thermal efficiency was from 180.64% at 1000 watt to 112.67% at 3700 watt in the case of CHP. The total thermal efficiency for CCHP system varied from 36.28% at 1000 watt to 63.4% at 3700 watt. Hence, for CCHP, the increase in total thermal efficiency was 150.72% at 1000 watt and 105.51% at 3700 watt. In CCP system, total thermal efficiency varied from 15.31% at 1000 watt to 32.2% at 3700 watt. So, in CCP, increase in total thermal efficiency was 5.80% at 1000 watt and 4.37% at full engine load. Since, the COP of VA system is less than 1, it takes more energy in the form of heat as input than the output in the form of cooling, and so, the increase in efficiency in case of CCP is extremely less as compared to that of CHP or CCHP.

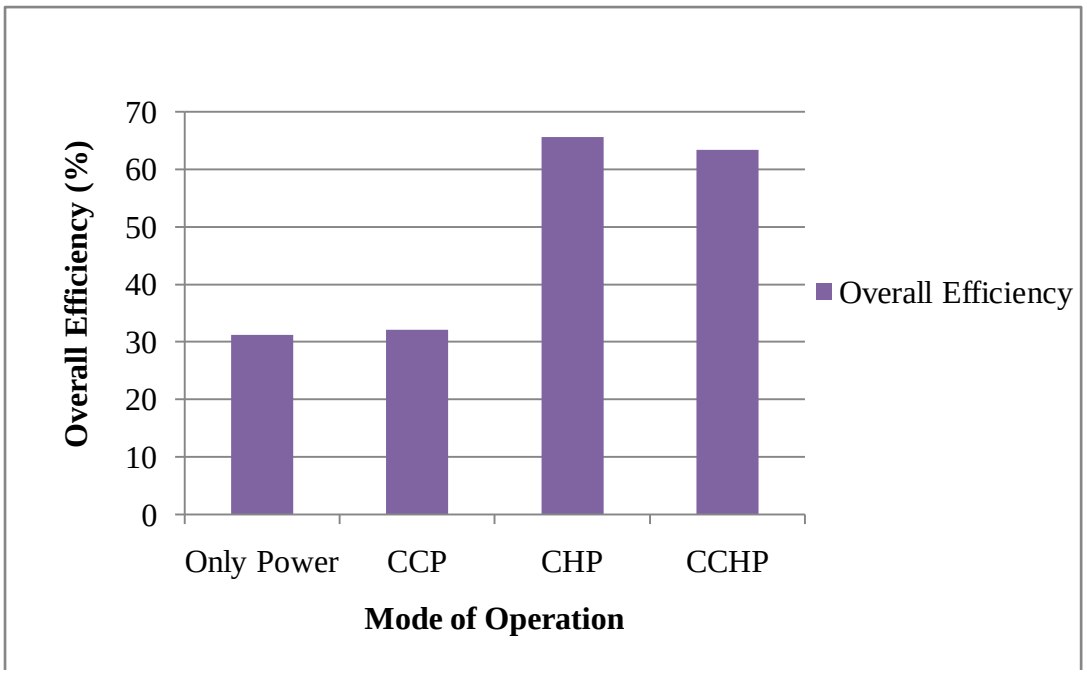

Fig.5.16 Comparison of overall efficiency for various modes at full engine load

5.6.3 Specific fuel consumption

The SFC for CHP varied from 0.206 kg/kWh at 1000 watt load to 0.127 kg/kWh at 3700 watt (full load) compared to 0.58 kg/kWh and 0.2716 kg/kWh respectively for single generation system. Hence, the reduction in SFC was 64.48% at 1000 watt and 53.24% at 3700 watt. The SFC for CCHP system varied from 0.231 kg/kWh at 1000 watt to 0.1323 kg/kWh at 3700 watt. Thus, the reduction in SFC for CCHP was 60.17% at 1000 watt and 51.29% at 3700 watt. In CCP system, SFC varied from 0.54 kg/kWh at 1000 watt to 0.2616 kg/kWh at 3700 watt. So, reduction in SFC for CCP system was 6.89% at 1000 watt and 3.68% at full load. Figure 5.17 shows the comparison of specific fuel consumption for various modes of operation at full engine load.

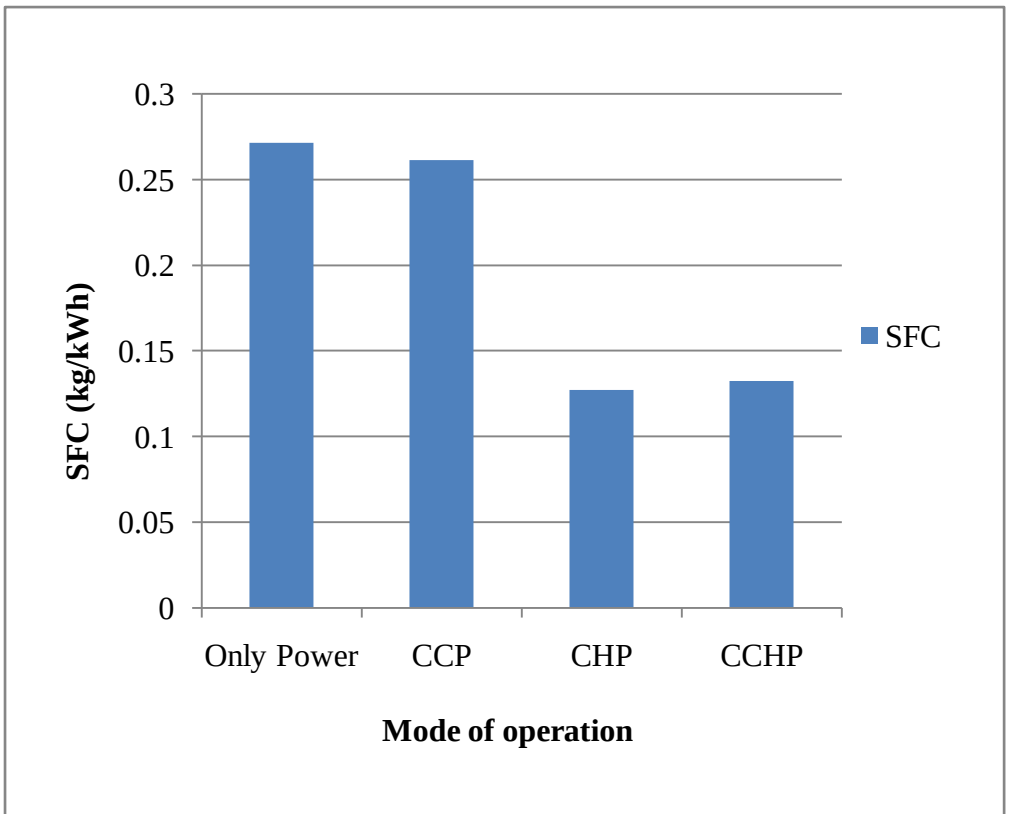

Fig.5.17 Comparison of SFC for various modes at full engine load

5.6.4 CO_2 emission in total useful output

The CO2 emission in kg/kWh for CHP varied from 0.456 kg/kWh at 1000 watt load to 0.2876 kg/kWh at 3700 watt (full load) compared to 1.22 kg/kWh and 0.623 kg/kWh respectively for single generation system. Hence, the reduction in CO_2 emission in kg/kWh was from 62.62% at 1000 watt to 53.83% at 3700 watt for CHP. The CO_2 emission in kg/kWh for CCHP system varied from 0.421 kg/kWh at 1000 watt to 0.265 kg/kWh at 3700 watt. So, the reduction in CO_2 emission in kg/kWh for CCHP system was 65.49% at 1000 watt and 57.46% at 3700 watt. In CCP system, CO_2 emission in kg/kWh varied from 1.19 kg/kWh at 1000 watt to 0.573 kg/kWh at 3700 watt. So, the percentage change of CO_2 emission in kg/kWh for CCP system was 2.45% at 1000 watt and 8.02% at full load. Figure 5.18 shows the comparison of CO_2 emission in useful energy output for various modes of operation at full engine load. CO_2 emissions in percentage are 4.5% less in CCHP as compared to CHP (fig. 5.7) at full engine load. The useful output (kW) is 2.98% less in CCHP as compared to CHP, therefore due to combined effect the CO_2 emissions (kg per kWh) are lower in CCHP as compared to CHP.

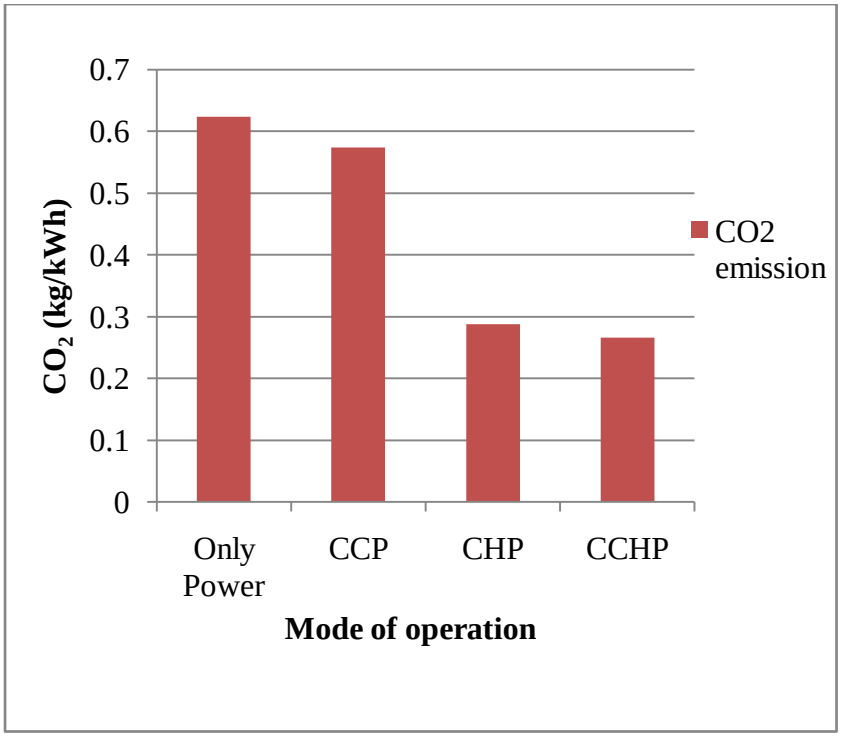

Fig.5.18 Comparison of CO_2 emissions for various modes at full engine load

5.6.5 Comparison of energy & exergy efficiency

Figure 5.19 shows the energy and exergy efficiency for single generation, CCP, CHP and CCHP systems at full engine load. For single generation, the energy efficiency was 30.85% at full load while the exergy efficiency was 29.69% at full load. The exergy efficiency of single generation was slightly lower than energy efficiency because chemical availability of fuel which is considered as the input in exergy analysis was slightly higher than the calorific value of fuel which is considered as the input in energy analysis [102]. It was seen from the graph in Fig. 5.19 that the exergy efficiency of CCP, CHP, and CCHP systems was lower than its energy efficiency. The exergy efficiency in the CCP, CHP and CCHP modes was marginally higher than that in single generation. This is due to the lower temperatures of the sources considered. Fig. 5.20 exergy balance diagram for the engine (only power mode) is provided for the better explanation. It is observed that 8.31 kW of exergy which is 34.9% of the exergy available in the fuel, is destroyed due to irreversibilities in the engine. Exergy lost in exhaust gas is 0.7016 kW in which 0.528 kW of exergy recovered for engine cooling & exhaust and 0.0853 kW of exergy recovered by VA system.

COP and exergetic efficiency of VA system was found to be 0.60 and 32.01% respectively from the modeling done by J. Aman et al. [103]. However, this modeling was done for a solar heated

10 kW air-cooled ammonia water absorption chiller. In contrast to that, in this experimental analysis, COP and exergetic efficiency of VA system was found to be 0.211 and 9.6% respectively.

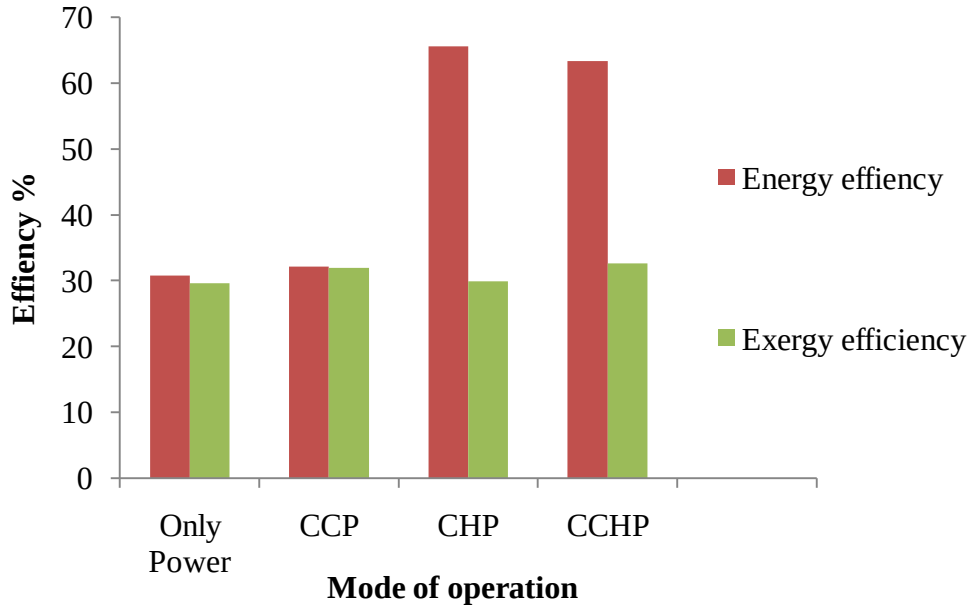

Fig.5.19 Comparison of energy and exergy efficiency for various modes at full engine load

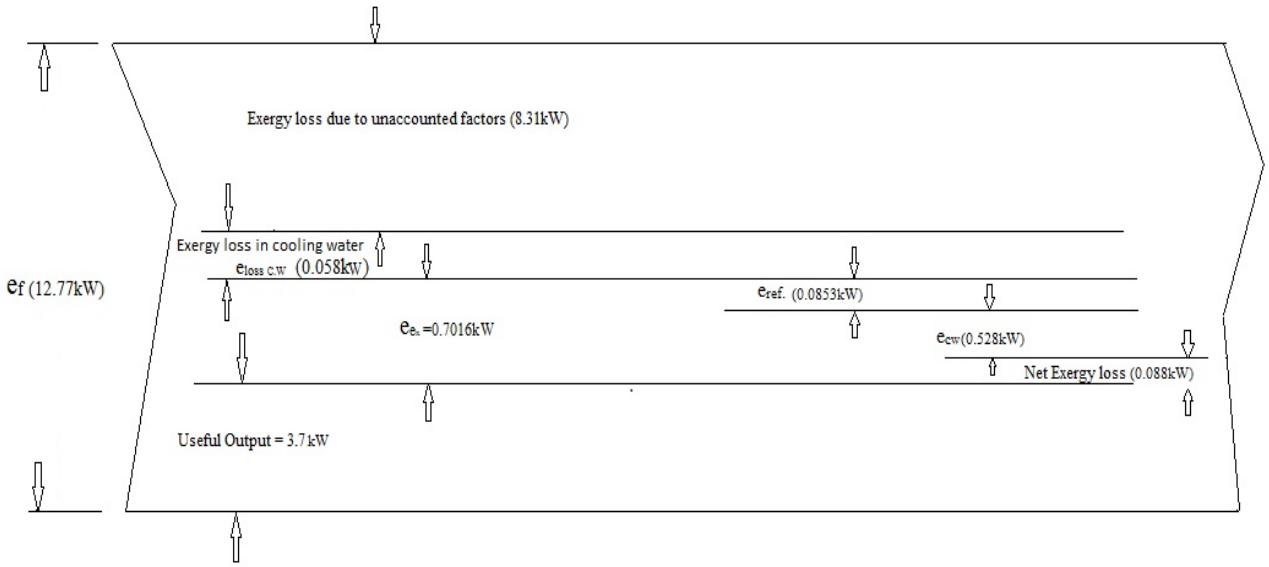

Fig. 5.20 Exergy balance diagram for the engine (only power mode)

5.7 Experimental optimization of the trigeneration system

Exhaust gas from engine was passed through the VA system for space cooling. In the trigeneration or CCHP mode, cooling water after extracting heat from engine block was designed to pass through the heat exchanger, where the other fluid was exhaust gas coming out from VA system generators. For the optimization of trigeneration system in CCHP mode, different VA units were operated one by one to obtain the best energy output in terms of space cooling and water heating.

It was observed that initially when only one VA unit was in operation, temperature of gases coming out from VA system generator and passing through the heat exchanger was 125^0C at 1000 W and 230^0C at full engine load i.e.3700 W. Similarly, the temperature of gases coming out from VA system generators and entering the heat exchanger was found to be 95^0C at 1000 W and 210^0C at full engine load, when the two VA units were in operation. It was also observed that if one or two VA units were in operation, then no space cooling effect was produced. Though the evaporator temperature of both the VA units (when only two VA units were in operation) reached 2^0C at full engine load, but it was still not sufficient to produce a cooling effect in the cabin. The total amount of heat recovered from engine exhaust and engine cooling system was 1.828 kW at 1000 W load and 4.510 kW at 3700 W engine load when only one unit of VA system was in operation and total amount of heat recovered from engine exhaust and engine cooling system was 1.70 kW at 1000 W load and 4.389 kW at 3700 W engine load when two VA units were operated. Figure 5.20 shows the variation of heat from engine coolant and engine exhaust with engine load in CCHP mode when one and two VA units were in operation.

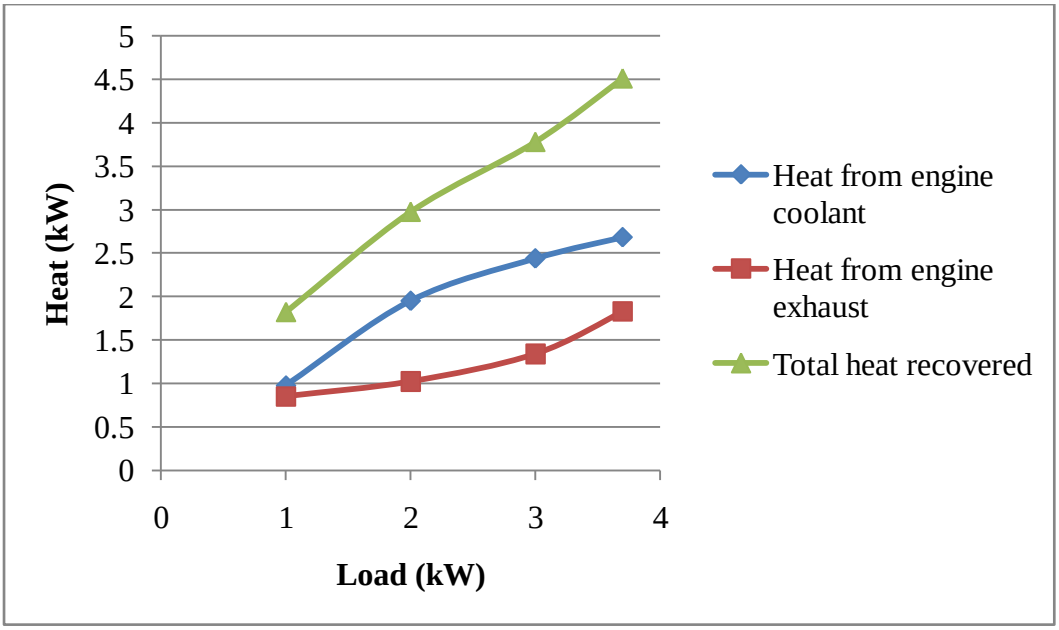

(a)

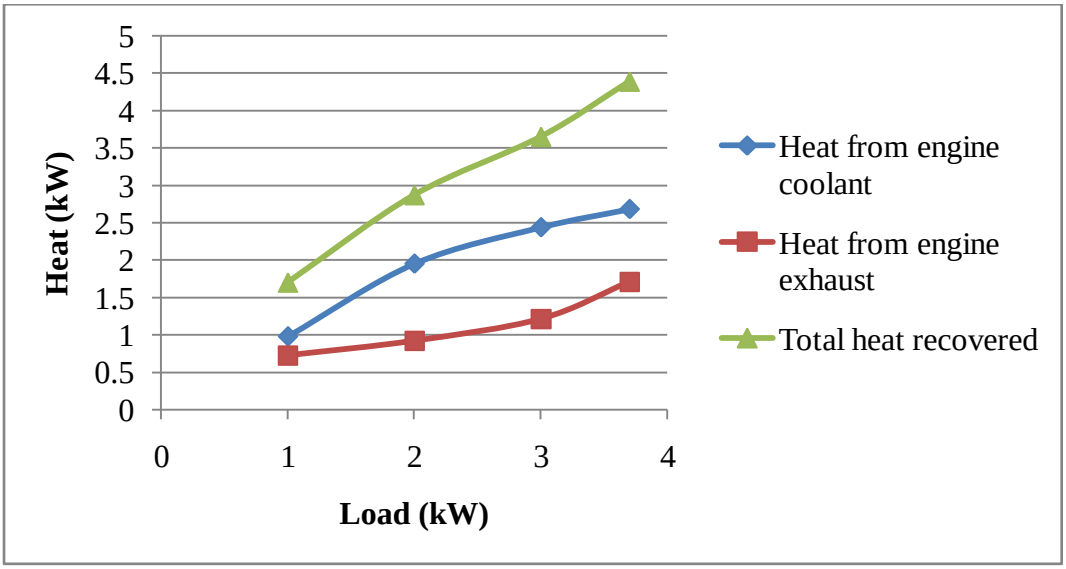

(b)

Fig.5.21 Variation of heat from engine coolant and engine exhaust with engine load in CCHP mode when **(a)** One VA unit and **(b)** Two VA units were in operation

When three units of VA system were in operation, then the temperature of gases coming out from VA system generators and entering the heat exchanger varied from 81^0C to 200^0C with the variation of engine load from 1000 W to 3700 W. In that situation space cooling effect was observed only at full engine load. In the beginning, only the top left generator was operated, keeping rest of the generator valves closed. When the temperature of top left generator reached about 100^0C, then the valve of top right generator of VA system was opened. In that condition, both, top left and top right units were in operation. Similarly, different permutations and combinations were applied for valves to be operated depending on the temperature condition of

each VA unit's generator. There were total 7 combinations for operation of VA units when three VA units were in operation. If G_1, G_2, G_3 and G_4 are considered as the top left, top right, bottom left and bottom right generators respectively and similarly E_1, E_2, E_3 and E_4 are considered as the top left, top right, bottom left and bottom right evaporators respectively, then the observed sequence of operation of VA units, when 3 VA units are in operation, is given in Table 5.2. At full engine load, when the three VA units were in operation, temperature difference of 4.5^0C was obtained between cabin and ambient. In that condition, cooling effect produced by VA system was 166 W at full engine load. The total amount of heat recovered from engine exhaust and engine cooling system varied from 1.58 kW at 1000 W to 4.26 kW at 3700 W. Figure 5.21 shows the variation of heat from engine coolant and engine exhaust with engine load in CCHP mode when three VA units were in operation.

Table 5.2 Sequences of operation of VA units when three VA units were in operation

S. No.	1	2	3	4	5	6	7
Sequences of operation	G_1	G_1, G_2	G_2	G_2, G_3	G_3	G_1, G_3	G_1, G_2 and G_3

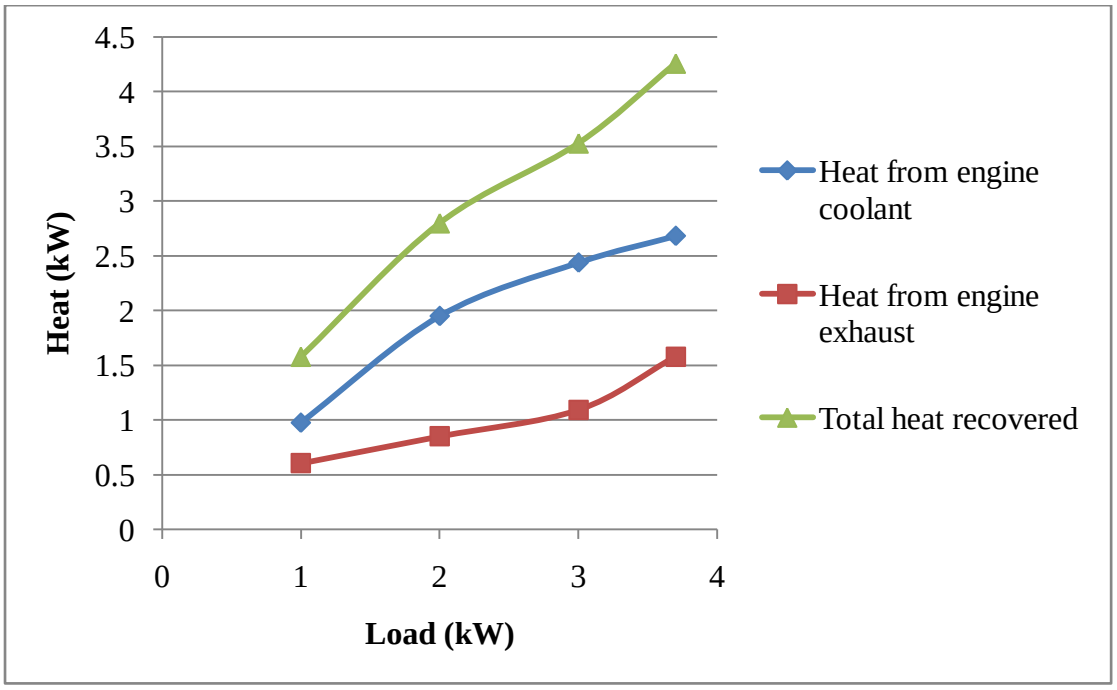

Fig.5.22 Variation of heat from engine coolant and engine exhaust with engine load when three VA units were in operation

When all the four units of VA system were in operation, then temperature of gases coming out from VA system generators varied from 70^0C to 185^0C with the variation of engine load from 1000 W to 3700 W. There were total 15 combinations for operation of VA units when all the four VA units were in operation which is already described in section 5.4 above. At full engine load, when all four units of VA system were in operation, remarkable temperature difference between cabin and ambient was obtained i.e. 6.5^0C. In that situation, cooling effect produced inside the cabin by VA system was 240 W at full engine load. The total amount of heat recovered from engine exhaust and engine cooling system varied from 1.46 kW at 1000 W to 4.19 kW at 3700 W. Figure 5.22 shows the variation of heat from engine coolant and engine exhaust with engine load in CCHP mode when all the four VA units were in operation.

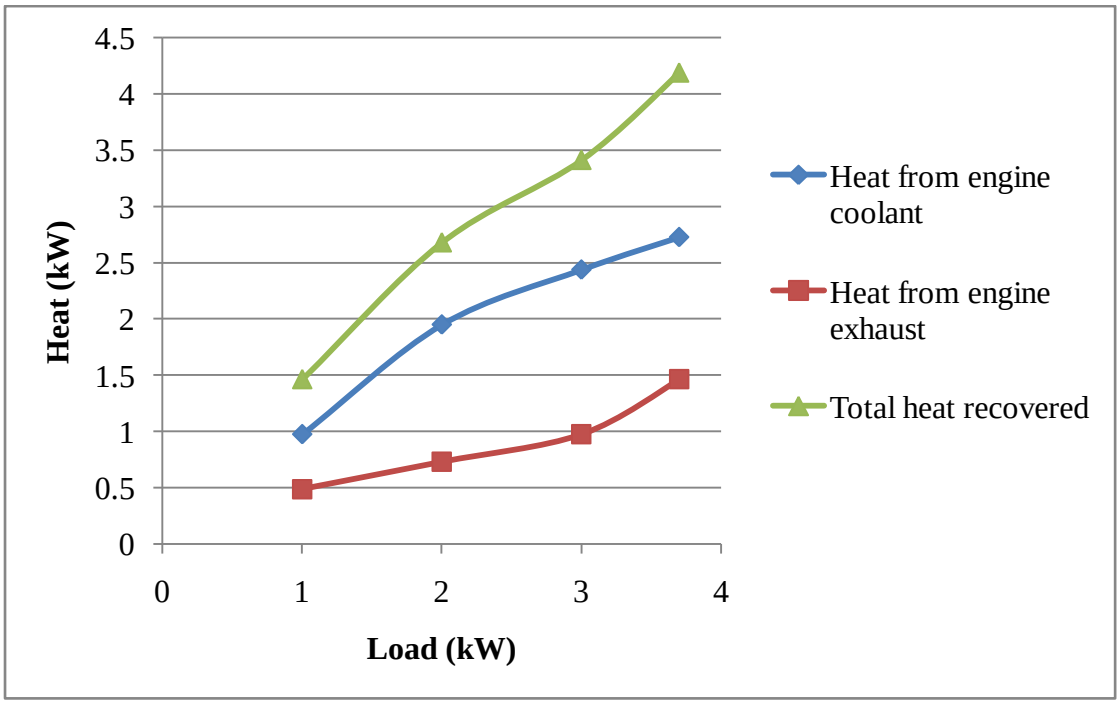

Fig.5.23 Variation of heat from engine coolant and engine exhaust with engine load in CCHP mode when all four VA units were in operation

Hence, with only one or two units of VA system in operation, only power and heating effect were obtained and no cooling effect was produced. Whereas, when either three or four units of VA system were in operation, it produced combined cooling, heating and power effect. Thus, trigeneration requirement was fulfilled when three or four units of VA system were in operation.

Figure 5.23 shows the variation of total useful output with the number of VA units in operation at full load. From the Figure, it was observed that total useful power output was 8.26 kW at full engine load when only one unit of VA system was in operation. Similarly, total useful power output was 8.13 kW at full engine load when two units of VA system were in operation. In both the situations, only power and heating effects were produced. Total useful output was 8.176 kW and 8.13 kW when three units and four units of VA system were in operation respectively. The cooling effect was more when all the four units of VA system were in operation. Thus, although total useful output was more when 3 units of VA system were in operation compared to that when all 4 units of VA system were in operation, however, cooling effect was substantially higher with 4 units compared to that with 3 units of VA system.

Hence, it can be safely concluded that in this size of set-up, using 3 units of VA system (i.e. approx. 150litres) generates an optimized trigeneration system. However, if more cooling effect is desired, then all four units of VA system should be put into operation, though sacrificing some output in terms of water heating. It is important to mention that the optimum results were obtained using the suggested sequence of operation of various units of the VA system.

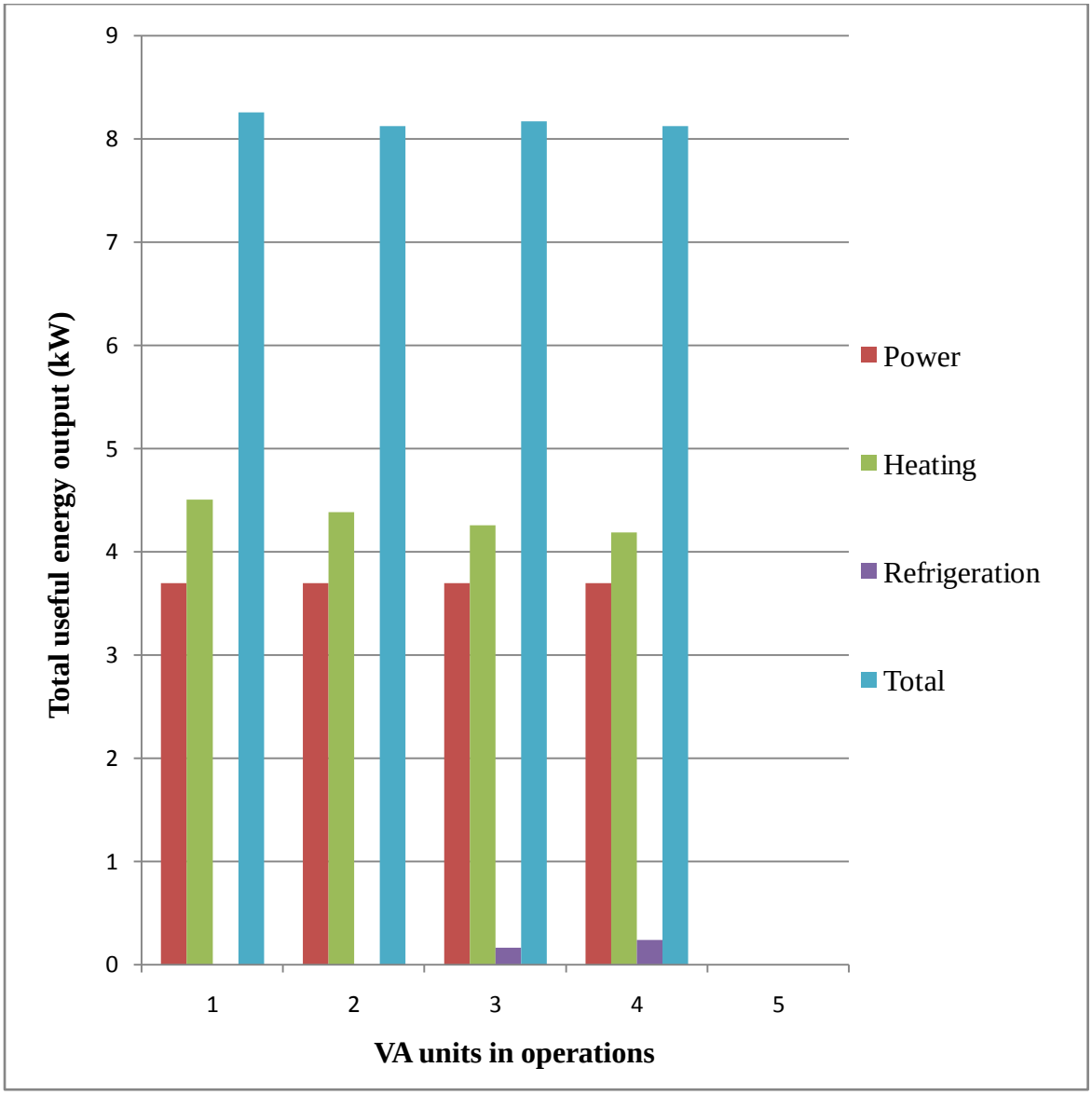

Fig.5.24 Variation of total useful energy output for different no. of VA units in operation

5.8 Mathematical Modeling

In the present research work, performance of CI engine operated micro trigeneration system for power, heating and space cooling was predicted by a simple model. In this model, a similar diesel engine was considered for trigeneration system, as the one used for the experimental study. The equation used for calculating of performance parameters of proposed model is presented in this section.

From available literature, different models of small capacity Kirloskar engines were selected and used for plotting of swept volume (in cc) vs. power of engine as shown in Fig. 5.24. The details are shown in Table 5.3.

Table 5.3: Variation of power with swept volume for various small Kirloskar engines

S.No.	Make	Power(kW)	Swept volume (cc)
1	AV1	3.7	553
2	TV1	5.18	661
3	DM10	7.4	948
4	DM14	10.36	1190

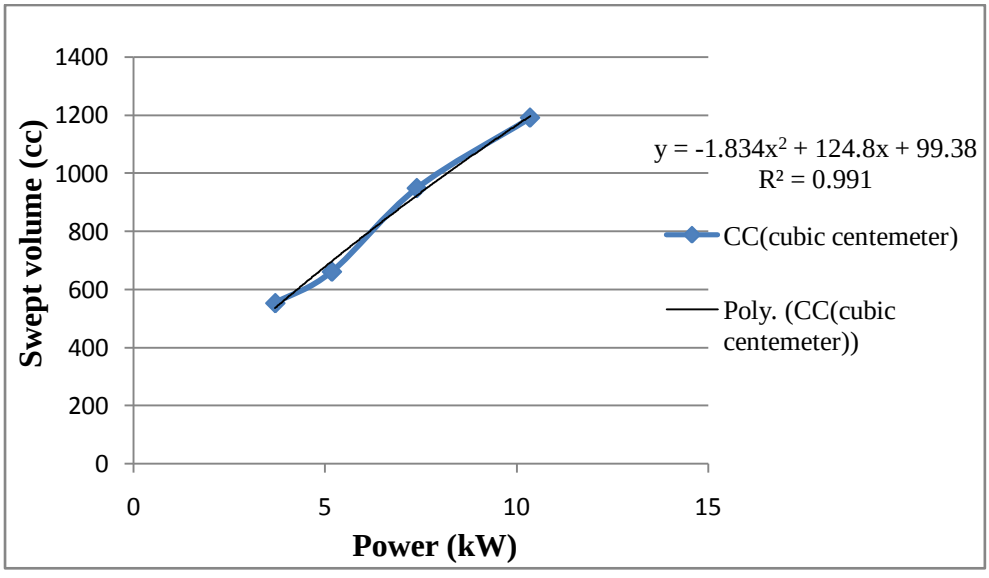

Fig.5.25: Swept volume vs. engine power for different agriculture engines

The graph shows a quadratic variation of swept volume (y) with power of engine (x) as:

$$y = -1.8347x^2 + 124.86x + 99.385$$

Further, this equation was used for determination of mass flow rate of air and mass flow rate of fuel in kg/sec at full load, assuming following parameters:

Volumetric Efficiency = 0.83; RPM = 1500; Density of air = 1.2 kg/m3;
Stoichiometric ratio = 19:1; COP = 0.55; Effectiveness of VA unit generator (ϵ) = 0.6

$$m_a = \frac{\text{Engine capacity in cubic centimeter} * \text{RPM} * \text{density of air} * \text{volumetric efficiency}}{2 * 60 * 10^6}\ kg/sec$$

$$m_a = \frac{(-1.834x^2 + 124.8x + 99.38) * 1500 * 1.2 * 0.83}{2 * 60 * 10^6}\ kg/sec$$

$m_a = 1.245 \times 10^{-5} \times (-1.834x^2 + 124.8x + 99.38)$ kg/sec

$m_f = 6.55 \times 10^{-7} \times (-1.834x^2 + 124.8x + 99.38)$ kg/s (where $m_f = m_a / 19$)

As total mass flow rate of exhaust gas is the sum of mass flow rate of air and that of diesel, it is given as:

$m_t = 1.31 \times 10^{-5} \times (-1.834x^2 + 124.8x + 99.38)$ kg/s

Heat available in exhaust gas, $Q_E = m_T \times C_p \times \Delta T$ $C_p = 1.005$ kJ/kg-K, $\Delta T = 320\ ^oC$

$Q_E = 1.31 \times 10^{-5} \times (-1.834x^2 + 124.8x + 99.38) \times 1.005 \times 320$ kW

$Q_E = 4.21 \times 10^{-3} \times (-1.834x^2 + 124.8x + 99.38)$ kW

Heat available in generator, $Q_g = \varepsilon \times Q_E$ (here ε for generator = 0.6)

Now heat available in generator, $Q_g = 2.52 \times 10^{-3} \times (-1.834x^2 + 124.8x + 99.38)$ kW

Refrigeration effect, $Q_R = COP \times Q_g$

Refrigeration effect, $Q_R = 1.39 \times 10^{-3} \times (-1.834x^2 + 124.8x + 99.38)$ kW

The modeling results calculated for heat available in exhaust gases and that for refrigeration effect show that only1/3rd of total heat available in exhaust gases was used for refrigeration. Rest of the heat is being supplied to the heat exchanger for hot water production.

Effectiveness of heat exchanger for hot water production = 0.7

$Q_{Heating} = 0.66 \times 4.21 \times 10^{-3} \times (-1.834x^2 + 124.8x + 99.38) \times 0.7$ kW

$Q_{Heating} = 1.945 \times 10^{-3} \times (-1.834x^2 + 124.8x + 99.38)$ kW

From the heat balance of four stroke, single cylinder diesel engine, 3.7 kW of heat is extracted by engine cooling jacket (same as electric output).

So total useful output:

$Q_{Totalusefuloutput} = Q_{ref} + Q_{enginecoolingjacketwater} + Q_{hotwaterafterheatexchanger}$ + b.p.

$Q_{Totalusefuloutput} = [1.39 \times 10^{-3} \times (-1.834x^2 + 124.8x + 99.38)] + 3.7 + [1.945 \times 10^{-3} \times (-1.834x^2 + 124.8x + 99.38)] + 3.7$

The efficiency of trigeneration system was calculated by the following equation:

$$\eta_{trigeneration} = \frac{\text{Total useful energy output}}{\text{Fuel input energy}}$$

$$\eta_{trigeneration} = \frac{[3.335 \times 10^{-3} \times (-1.834x^2 + 124.8x + 99.38)] + 7.4}{6.55 \times 10^{-7} \times (-1.834x^2 + 124.8x + 99.38) \text{X LCV}}$$

Figure 5.25 shows the comparison of useful energy output, overall efficiency, CO_2 emissions and SFC for theoretical & experimental results at 3.7 kW engine load.

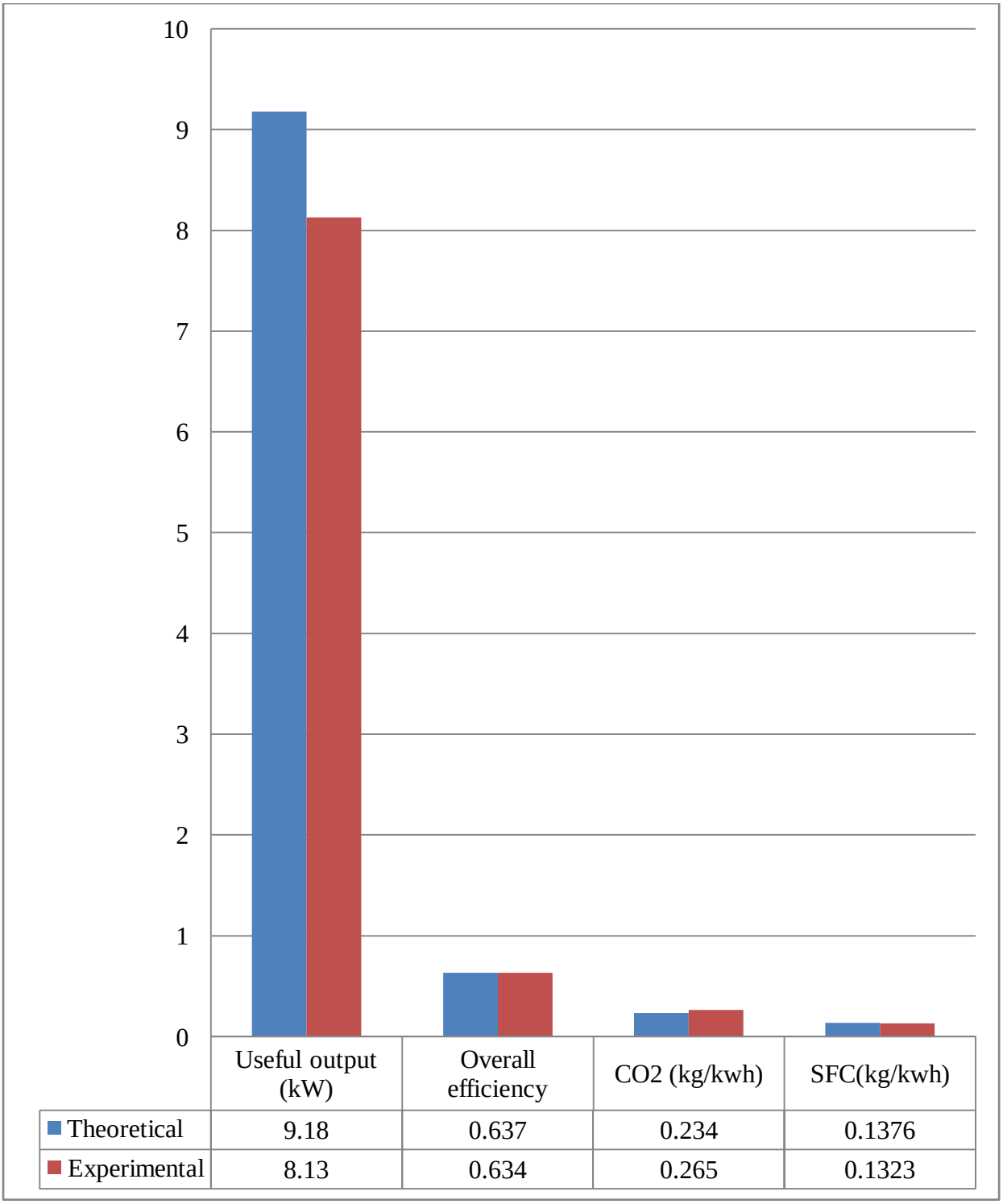

	Useful output (kW)	Overall efficiency	CO2 (kg/kwh)	SFC(kg/kwh)
Theoretical	9.18	0.637	0.234	0.1376
Experimental	8.13	0.634	0.265	0.1323

Fig.5.26: Comparison of useful energy output, overall efficiency, CO_2emissions and SFC for theoretical & experimental results at 3.7 kW engine load

CHAPTER 6
CONCLUSIONS

6.1 Conclusions

In this study, design and development of a CI engine operated micro trigeneration system was done and performance and emissions parameters of the above system were analyzed. Following conclusions can be drawn from the experimental study of CI engine operated micro trigeneration system:

1. BSFC and BTE for single generation, CCP, CHP and CCHP systems are nearly the same. This proves that integration of vapor absorption system and/or heat exchanger does not adversely impact the performance of engine generator.

2. Trigeneration system developed was more efficient, less polluting and more economical than the single generation system.

3. CO_2 emission per kWh of useful energy output at full engine load decreased in CHP, CCHP and CCP modes by 53.83%, 57.46% and 8.02% respectively compared to that of single generation system which is a substantial reduction in CO_2 emission. The impact in case of CCP is less because the COP of VA system is less than 1, so it takes more input energy in the form of heat than the output energy in the form of cooling.

4. The decrease in specific fuel consumption for CHP, CCHP and CCP systems over single generation system was 53.24%, 51.29% and 3.68% respectively at full engine load.

5. The useful energy output of the engine with single generation is only the brake power but in case of CHP, CCHP and CCP system, useful energy output is the sum of brake power along with the heating and cooling effects as the case may be. The useful energy output at full engine load for CHP, CCHP and CCP was found to be increased by 126.48%, 119.86% and 7.83% respectively compared to that of single generation.

6. The total thermal efficiency at full engine load for CHP, CCHP and CCP was increased by 112.67%, 105.31% and 4.37% respectively compared to that of single generation.

7. Exergy efficiency of the CHP, CCHP and CCP mode was slightly higher than the exergy efficiency of single generation (power only) system. It means energy is more effectively utilized in the integrated system compared to that in single generation system.

8. A simple mathematical model was developed for simulating the performance of micro-trigeneration system for the same CI engine but with optimum system components for power, heating and space cooling.

9. No adverse impact on any parameter was found while operating on cogeneration or trigeneration system as compared to single generation system.

10. The results obtained from the present research work show that development of CI engine operated micro trigeneration system for power, heating and space cooling is feasible and micro trigeneration systems have potential to mitigate global warming and may be proved as useful tool for sustainable development of the world.

6.2 Future Work

Although it was tried to cover the details of Micro-Trigeneration system developed as much as possible but there is always scope for future work in research field and the future scope of the present work is presented as following:

- To improve the overall performance of such trigeneration system, the performance of VA system needs to be improved. And for this, there is further scope for improvement in the design of VA system to recover heat somewhat more effectively by way of (i) improving generator effectiveness incorporating fins, (ii) reducing the exhaust pipe length and number of bends, and (iii) selecting VA system with capacity best suited to the application i.e. having one VA unit of desired capacity rather than four smaller units.

- For matching the variable energy demand profile of a building, storage devices such as battery for electricity storage, hot water storage tank for storing heat etc. can be incorporated in the Trigeneration system.

- In the present work, limited models targeting specific tasks have been developed. In future, a more comprehensive Trigeneration simulation model can be developed which can simulate the energy demand of a building integrated with Trigeneration system.

- In present study, diesel oil have been used as an fuel source for CI engine operated micro-Trigeneration system for power, heating and space cooling but in future alternate fuel sources not limited to oils but also gaseous fuel such as biogas etc can be tested.

- Economic analysis of micro-Trigeneration working on different alternate fuels can be done considering the availability and prices of the fuels.

APPENDIX-A

ERROR ANALYSIS

The values of various parameters obtained during the experiments could have errors or uncertainties due to operating conditions, environmental conditions, experimental methods adopted, calibration of equipments, accuracy and precision of equipments, human observations, test case planning, etc. Measurement errors fall into two main categories such as Systematic error and Random error. Imperfect calibration of measuring instruments (zero error), changes in environment which interfere with the measurement process and imperfect methods of observation caused the main sources of systematic error. Random error is caused by inherently unpredictable fluctuations in the readings of a measurement apparatus or in the experimenter's interpretation of the instrumental reading. In this investigation, the uncertainties were estimated from the minimum values of measured values as far as the individual measurements are concerned. To calculate the combined uncertainty of measurements a root-sum-square method was used. If a physical fundamental depends on n number of parameters, the combined uncertainties of each function was calculated by Pythagorean summation of uncertainties given by the equation.

$$z = f(x_1, x_2, x_3, x_4, \ldots\ldots x_n)$$

$$\sigma_z^{\,2} = \left[\frac{\partial f}{\partial x_1}\right]^2 \sigma_{x_1}^{\,2} + \left[\frac{\partial f}{\partial x_2}\right]^2 \sigma_{x_2}^{\,2} + \left[\frac{\partial f}{\partial x_3}\right]^2 \sigma_{x_3}^{\,2} + \ldots\ldots\ldots\ldots\ldots\ldots\ldots + \left[\frac{\partial f}{\partial x_n}\right]^2 \sigma_{x_n}^{\,2}$$

σ_z= uncertainty of the function

σ_{x_n} = uncertainty of the parameter

f= function

x_n= parameter of the measurement

n= number of variables

Uncertainty analysis for micro-trigeneration system working on diesel fuel as baseline case is presented here. The resolution of the measurements and the maximum uncertainties in the calculated results are given in Table A1.

Table A1: Percentage uncertainty in measurement of different quantities

Measured quantity	**Range of experiment**	**Resolution**	**% Uncertainty**
CO	0-10 % vol.	0.01%Vol.	±0.4 %
CO_2	0-20 % vol.	0.1%Vol.	±0.4 %
HC	0-20,000 ppm	1 ppm	±0.3 %
NO_X	0-5000 ppm	1 ppm	±0.3 %
Smoke	0-100 %	0.1 %	±0.18 %
Load	0-3700 W	100 W	±0.17 %
Fuel vol. flow	0-100 ml	±1 ml	±1 %
BTE	-	-	±1.2 %
BSFC	-	-	±1.2 %

APPENDIX- B

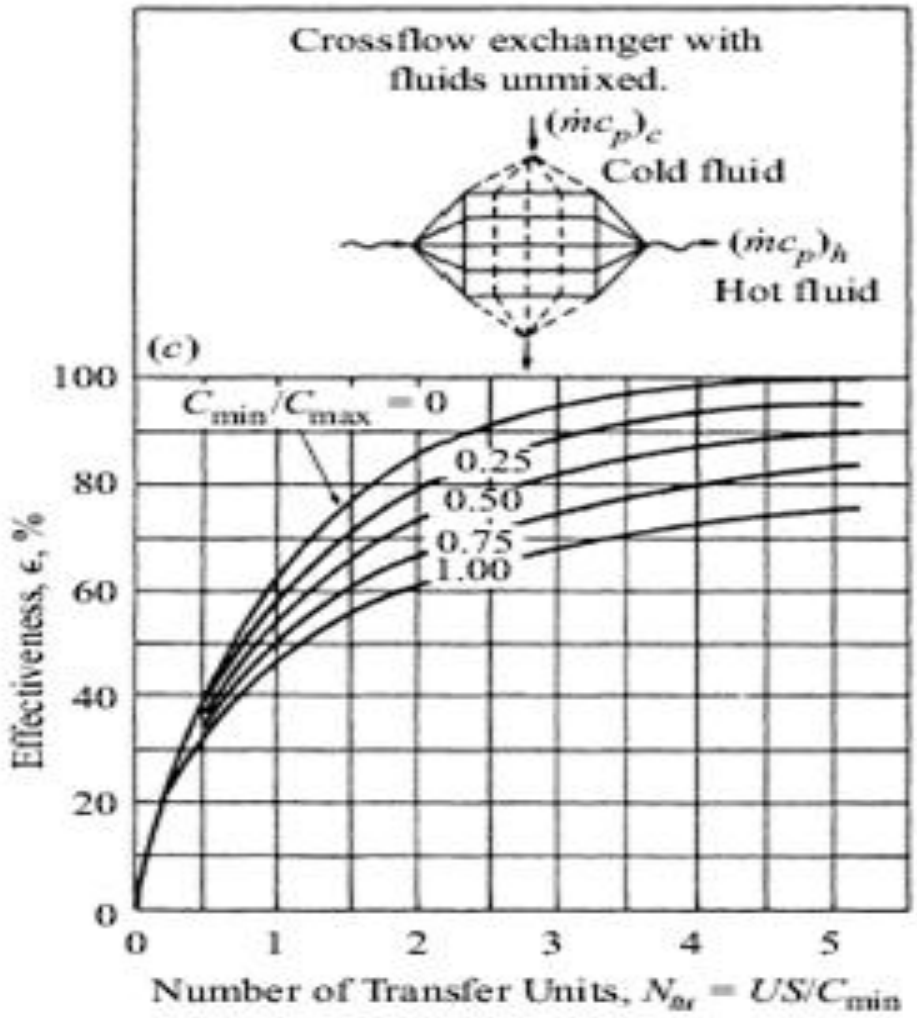

Fig.A.1 NTU-effectiveness chart for cross-flow heat exchanger

APPENDIX- C

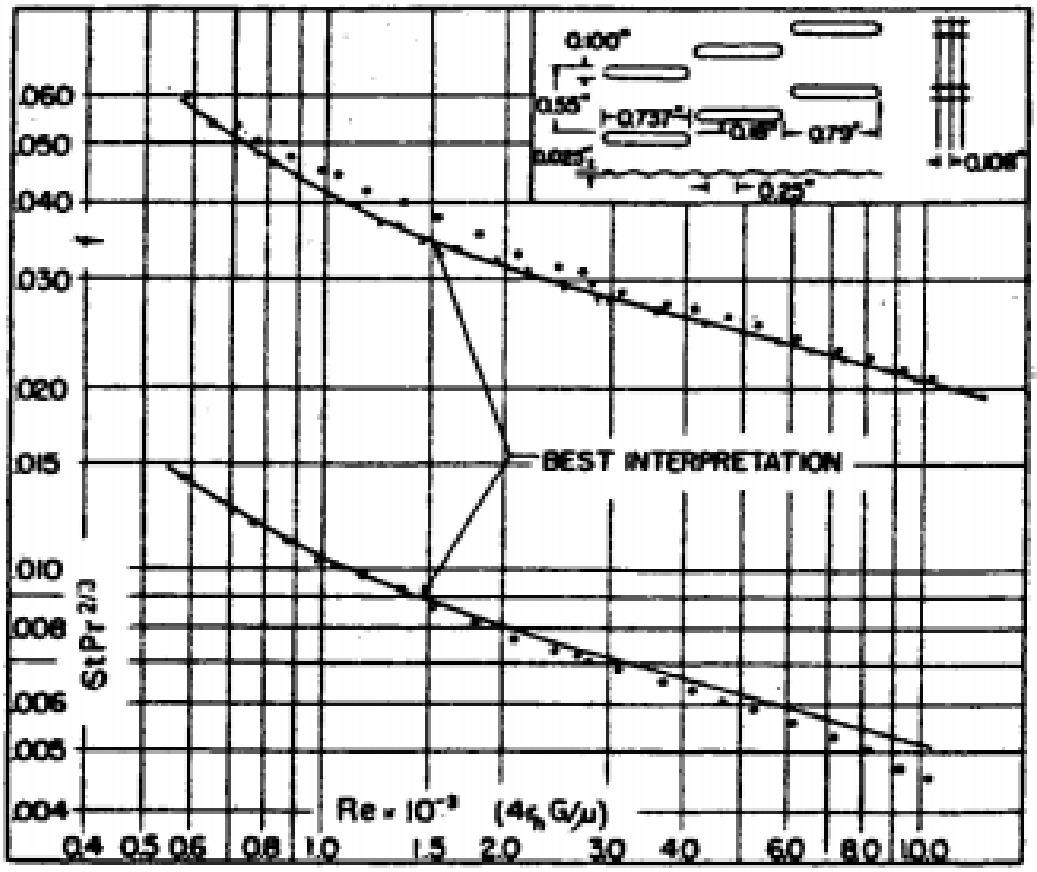

Fin pitch = 9.29 per in = 366 per m

Flow passage hydraulic diameter, $4r_h$ = 0.01352 ft = 4.12×10^{-3} m

Fin metal thickness = 0.004 in, copper = 0.102×10^{-3} m

Free-flow area/frontal area, σ = 0.788

Total heat transfer area/total volume, α = 228 ft²/ft³ = 748 m²/m³

Fin area/total area = 0.814

Fig.A.2 Chart of Stanton number and friction factor for surface 11.32-0.737-SR

APPENDIX- D
Coefficient of Performance (COP) for VAR System

COP is the ratio of cooling effect to the amount of heat supplied to the generators of VA system. In this work engine exhaust gas was used as source of heat supplied to the generators. Mathematically, expression of the COP for vapor absorption system was calculated using the following equation:

$$COP_{VA} = \frac{E_{ref}}{E_{gen}}$$

The heat supplied to the generators of VA system was calculated by the following formula:

$$E_{gen} = \epsilon C_{\min}(T_{hi}\text{-}T_{ci}) \text{ kW}$$

Here, $\epsilon$is the effectiveness of the generator of VA system. $C_{min}$is the minimum heat capacity and $T_{hi}$and $T_{ci}$are the temperatures of the hot fluid and cold fluid at inlet of VA system generator respectively.

The expression of refrigeration effect produced by VA system is given by:

$$E_{ref} = UA\{T_{ambient} - T_{cab}\}k\text{W}$$

The value of UA can be calculated by:

$$\frac{1}{UA} = \frac{1}{h_i A_i} + \sum\frac{\delta}{kA} + \frac{1}{h_0 A_0}$$

Where, h_i is the convective heat transfer coefficient of air of the refrigerator inside wall, h_0 is the convective heat transfer coefficient of air of the refrigerator outside wall, $A_i$and $A_0$are areas of inside and outside the refrigerated walls respectively. Now,

$$\sum\frac{\delta}{kA} = \frac{\delta_1}{k_1\ A_1} + \frac{\delta_2}{k_2\ A_2} + \frac{\delta_3}{k_3\ A_3} + \frac{\delta_4}{k_4\ A_4} + \frac{\delta_5}{k_5\ A_5} + \frac{\delta_6}{k_6\ A_6} + \frac{\delta_7}{k_7\ A_7} + \frac{\delta_8}{k_8\ A_8}$$

Here,$k_1, k_2, k_3, k_4, k_5, k_6, k_7$and $\delta_1, \delta_2, \delta_3, \delta_4, \delta_5, \delta_6, \delta_7$are the thermal conductivities & thickness of nitrile rubber, glass wool, thermocol, ply sheet, plaster of Paris, extruded polystyrene insulated sheet and aluminum foils respectively. $A_1, A_2, A_3, A_4, A_5, A_6, A_7$are the areas of back side of VA

system, area of refrigerated side of VA system, side wall of cabin, ply sheet area, generators pipe area, inside area of cabin and pipe area for the flow of gases respectively.

Table A2: Thermal conductivity of different materials

Material	Thermal Conductivity, k (W/mK)
Asbestos rope	0.20
Glass wool	0.03
Plaster of Paris	0.56
Nitrile rubber	0.255
Thermocol	0.036
Extruded polystyrene sheet	0.037
Ply sheet	0.13
Aluminum foil	138

APPENDIX- E
The formula for exergy calculations

The exergy of a flow stream is determined by simply adding the flow exergy relation to the exergy relation in for non-flowing fluid,

$$X_{\text{flowing fluid}} = X_{\text{non flowing fluid}} + X_{\text{flow}} \quad \text{(i)}$$

Where,

$$X_{\text{non flowing fluid}} = (u-u_0) + P_0(v-v_0) - T_0(s-s_0) + (V^2/2) + gz, \quad \text{(ii)}$$

If, u_0, v_0, s_0 are the properties of the system evaluated at the dead state and u, v, s are the property of the system evaluated at the given state. Then,

$$X_{\text{flowing fluid}} = (u-u_0) + P_0(v-v_0) - T_0(s-s_0) + (V^2/2) + gz + (P-P_0)V$$

$$= (u+PV) - (u_0+P_0V_0) - T_0(s-s_0) + (V^2/2) + gz$$

$$= (h-h_0) - T_0(s-s_0) + (V^2/2) + gz \quad \text{(iii)}$$

The final expression is called flow (or stream) exergy, and is denoted by φ

Flow exergy:

$$\varphi = (h-h_0) - T_0(s-s_0) + (V^2/2) + gz \quad \text{(iv)}$$

Then the exergy change of a fluid stream as it undergoes a process from state 1 to state 2 become

$$\Delta\varphi = \varphi_2 - \varphi_1 = (h_2-h_1) - T_0(s_2-s_1) + [(V_2^2-V_1^2)/2] + g(z_2-z_1) \quad \text{(v)}$$

For fluid streams with negligible kinetic and potential energies, the kinetic and potential energy terms drop out. So, the reduced equation will be as follow:

$$\Delta\varphi = \varphi_2 - \varphi_1 = (h_2-h_1) - T_0(s_2-s_1) \quad \text{(vi)}$$

Note that the exergy change of a closed system or a fluid stream represents the maximum the amount of useful work that can be done (or the minimum amount of useful work that needs to be supplied if it is negative) as the system changes from state 1 to 2 in a specified environment, and represents the reversible work W_{rev} .It is independent of the type of process executed, the kind of system used, and the nature of energy interactions with the surrounding. Also note that the exergy

of a closed system cannot be negative, but the exergy of a flow stream can at pressure below the environment pressure P_0.

The change in entropy can be found by the using following expression:

We know that

$$Tds = dH - Vdp$$

$$\int_1^2 dS = \int_1^2 \frac{mCpdT}{T} - \int_1^2 \frac{Vdp}{T} = \int_1^2 mCp\frac{dT}{T} - \int_1^2 mR\frac{dP}{P}$$

$$where, \quad \frac{V}{T} = \frac{mR}{p}$$

$$S2 - S1 = mCp\ln\frac{T2}{T_1} - mR\ln\frac{p2}{p_1}$$

At constant pressure the change in entropy will be:

$$S2 - S1 = mCp\ln\frac{T2}{T_1} \qquad \text{(vii)}$$

Put the equation no. vii in equation vi and we can get the following final equation

$$\Delta\varphi=\varphi_2-\varphi_1= (h_2-h_1) - mCp\ln\frac{T2}{T_1}$$

REFERENCES

1. http://www.eia.gov/forecasts/ieo/pdf/0484(2013).pdf Last accessed on Oct. 7, 2015.
2. http://www.iea.org/publications/freepublications/publication/KeyWorld2014.pdf Last accessed on Oct. 7, 2015.
3. http://www.worldenergy.org/wpcontent/uploads/2012/09/wec_transport_scenarios_2050.pdf Last accessed on Oct. 9, 2015.
4. http://mospi.nic.in/Mospi_New/upload/Energy_Statistics_2013.pdf Last accessed on Oct. 9, 2015.
5. Chaturvedi, V., Eom, J., Clarke, L. E., & Shukla, P. (2011, Dec). Retrieved March 2014, from Joint Global Change ResearchInstitute: http://www.globalchange.umd.edu/wpcontent/uploads/2011/12/CMM_IndiaBuilding_Chaturvedi.pdf Last accessed on Oct. 7, 2015.
6. http://www.gbpn.org/sites/default/files/08.%20INDIA%20Baseline_TR_low.pdf Last accessed on Oct. 7, 2015.
7. Climate Works Foundation. (2010). Reducing GHG Emissions in the Building Sector in India: A Strategy Paper. http://www.climateworks.org/imo/media/doc/Policies%20That%20Work_Overview%20Report.pdf Last accessed on Oct. 10, 2015.
8. http://www.iea.org/publications/freepublications/publication/co2emissionfromfuelcombustionhighlights.pdf Last accessed on Oct. 7, 2015.
9. Hongdong Yu, "The Design, testing and analysis of a Biofuel micro trigeneration system", A thesis submitted to the Newcastle University in partial fulfillment of the requirements for the degree of doctor of philosophy, October 2012. Last accessed on Jan. 7, 2015.
10. Morelli DT 1997 "Thermoelectric devices, In: Trigg GL", Immergut E H (eds.) Encyclopedia of Applied Physics. Wiley – VCH, New York, Vol. 21, pp. 339 – 54. Last accessed on Dec. 5, 2014.
11. F. Stabler, "Automotive applications of high efficiency thermoelectric", Proceedings of DARPA/ONR/DOE high efficiency thermoelectric workshop, 2002, 1-26. Last accessed on Oct. 7,2014.

12. R. Saidur, M. Rezaei, W. K. Muzammil, M.H. Hassan, S. Paria, M. Hasanuzzaman, "Technologies to recover exhaust heat from internal combustion engines", International Journal of Renewable and Sustainable Energy Reviews 16 (2012) 5649–5659.
13. Yu C, Chau KT. "Thermoelectric automotive waste heat energy recovery using maximum power point tracking", Energy Conversion and Management 50(6) (2009), 1506–12.
14. Basel I. Ismail, Wael H. Ahmed, "Thermometric Power Generation Using waste heat energy as an alternative green technology", Recent Patents on electrical engineering 2 (2009), 27 – 39. http://www.researchgate.net/profile/Wael_Ahmed2/publication/228637825_Thermoelectric_Power_Generation_Using_Waste_Heat_Energy_as_an_Alternative_Green_Technology/links/0c96052395416712fe000000.pdf Last accessed on Feb. 7, 2014.
15. DM Rowe. "Thermoelectric waste heat recovery as a renewable energy source", International journal innovative Energy System and Power, 2006:1: 13-23.http://www.ewp.rpi.edu/hartford/~lewisl2/Engineering%20Project/Other/References/THERMOELECTRIC%20WASTE%20HEAT%20RECOVERY%20AS%20A%20RENEWABLE%20ENERGY%20SOURCE%20%20David%20Michael%20Rowe.pdf Last accessed on March 7, 2014.
16. David Michael Rowe, Review on Thermoelectric Waste Heat Recovery as a Renewable Energy Source, International Journal of innovations in Energy System and Power, Vol.1 No.1, November 2006. Last accessed on April 15, 2014.
17. CT Hsu, GY Huang, HS Chu, B Yu, DJ Yao. "Experiments and simulations on low-temperature waste heat harvesting system by thermoelectric power generators", Applied Energy 88(4) (2011), 1291–7.
18. SB Riffat, X Ma, Thermoelectrics: "A Review of Present and potential Applications", Applied Thermal Engineering 23 (2003), 913-935.
19. L Chen, J Li, F Sun, C Wu, "Performance optimization of a two stage semi conductor thermoelectric generator", Applied Energy 82 (2005), 300 – 312.
20. A Duparchy, P Leduc, G Bourhis, C Ternel. "Heat recovery for next generation of hybrid vehicles: simulation and design of a Rankine cycle system", World Electric Vehicle Journal Vol.3 ISSN 2032-6653, 2009. http://www.evs24.org/wevajournal/php/download.php?f=vol3/WEVJ3-3260191.pdf. Last accessed on Oct. 15, 2014.
21. I Vaja, A Gambarotta. "Internal combustion engine (ICE) bottoming with organic Rankine cycles (ORCs)", Energy 35(2) (2010), 1084–93. Last accessed on Sept. 7, 2014.

22. H Chen, "Converting low grade heat into electrical power", Available at http://www.eng.usf.edu/hchen4/index.html Last accessed on Oct. 17, 2014.
23. B Liu, K Chien, C Wang. "Effect of working fluids on organic Rankine cycle for waste heat recovery", Energy 29 (2004), 1207 – 17. Last accessed on May 7, 2014.
24. DiPippo R. "Second Law assessment of binary plants generating power from low-temperature geothermal fluids", Geothermics, 33 (2004), 565–86. Last accessed on May. 7, 2015.
25. H Chen, DY Goswami, EK Stefanakos. "A review of thermodynamic cycles and working fluids for the conversion of low-grade heat", Renewable and Sustainable Energy Reviews 14 (2010), 3059–67.
26. H. Yamaguchi, Zhang, X. R., Fujima,, M. Enomoto & N. Sawada: "Solar energy powered Rankine cycle using supercritical CO_2", Applied Thermal Engineering 26, 2345 – 2354.
27. JC Conklin, JP Szybist. "A highly efficient six-stroke internal combustion engine cycle with water injection for in-cylinder exhausts heat recovery", Energy 35 (2010), 1658–64.
28. B. Crower Method and apparatus for operating an internal combustion engine. United States patent application 20070022977; 2005. http://www.freepatentsonline.com/20070022977.pdf Last accessed on Nov. 7, 2014.
29. Dyer LH. Internal combustion engine. United States patent US 1339176A, 1920. http://patentimages.storage.googleapis.com/pdfs/US1339176.pdf Last accessed on Nov. 7, 2014.
30. Kellogg-Smith O. Internal combustion and steam engine. United States patent 4143518; Mar 13, 1979. http://patentimages.storage.googleapis.com/pdfs/US4143518.pdf Last accessed on Nov. 7, 2014.
31. GJ Larsen. Engine with a six-stroke cycle, variable compression ratio, and constant stroke. United States patent 4,736,715; 1988. http://patents.com/us-4736715.html Last accessed on Nov. 7, 2014.
32. DM Prater. Multiple stroke engine having fuel and vapor charges. United States patent 6,253,745; 2001. http://patentimages.storage.googleapis.com/pdfs/US6253745.pdf Last accessed on Nov. 7, 2014.
33. H Rohrbach, R Tamins. "Engine having alternate internal-combustion and fluid pressure power strokes", United States patent 2,671,311; 1954.

http://patentimages.storage.googleapis.com/pdfs/US2671311.pdf Last accessed on Nov. 7, 2014.

34. S Singh. "Computer controlled multi-stroke cycle power generating assembly and method of operation", United States patent 7,021,272; 2006. http://patentimages.storage.googleapis.com/pdfs/US7021272.pdf Last accessed on Nov. 7, 2014.

35. RC Tibbs. "Six cycle combustion and fluid vaporization engine", United States patent 3,964,263; 1976 http://patentimages.storage.googleapis.com/pdfs/US3964263.pdf Last accessed on Nov. 7, 2014.

36. Mingxi Liu, "Energy Efficient operation strategy design for the combined cooling, heating, and power system", A Thesis submitted in Partial fulfillment of the requirement for the Degree of Master of Applied Science in Department Of Mechanical Engineering in University of Victoria.

https://dspace.library.uvic.ca/bitstream/handle/1828/4002/Liu_Mingxi_MASc_2012.pdf?sequence=12&isAllowed=y Last accessed on Dev. 12, 2014.

37. D.W. Wu, and R.Z. Wang, "Combined cooling, heating and power: A Review" Progress in Energy and Combustion Science 32 (2006), 459-495.

38. Kamal Kishore Khatri, "Studies on Straight Vegetable Oil – Diesel Blend Operated Trigeneration System", A Thesis submitted in fulfillment of the requirements for the degree of Doctor of Philosophy, Department of Mechanical Engineering, MNIT, Jaipur, July, 2010. Last accessed on Nov. 7, 2014.

39. A report on "Residential Cogeneration System: A Review of the Current Technologies", A Report of Subtask A of FC + COGEN-SIM The Simulation of Building Integrated Fuel Cell and Other Cogeneration Systems. Annex 42 of the International Energy Agency, Energy Conservation in Buildings and Community Systems program, First published: April 2005, Available at http://www.ecbcs.org/docs/Annex_42_Review_Residential_Cogen_Technologies.pdf.

40. D. Dentice, M Accadia, M.Sasso, S. Sibilio,L. Vanoli, "Micro-Combined Heat and Power in Residential and Light Commercial Applications", Applied Thermal Engineering 23,(2003), 1247-1259.

41. R.Patrascu, E. Minciuc, "Comparative analysis of different combined heat and power generation: fuel cells, gas turbine, internal combustion engine", 4th IASME/WSEAS

International conference on Energy, Environment, and Sustainable Development (EEESD 08), Algarve, Portugal, June 11- 13, 2008, pp 27 – 31.

http://www.worldses.org/books/2008/algarve/new-aspects-of-energy-environment-ecosystems.pdf Last accessed on Nov. 7, 2014.

42. F.RODICA, D.ANDREI, "Small scale cogeneration – a viable alternative for Romania", 4th IASME/WSEAS International conference on Energy, Environment, and Sustainable Development (EEESD 08), Algarve, Portugal, June 11- 13, 2008, pp 60-66.http://www.wseas.us/e-library/conferences/2008/algarve/EEESD/008-588-176.pdf Last accessed on Nov. 11, 2014.

43. M. Ozdenefe,U. Atikol, "Assessing the applicability of trigeneration in the hotel sector", Proceedings of the 5th IASME/WSEAS International Conference on Energy & Environmental (EE-10) University of Cambridge, UK February 23- 25. 2010, pp 299-304.

http://www.wseas.us/e-library/conferences/2010/Cambridge/EE/EE-48.pdf Last accessed on Nov. 7, 2014.

44. J.Van Bael, E. Peeters, "Evaluation of the First Micro Combined Heat and Power for Social Housing in Belgium", Proceedings of the 6th WSEAS International Conference on Power Systems, Lisbon, Portugal, September 22-24, 2006, pp.165-168.

http://www.wseas.us/e-library/conferences/2006lisbon/papers/517-305.pdf Last accessed on Nov. 7, 2014.

45. J.Zarinchang, A. Yarmahmoudi, "Optimization of Stirling Engine Heat Exchangers Selected papers from the WSEAS Conference Santander", Cantabria, Spain, September 23 – 25, (2008), 143 – 150.

http://www.wseas.us/e-library/conferences/2008/spain/selected/selected17.pdf Last accessed on Nov. 13, 2014.

46. Residential Micro CHP Using Stirling Engines, Emerging Technologies & Practices, ACEEE 2004.

47. V. Dorer,R. Weber, A. Weber"Performance Assessment of fuel cell Micro cogeneration systems for Residential Buildings", Energy and Buildings 37(2005), 1132- 1146.

48. G.R. Simader, R.Krawinkler, G. Trnka, "Micro CHP systems: state of the art", Final Report, Deliverable 8 (D8) of Green Lodges Project (EIE/04/252/S07.38608), Austrain Energy Agency, Vienna, 2006.http://ec.europa.eu/energy/intelligent/projects/sites/iee-projects/files/projects/documents/green_lodges_micro_chp_state_of_the_art.pdf Last accessed on Nov. 7, 2014.

49. H.L. Onovwiona, V.I. Ugursal, "Residential Cogeneration Systems: Review of the Current Technology", Renewable and Sustainable Energy Reviews 10(2006), 389- 431.

50. "Micro CHP Systems for Residential Applications", 2006, Final Report, United Technologies Research Center.

http://nechpi.org/wp-content/uploads/2012/06/MICRO-CHP-UTC.pdf Last accessed on Dec. 7, 2014.

51. B. Aoun, "Micro Combined Heat and Power Operating on Renewable Energy for Residential Building", Doctoral Thesis, Ecole Nationale Superieure des mines de Paris, 2008.https://tel.archives-ouvertes.fr/pastel-00005092/document. Last accessed on Nov. 7, 2014.

52. COGEN Europe (The European Association for the Promotion of Cogeneration, www.cogen.org). The European educational tool on cogeneration, 2nd December 2001.

53. WADE (World Alliance of Decentralize Energy, www.localpower.org). Guide to decentralized energy technologies 2002.

http://www.bioturbine.org/Publications/PDF/WADEDETechnologies.pdf Last accessed on Nov. 7, 2014.

54. Trina Masepohl, The National Renewable Energy Laboratory (NREL).On site power systems for laboratories, 2003.
www.nrel.gov/docs/fy04osti/33978.pdf Last accessed on Nov. 7, 2014.

55. IEA (The International Energy Agency).Distributed Generation in liberalized electricity markets, 2002.

56. COGEN Europe "Decentralized generation technologies – potentials, success factors and impact in the liberalized EU energy markets", Final Report, October 2002.

57. A joint project of the Gas Research Institute (GRI) and the National Renewable Energy Laboratory (NREL), prepared for office of Energy Efficiency and Renewable Energy (EERE), November 2003.

www.nrel.gov/docs/fy04osti/34783.pdf Last accessed on Nov. 7, 2014.

58. A. M.Papadopoulos, S. Oxizidis, N. Kyriakis, "Perspective of solar cooling in view of the development in the air conditioning sector", Renewable and Sustainable Energy Reviews7 (2003), 419-38.

59. G. Foley, R. DeVault, R. Sweetser , "Future of absorption technology in America: a critical look at the impact of BCHP and innovation", Advanced building systems – 2000 conference, USA: 2000.

Available http://energy.gov/sites/prod/files/2013/11/f4/absorption_future.pdf

60. R.Z. Wang, R.G. Oliveria, "Absorption refrigeration – an efficient way to make good use of waste heat and solar energy", Progress of Energy Combustion 32 (2006),424-58.

61. K. Daou, RZ.Wang, ZZ Xia,"Desiccant cooling air conditioning: A review", Renewableand Sustainable Energy Reviews10 (2006),55-77.

62. P.Srikhirin, S.Aphornratana, S.Chungpaibulpatana, "A Review of absorption refrigeration technologies", Renewableand Sustainable Energy Reviews 5 (2001),343-72.

63. Broad non electric chiller model selection & design manual, Broad Air conditioning Co. Ltd.

http://www.broadusa.com/index.php/lieterature/doc_download/42-broad-x-non-electric-chiller Last accessed on Nov. 7, 2014.

64. N .Velazquez, R. Best, "Methodology for the energy analysis of an air cooled GAX absorption heat pump operated by natural gas and solar energy", Applied Thermal Engineering, 22 (2002), 1089-1103.

65. D. Zheng, W. Deng, H Jin, J. Ji "α-h diagram and principle of exergy coupling of GAX cycle", Applied Thermal Engineering, 27 (2007), 1771-1778.

66. V.Sabatelli, G.Fiorenza, D. Marano,"Technical status report on solar desalination and solar cooling", A Technical report of the EU-project "NEGST (New Generation of Thermal Solar Systems)" WP5.D1:2007. Available from: http:\\www.swt-technologie.de\html\ publicdeliverables3.html. Last accessed on Nov. 15, 2014.

67. W. Ryan, New developments in gas cooling. ASHRAE J 44(4) (2002), 23-26.

68. J. Deng, R. Z. Wang, G. Y. Han, "A review of thermally activated cooling technologies for combined cooling heating and power systems", Progress in Energy and Combustion Science 37 (2011), 172-203.

69. T. Nunez, "Thermally driven cooling: Technologies, development and applications", Journal of Sustainable Energy, Vol. 1 No. 4, December, 2010. www.energy-cie.ro/archives/2010/nr_4/v4-03_nunez_thomas.pdf Last accessed on Nov. 20, 2014.

70. OJ Ryan, "A micro cooling, heating, and power (m- CHP) instructional module", A MS thesis, Mechanical Engineering Department, Mississippi State University, Mississippi, December 2005. http://sun.library.msstate.edu/ETD-db/theses/available/etd-11092005-123751/unrestricted/All_Thesis.pdf. Accessed on April 14, 2014.

71. M. Jradi, S. Riffat, “Trigeneration system: Energy policies, prime movers, cooling technologies, configurations and operation strategies”, Renewable and sustainable energy reviews 32 (2014), 396-415.

72. D. Ziher, A. Poredos, “Economics of a trigeneration system in a hospital”, Applied Thermal Engineering 26 (2006), 680-687.

73. J. Bassols, B. Kuckelkorn, J. Langreck, R. Schneider, H. Veelken, “Trigeneration in the food industry”, Applied Thermal Engineering 22 (2002), 595-602.

74. M.V. Biezma, J.R. San Cristóbal, Investment criteria for the selection of cogeneration plants – a state of the art review, Applied Thermal Engineering 26 (5–6) (2006), 583–588.

75. A. Napolitano, G. Franchini, A. Perdichizzi, W. Sparber, Design Criteria for Trigeneration Systems Coupled with Solar Thermal Collectors, 64◦ Congresso Nazionale ATI, L’Aquila, Italy, 2009.

76. A.Arteconi, C. Brandoni, F. Polonara, “Distributed generation and trigeneration: Energy saving opportunities in Italian supermarket sector”, Applied Thermal Engineering 29 (2009), 1735-1743.

77. E. Cardona, A. Piacentino, A methodology for sizing a trigeneration plant in Mediterranean areas, Applied Thermal Engineering 23 (2003), 1665–1680.

78. A Moran, ‘Micro CHP modeling and simulation using thermodynamic cycles’, A MS thesis, Department of Mechanical Engineering, Mississippi State University, Mississippi, 2006. http://sun.library.msstate.edu/ETD-db/theses/available/etd-11102006-003810/unrestricted/AlanMoranThesis.pdf. Accessed on April 17, 2014.

79. G.Angrisani, A.Rosato, C.Roselli, M.Sasso, S.Sibilio, Experimental results of a micro trigeneration installation, Applied Thermal Engineering 38 (2012), 78-90.

80. Giovanni Angrisani, Carlo Roselli, Maurizio Sasso, Francesco Tariello, “Dynamic performance assessment of a micro-trigeneration system with a desiccant-based air handling unit in Southern Italy climatic conditions”, Energy Conservation and Management 80 (2014), 188-201.

81. S.P.Borg, N.J.Kelly, High resolution performance analysis of micro trigeneration in an energy efficient residential building, Energy and Buildings 67 (2013), 153- 165.

82. Jian Deng, Ruzhu Wang, Jingyi Wu, Guyong Han, Dawei Wu, Sheng Li, “ Exergy cost analysis of a micro trigeneration system based on the structural theory of thermoeconomics”, Energy 33(9) (2008), 1417- 1426.

83. J.Y.Wu, J.L. Wang, S.Li, R.Z.Wang, Experimental and simulative investigation of a micro CCHP (micro combined cooling, heating and power) system with thermal management controller, Energy 68 (2014), 444-453.

84. Y. Huangfu, J.Y. Wu, R.Z. Wang, X.Q. Kong, B.H. Wei, "Evaluation and analysis of novel micro scale combined cooling, heating and power (MCCHP) system", Energy Conversion and Management 48 (2007), 1703-1709.

85. J. Godefroy, R. Boukhanouf, S. Riffat, "Design, testing and mathematical modelling of a small-scale CHP and cooling system (small CHP-ejector trigeneration)", Applied Thermal Engineering 27 (2007), 68-77.

86. X.Q. Kong, R.Z. Wang, J.Y. Wu, X.H. Wang, Y. Hunangfu, D. W. Wu, Y.X.Xu, "Experimental investigation of a micro combined cooling, heating, and power system driven by a gas engine", International Journal of Refrigeration 28 (2005) 977-987.

87. Yaodong Wang, Ye Huang, Elijah Chiremba, Anthony P.Roskilly, Neil Hewitt, Yulong Ding, Dawei Wu, Hongdong Yu, Xiangping Chen, Yapeng Li, Jincheng Huang, Ruzhu Wang, Jingyi Wu, " An investigation of a household size trigeneration running with hydrogen" Applied Energy 88 (2011), 2176-2182.

88. Yaodong Wang, Ye Huang, Anthony P. Roskilly, Yulong Ding and Neil Hewitt, "Trigeneration running with raw jatropha oil", Fuel Processing Technology 91(3) (2010), 348-353.

89. Andre Alexio Manzela, Sergio Morais Hanriot, Luben Cabezas Jose Ricardo Sodre "Using engine exhaust gas as energy source for an absorption refrigeration system", Applied Energy 87 (2010), 1141-1148.

90. Lin Lin, Yaodong Wang, Tarik Al-Shemmeri, Tom Ruxton, Stuart Turner, Shengchuo Zeng, Jincheng Huang, Yunxin He, Xiaodong Huang, "An Experimental investigation of a household size trigeneration", Applied Thermal Engineering 27(2007), 576-585.

91. Operating manual of Kirloskar Oil Engines, "Specifications of Kirloskar Single Cylinder water cooled diesel engine AV1".

92. Technical specifications of Acrylic body low flow rotameter Available at: www.cvgtechnocraft.com/acrylic_body_rotameter.htm Last accessed on Nov. 7, 2014.

93. Specifications of Domestic type Rahul make water flow meters, Available at http://www.rahulmeters.com/?page_id=91

94. Operating Manual of AVL DITEST, AVL, Austria "AVL DiGas 4000 light". www.avlditest.com/fileadmin/image/pdf_english/AVL_abgastester_Serie4000_E_070329.pdf
95. Operating Manual of AVL 437 smoke meter.
96. Operating Manual for "Vapor absorption refrigeration test Rig", Supplier of equipment-T.T.E., Bangalore.
97. A technical design report on combined emergency power and refrigeration source, by design group of the capstone design course MIM U702.

http://iris.lib.neu.edu/cgi/viewcontent.cgi?article=1016&context=mech_eng_capstone
98. Kotas, R.J., "The exergy method of thermal plant analysis", Reprint edition 1995, Krieger, Malabar, FL.
99. P Tan, Z Hu, D Lou, "Regulated and unregulated emissions from a light-duty diesel engine with different sulfur content fuels", Fuel 88(2009), 1086–91.
100. Rahul Goyal, Dilip Sharma, S.L.Soni, Pradeep Kumar Gupta, Dheeraj Johar, Deepesh Sonar, "Performance and emission analysis of CI engine operated micro trigeneration system for power, heating and space cooling", Applied Thermal Engineering 75 (2015), 817-825.
101. Kamal Kishore Khatri, Dilip Sharma, S.L.Soni, Deepak Tanwar, "Experimental investigation of CI engine operated Micro Trigeneration system", Applied Thermal Engineering 30 (2010), 1505-1509.
102. V. Pandiyarajan, M.Chinnappandian, V.Raghavan, R.Velraj, "Second law analysis of a diesel engine waste heat recovery with a combined sensible and latent heat storage system", Energy policy 39 (2011), 6011-6020.
103. J. Aman, D. S.-K. Ting, P. Henshaw, "Residential solar air conditioning: energy and exery analyses of an ammonia – water absorption cooling system", Applied Thermal Engineering 62 (2014), 424-432.

PUBLICATIONS

Research Papers published/accepted in Journals:

1. Rahul Goyal, Dilip Sharma, S. L. Soni, Pradeep Kumar Gupta, Dheeraj Johar, An experimental investigation of CI engine operated micro-cogeneration system for power and space cooling, Energy Conversion and Management, 89 (2015) 63-70. (3.590 SCI)
2. Rahul Goyal, Dilip Sharma, S. L. Soni, Pradeep Kumar Gupta, Dheeraj Johar, Deepesh sonar, Performance and emission analysis of CI engine operated micro trigeneration system for power, heating and space cooling, Applied Thermal Engineering, 75, (2015) 817-825. (2.624 SCI)

Research Papers presented or published in International Conferences/Conventions:

1. Rahul Goyal, Dilip Sharma, S. L. Soni, Pradeep Kumar Gupta, Dheeraj Johar, Experimental Optimization of CI Engine Operated Micro-Trigeneration System for Power, Heating and Space Cooling, 14th International Conference on "Sustainable Energy Technologies-SET 2015, 25- 27 of August 2015, Nottingham, UK.
2. Rahul Goyal, Dilip Sharma, S. L. Soni, A review of various waste heat recovery technologies in I.C. engine, International Conference on "Advance Trends in Engineering and Technology (ICATET) 2013" 1^{9th} December to 2^{0th} December 2013 organized by Arya college of Engineering & I.T. Kukas, Jaipur.
3. Rahul Goyal, Dilip Sharma, S. L. Soni, A review of combined cooling, heating and power systems, International Conference on "Alternative Fuels for I C Engines" ICAFICE-2013 6th February to 8th February, 2013 organized Department of Mechanical Engineering, MNIT Jaipur.
4. Rahul Goyal, Dilip Sharma, S. L. Soni, A review of trigeneration system, International Seminar on "Conservation of Energy" 9th November to 10th November, 2011 organized by Shankara Group of Institutions in collaboration with Republic of Lithuania, Kukas, Jaipur.

Research Papers presented or published in National Conferences/Conventions:

1. Rahul Goyal, Dilip Sharma, S. L. Soni, Cogeneration in Group industry, National Conference on "Energy Efficient System Design and Manufacturing- EESDM, 2012" 30th March to 31st March, 2012, organized by Vivekananda institute of technology, Jaipur.
2. Rahul Goyal, Dilip Sharma, S. L. Soni, Dheeraj Johar, Experimental investigation of CI engine operated waste heat operated cooker, National Conference on "Energy Efficient System Design and Manufacturing- EESDM, 2012" 30th March to 31st March, 2012, organized by Vivekananda institute of technology, Jaipur.